OPTIMAL ALLOCATION OF REACTIVE POWER TO MITIGATE FAULT DELAYED VOLTAGE RECOVERY

A Thesis
Presented to
The Academic Faculty

by

Sandhya Madan

In Partial Fulfillment
of the Requirements for the Degree
Master of Science in the
School of Electrical and Computer Engineering

Georgia Institute of Technology
August 2010

OPTIMAL ALLOCATION OF REACTIVE POWER TO MITIGATE FAULT DELAYED VOLTAGE RECOVERY

Approved by:

Dr. A.P. Meliopoulos, Advisor
School of Electrical and Computer Engineering
Georgia Institute of Technology

Dr. S. Deng
School of Industrial and Systems Engineering
Georgia Institute of Technology

Dr. M. Begovic
School of Electrical and Computer Engineering
Georgia Institute of Technology

Dr. R.G. Harley
School of Electrical and Computer Engineering
Georgia Institute of Technology

Date Approved: 06/18/2010

ACKNOWLEDGEMENTS

I would like to thank my advisor Dr. A.P. Meliopoulos for an opportunity to work on this project and his continued guidance. I would also like to thank the committee, Dr. Miroslav Begovic, Dr. Ronald Harley and Dr. Shijie Deng for their time.

During the course of my Masters, I have had the opportunity to exchange ideas with many of my fellow students, and this has helped me a great deal in my research. For this, I would like to thank Curtis Roe, Yonghee Lee, Nathan Ainsworth, Stephanie Gossman, Sungyun Choi and Vangelis Farantatos. I would particularly like to thank Dr. George Stefopoulos for taking the time to help me during the course of my research, and also for providing many valuable pointers.

I would like to thank my parents for their love and support, this has continued to be a source of encouragement.

TABLE OF CONTENTS

LIST OF TABLES

LIST OF FIGURES

LIST OF SYMBOLS AND ABBREVIATIONS

α_1	Weight for investment cost
α_2	Weight for installation cost
α_3	Weight for operating cost
β_1	Weight for voltage deviation
β_2	Weight for recovery time
β_3	Weight for voltage oscillations
AVR	Automatic Voltage Regulator
$C(X_{i,k})$	Cost of State – i for Stage – k
$C^*(X_{i,k})$	Optimal cost from the start of planning period to State – i, Stage – k
HVDC	High Voltage Direct Current
IEEE	Institute of Electrical and Electronics Engineers
kV	kilovolt
MVA	MegaVoltAmpere
MVAr	MegaVoltAmpere-reactive

OAODVAR	Optimal Allocation of Dynamic VoltAmpere-reactive
pu	per-unit
PV	Photovoltaic
RTS	Reliability Test System
STATCOM	Static Synchronous Compensator
SVC	Static VoltAmpere-reactive Compensator
$T(X_{i,k} \rightarrow X_{j,k+1})$	Transition cost from State – i, Stage – k to State – j, Stage – k+1
t_{ri}	Recovery time for dynamic load bus 'i'
VAr	VoltAmpere-reactive
V_{ni}	Nominal voltage at dynamic load bus 'i'
V_{osci}	Magnitude of voltage oscillation at dynamic load bus 'i'
V_{ti}	Terminal voltage at dynamic load bus 'i'
WinIGS	Windows Integrated Grounding System
$X_{i,k}$	State – i at Stage – k
ZIP	Impedance, Current, Power (Load Models)

SUMMARY

The Masters Thesis research focuses on reactive power and voltage control during and following major power system disturbances such as faults and subsequent loss of transmission line(s) or generator(s), voltage recovery phenomena following successful fault clearing, dynamic swings of power systems and local voltage suppression, etc. During these events, load and other system dynamics may cause reactive power deficiencies and system voltage issues such as delayed voltage recovery. These phenomena may lead to secondary events such as tripping of loads and/or circuits. Dynamic VAr sources such as generators, static VAr compensators (SVCs), STATCOMs etc and to a lesser degree static VAr sources such as capacitor or reactor banks, can help the system recover from these contingencies by providing fast modulation of the reactive power. Because of the higher cost of dynamic VAr resources, it is important to optimize the deployment of these devices by minimizing the total installed capacity of dynamic VAR resources while meeting the technical requirement and achieving the necessary performance of the system. We refer to this problem as the optimal allocation of dynamic VAR sources (OAODVARS). OAODVARS has been addressed with traditional analytic methods as well as with Artificial Intelligence methods such as genetic algorithms and Tabu search using mostly power flow type models. Both type of methods, as reported in the literature, have not provided satisfactory solutions because they ignore system dynamics and especially load dynamics, in other words they are based on power flow type models. In addition the AI methods have been proved to be extremely inefficient. We propose a new approach that has the following two advantages: (a) it is based on a realistic model that captures system dynamics and (b) it is based on the efficient successive approximation dynamic programming. The solution is provided as a sequence

of planning decisions over the planning horizon. The proposed method will be demonstrated on the IEEE 24-bus reliability test system.

CHAPTER 1

INTRODUCTION

1.1 Problem Statement

Voltage stability issues are a major concern in view of increasing load demands. Sudden increase in loads, both industrial and residential, causes major disturbances and transients in the voltage of the power system grid with potential secondary effects such as load disruption, unwanted relay operations, etc. These disturbances affect the power system stability and recovery depends on how well the system has been designed to deal with these contingencies.

Transients can occur in the system due to loading, loss in transmission lines or generating units, faults etc. The system recovery after these transients depends on the dynamic loads in the system, such as induction motors, as well as amounts of reactive power installed. The existence of these loads demands additional reactive power support after contingencies. This is significant in most power systems as they operate close to their loading limits.

The main measure of power system reliability after these transients is the voltage recovery after these transients. The dynamic loads in the system require increased reactive power during this period. If the reactive power support in the system is inadequate, these loads may show delayed recovery. The protection system for the induction motors may cause tripping. This increases the economic losses incurred due to the faults.

Static and dynamic reactive power sources installed at different locations in the system can provide fast modulation of reactive power, thereby helping the system recover.

Given a power system, the ideal magnitude and location of the SVC to be installed is to be found so that the system is able to recover from any faults, increase in loads, or other contingencies. Since SVCs are relatively expensive devices, the amount and locations of SVC should be optimized.

1.2 Research Objectives

The following tasks have been carried out to improve the stability of the test system:

- Literature study of previous research on static VAr compensators used to improve voltage stability.
- Formulation of the proposed approach.
- Solution Methods of the optimization problem above.
- Example Results

This optimization approach is an application of dynamic programming to the problem. The reactive power installation problem is viewed as a multistage decision making process over a planning horizon of 5 to 10 years. Dynamic programming approach is applied to obtain the most optimal decisions to be taken at each stage. The method is demonstrated on an example distribution system.

CHAPTER 2

BACKGROUND AND LITERATURE REVIEW

This chapter provides an overview of stability phenomena, voltage recovery issues and previous mitigation techniques applied to alleviate these problems. The concepts of static and dynamic stability are explained. The focus of this thesis is dynamic voltage stability, and voltage recovery after a contingency is illustrated with an example distribution system. The effect of slow voltage recovery on loads is evident from these examples.

In the second part of the chapter, various optimization algorithms that have been used for reactive power allocation are explained.

2.1 Stability in Power Systems

Instability can occur in a power system by a variety of phenomena. In general, three major types of voltage stability can be identified, (1) Static Voltage Stability, (2) Dynamic Voltage Stability, (3) Transient Voltage Collapse. The three voltage stability types will be described next.

2.1.1 Static Voltage Stability

AC circuits can transmit limited amounts of power, the limit is dependent upon the operating voltage of the circuit and the impedance of the circuit. As power is routed through an AC transmission line, the voltage decreases with increased load. At some

point the voltage collapses indicating that the line has reached its maximum transfer capability. Figure 2.1 indicates this behavior and it is normally referred to as the nose curve. Static voltage stability studies are concerned with the computation of the location of the collapse point (tip of nose curve) and the distance of an operating point from that limit. The point at which the voltage collapses is called the nose point and is determined as that point where the voltage drastically collapses on further loading.

Static voltage stability studies are done by slowly loading the power system in incremental steps and studying the response of the system to the loads. The loads are increased by a factor called the loading factor and the control of the system is studied using the controllability factor. The P-V and V-Q curves at the buses where loading is done provides relationships between the system load changes and the load variations.

The procedure for plotting the nose curve involves increasing the loading at selected buses and applying power flow algorithms to determine the bus voltages and powers. The shape of the in the curve in Figure 2.1 depends on the load at the load centers. During unstable conditions, capacitor banks along with motors may cause the voltage to drop steeply for even small increases in power [15].

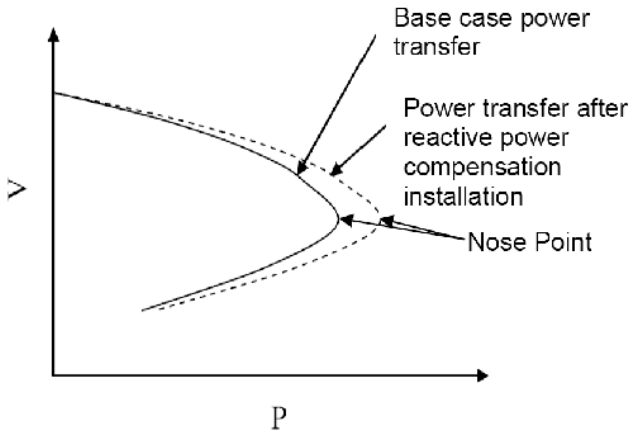

Figure 2.1: PV Characteristics for Static Instability

For generating the V-Q curves, a MVAr generator is used at the required bus and the bus voltage is varied, allowing for the computation of the MVAr requirement [12].

The loads used in the static voltage stability studies are considered as constant impedance, constant current and constant power models (ZIP Models). However, 60% of the loads used are induction motor loads and these loads do not follow the behavior of any of the above load models during instability. When these considerations are taken into account, stability limits found are more realistic and lower than the stability limits found without the induction motor loads [13].

2.1.2 Dynamic Voltage Collapse

Dynamic voltage collapse occurs when sudden changes in reactive power requirements occur in a system such as clearing a fault, rapid load change or isolation of transmission lines. During these disturbances, if the dynamic VAr sources do not compensate for these requirements, the system reactive power will decay. This decay causes decreases in line charging and bus voltages. During this period, there is also a rise in the real power losses. The bus voltage magnitudes are determined by reactive power flow and the currents are determined by the real power flow.

The generators in the system try to compensate for the reactive power imbalance in the system. If the reactive power load is less than the reactive power loss, the generators may support this reactive power requirement. Thus, a wider area is affected by the disturbance [9].

The loads connected to the network may be voltage sensitive and may stop working if the voltage continues to remain below a predefined level. If a fault occurs, the

voltage suddenly dips and then increases to another value below the nominal value after the fault is cleared. The voltage approaches the nominal value from this post fault value slowly. This period of recovery depends on the induction motor loads connected to the system [6].

Faults on a transmission line contribute the most to dynamic voltage instability. Three phase faults occurring near the load bus show a profound effect on the dynamic instability of the system. In transient events, stability can be increased and a voltage collapse can be avoided by using fast-tracking devices that are able to immediately supply reactive power to the system [5].

Dynamic instability can also occur when the automatic voltage regulator loop connected to a generator amplifies the oscillations rather than damp them. After a fault, when negative damping is introduced, the system tends to proceed into undamped oscillations. This may occur at a weakly connected generating station when the loads are located at a significant distance from the plant [15].

Within the first few seconds of the disturbance, the fast dynamics of the system collapse, affecting the faster components in the system. There is a time separation between the static and dynamic phenomena. This is exploited when studying the dynamics of the system. The components taken into account during these first few seconds include synchronous generators, AVR, induction motors, HVDC devices, tap changers and switchable shunt capacitors. [7], [8].

The phenomenon of dynamic voltage collapse occurred in the 2004 blackout in Northeastern US and Canada. A flashover in a transmission line caused the line to be isolated from the system. This subsequently increased the loading on the other transmission lines. Some of the transmission lines exceeded their power transfer limits

and also tripped. Figure 2.2 shows how the tripping of various transmission lines increased the loading on other lines [19].

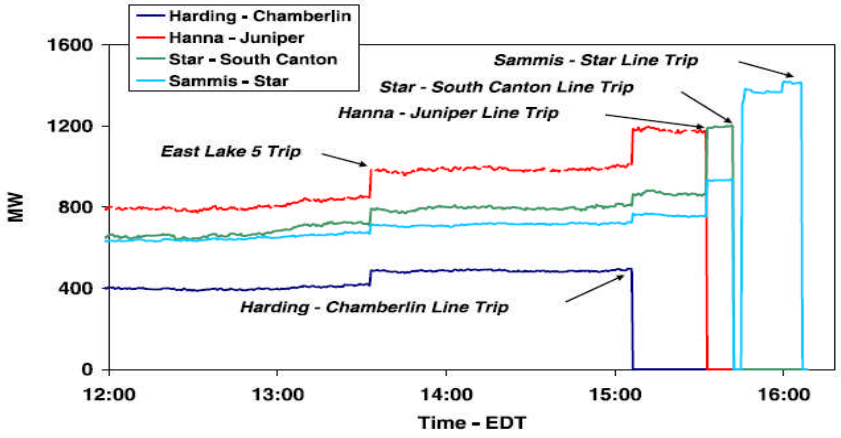

Figure 2.2: Increase in transmission line loading due to tripping of various lines [19]

Due to this, the voltage in the system decreased and the reactive power requirement of the system increased. Figure 2.3 shows the various transmission line voltages.

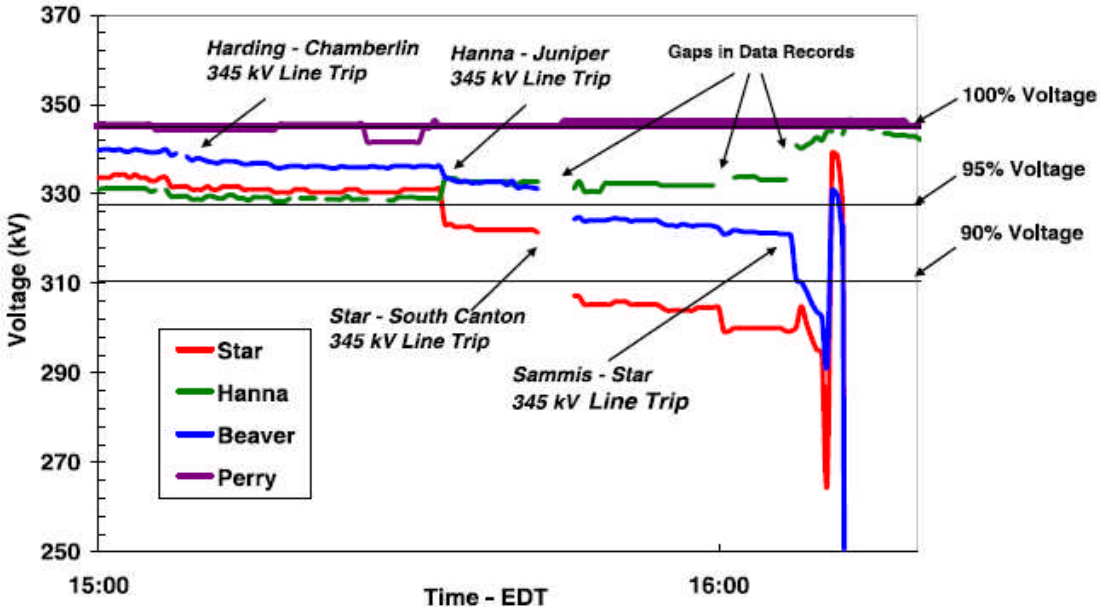

Figure 2.3: Transmission voltages at various lines in the system [19]

2.1.3 Transient Voltage Collapse

This phenomenon occurs when generating units oscillate and generate large transient phase angle differences among various parts of the system. The voltage near the center of the oscillations reduces significantly and possibly a full voltage collapse may occur.

A system containing two generating stations connected by a transmission line undergoing transient voltage collapse has been modeled on WinIGS. The transmission line is 80.0 miles long and is a 3-phase overhead conductor. The two generators are rated at 115kV. The generator connected to BUS 2 is in phase with the generator at BUS 1. Figure 2.4 shows the test system 1 used in this case.

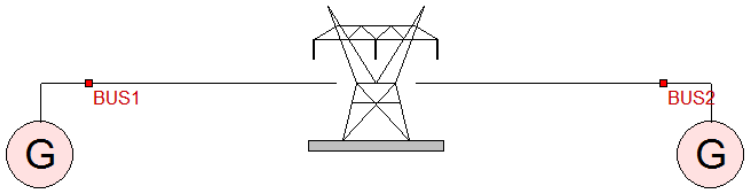

Figure 2.4**:** Single – Line Diagram of Test System 1

Figure 2.5 shows the voltages at different points on the line for the three phases.

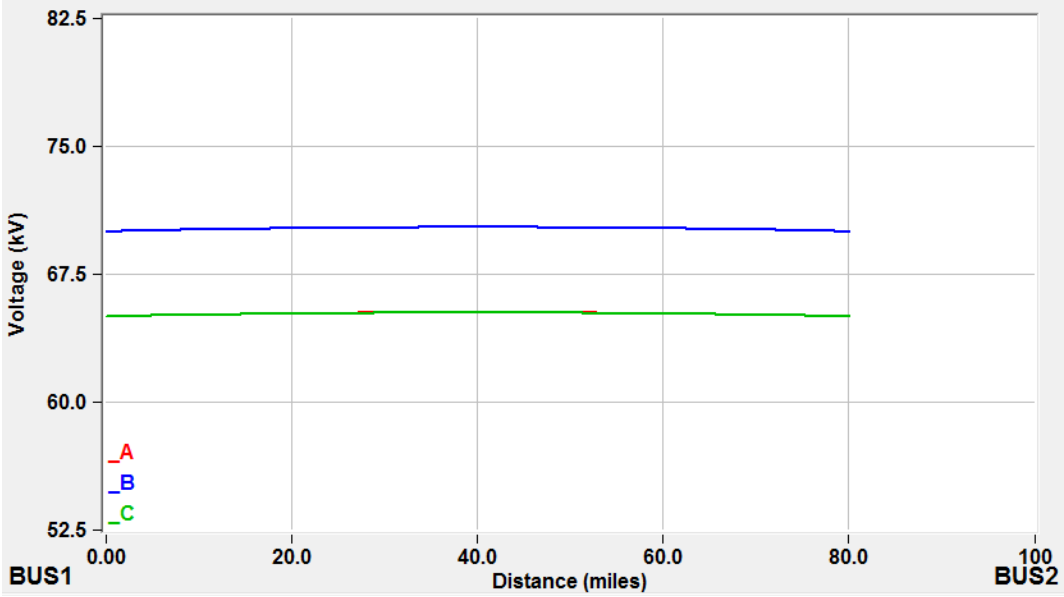

Figure 2.5: Voltage profile on the line of Test System 1

The generator connected at bus 2 is now made to operate out of phase by 180^0 with the generator at bus 1. This causes the voltage at the midpoint of the line to reduce to 0. Figure 2.6 shows the voltage profile for the above case.

When the generator at bus 2 is out of phase by 120^0, the voltage is still below the nominal value and reduces to a minimum at a particular point on the line. Figure 2.7 shows the voltage profile for this case.

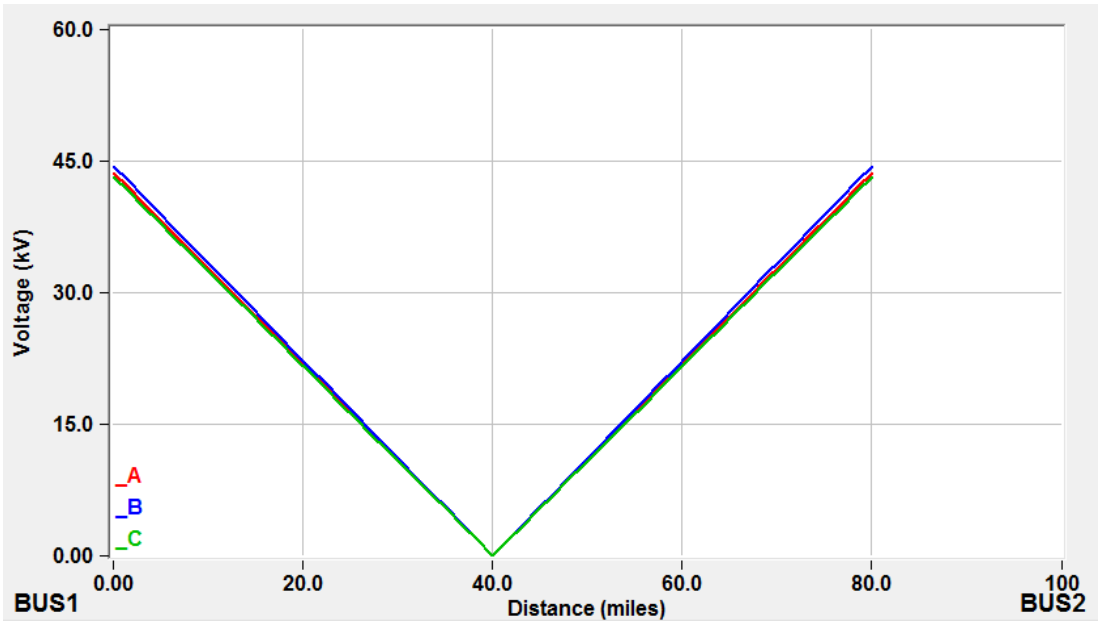

Figure 2.6: Voltage profile for the line with generator out of phase by 180^0

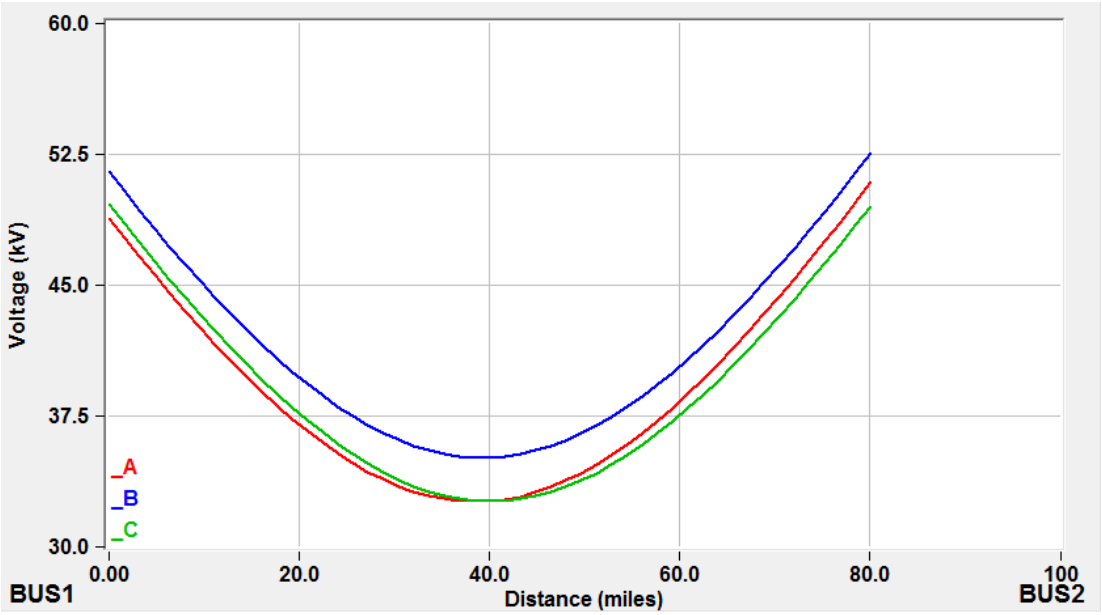

Figure 2.7: Voltage profile for the line with generator out of phase by 120^0

2.2 Voltage Recovery Phenomena

Apart from static VAr controllers, capacitor banks and other VAr sources have also been used to supply reactive power, especially during major disturbances. At locations near a disturbance, the system loads tend to draw heavy reactive currents from the system. After the fault has been cleared, the recovery of the voltage to its initial nominal values depends on the loads connected to the system and how fast the faults have been cleared.

Voltage recovery after balanced and unbalanced reduction in voltages takes place when the circuit breaker isolates the fault and the fault has been cleared. During balanced faults, all the three phases experience the same dip in voltage while unbalanced faults cause unequal reduction in voltages in the three phases. Figure 2.8 shows the recovery of voltage after a dip due to a three phase to ground fault [18]

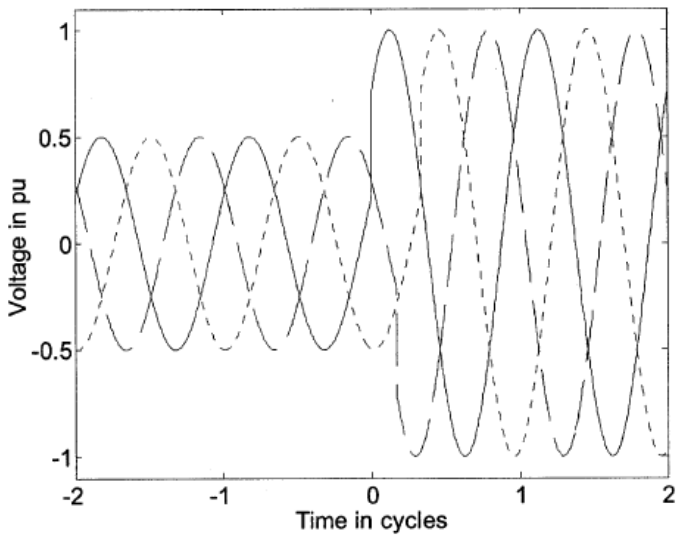

Figure 2.8: Voltage recovery after a three phase to ground fault [18]

During a fault in the Metro Atlanta area in 1999, the fault was not cleared completely. This led to a drop in the voltage from the nominal value. Due to breaker

failures, the transmission line was not able to recover the voltage immediately. The induction motors connected to the system decelerated and increased the reactive power requirement on the system. These loads were then disconnected from the system. About 15 seconds after the fault, the system was able to recover the voltage. However, due to the lost loads, there was a voltage overshoot. As the motors were connected and accelerated, the voltage returned to its normal value. Figure 2.9 shows the voltages and real and reactive powers of the motors at different time instants during this period [17].

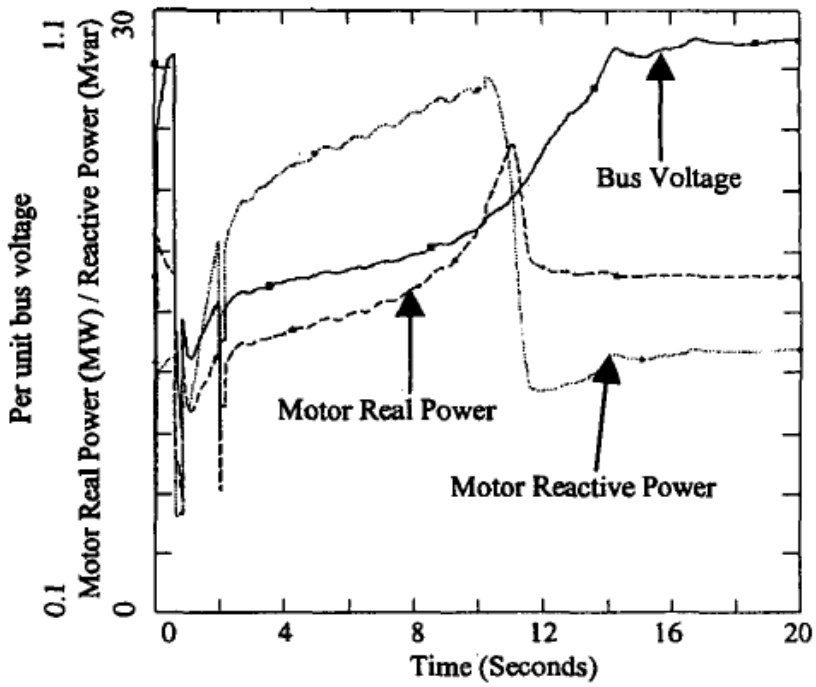

Figure 2.9: Voltage of line, real and reactive powers of motors during a fault in the Metro Atlanta area [17]

Voltage recovery of the system is affected to a great extent by the motor initial currents and the in-rush currents in transformers. The latter influences the voltage recovery when the feeders are energized after a fault. Two approaches can be used to study the effects of motor and transformer currents on voltage stability, the quasi static model and the full domain transient model.

2.2.1 Quasi Static Model

The first model is a quasi-static model. In this model, the system is studied in the frequency domain. The magnitude of the voltages is studied, and the fast transients are ignored. The slow-acting dynamics, particularly that of the induction motor loads gain precedence in this model. The electric transients due to the shunt elements such as inductors and capacitors are not considered.

The voltages and currents are expressed as real and imaginary terms and the expression for current is expressed for any node as follows:

$$\begin{bmatrix} I_r^k \\ I_i^k \\ 0 \end{bmatrix} = y_{eq\_real}^k \begin{bmatrix} V_r^k \\ V_i^k \\ y^k \end{bmatrix} + \begin{bmatrix} x^{kT} f_{eq\_real1}^k x^k \\ x^{kT} f_{eq\_real2}^k x^k \\ \cdots \end{bmatrix} - b_{eq\_real}^k$$

This form can also be used for dynamic component modeling after the differential equations have been converted to algebraic equations [16].

2.2.2 Full Time-Domain Transient Model

In this model, the fast dynamics can also be included. All the dynamic generating units, loads and other power system components are considered. It can also model the nonlinearities in the components as well as saturation. In this model, each component is represented using its differential equation. This set of differential equations is integrated and represented in the following general form:

$$\begin{bmatrix} i^k(t) \\ 0 \end{bmatrix} = A^k \cdot \begin{bmatrix} x^k(t) \\ y^k(t) \end{bmatrix} + \begin{bmatrix} X^{k\,T} F_1^k X^k \\ \dots \\ X^{k\,T} F_n^k X^k \end{bmatrix} - b^k$$

2.3 Voltage Recovery in Test Systems

Investigation has been done in [16] into voltage recovery in distribution systems after major contingencies. This section illustrates the results obtained.

Using a 25kV transmission/distribution test system (

Figure 2.10), three phase faults were simulated by [16] and the voltage profiles at different buses for a period of time after the disturbance was analyzed. Figure 2.11 shows the voltage recovery for a period of about 3 seconds after the fault has been induced. The fault has been applied on the transmission side and the voltage shown corresponds to the distribution side of the substation. At this level, the recovery is very slow and does not reach the nominal value of 1.0pu.

Induction motor voltages at the 480V bus show a faster recovery (Figure 2.11). Figure 2.13 shows the reactive power absorption by the motors after fault. Both active and reactive powers reach a very high value in the post fault period. If the motors stall, they begin to absorb very high values of reactive power and do not return to their normal operating speeds [16].

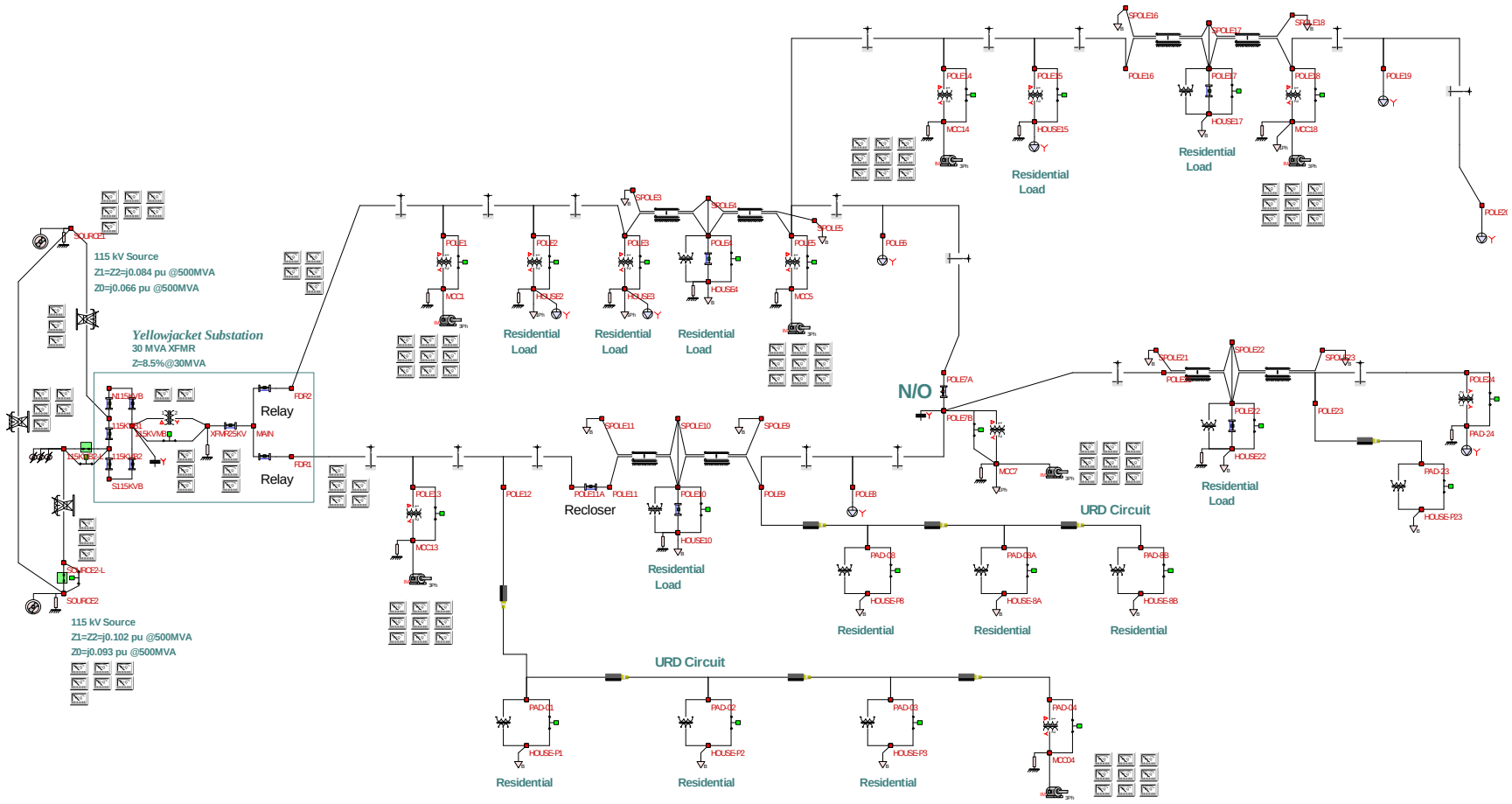

Figure 2.10: 25kV Transmission/Distribution System [16].

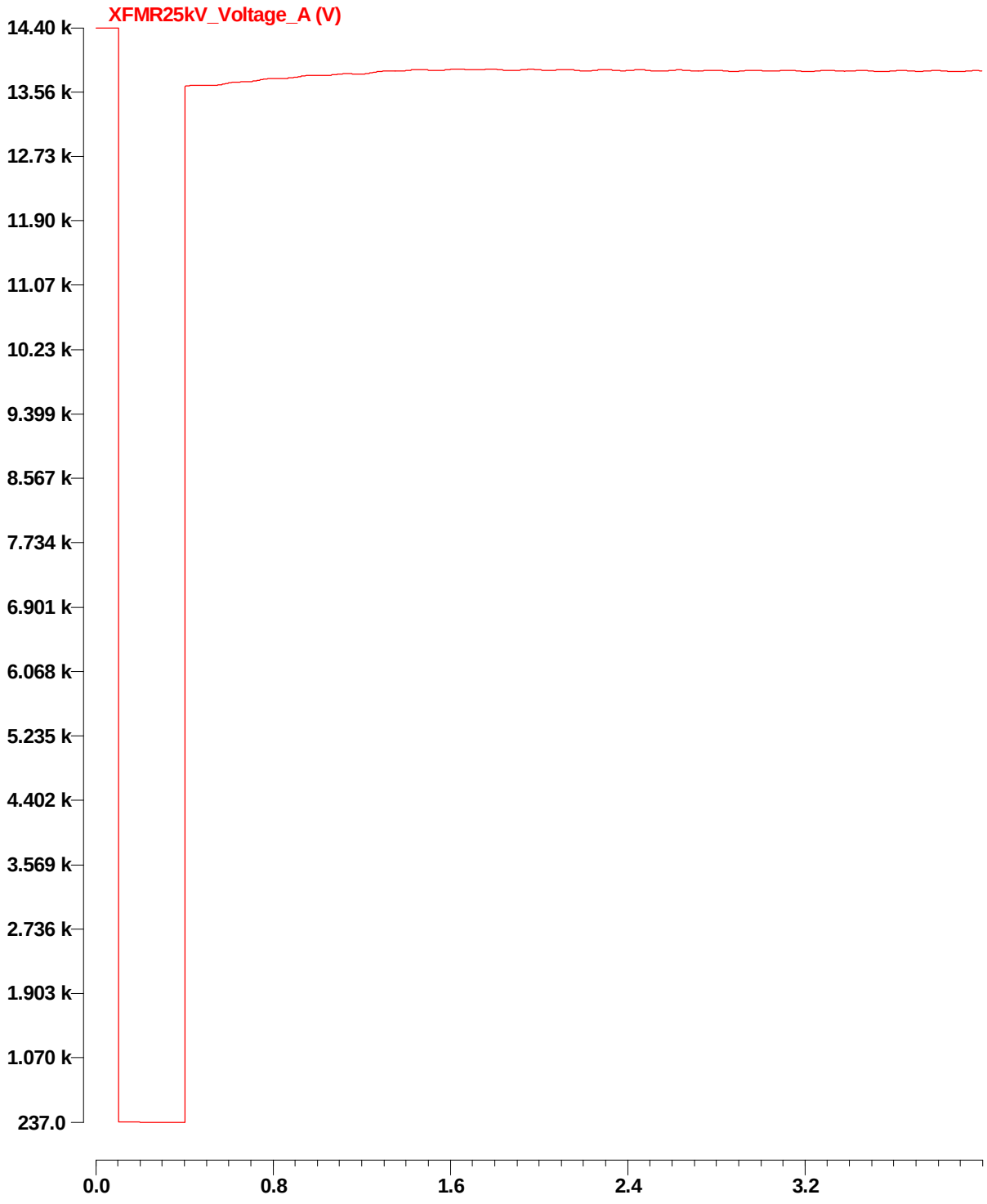

Figure 2.11: Voltage at the distribution side [16]

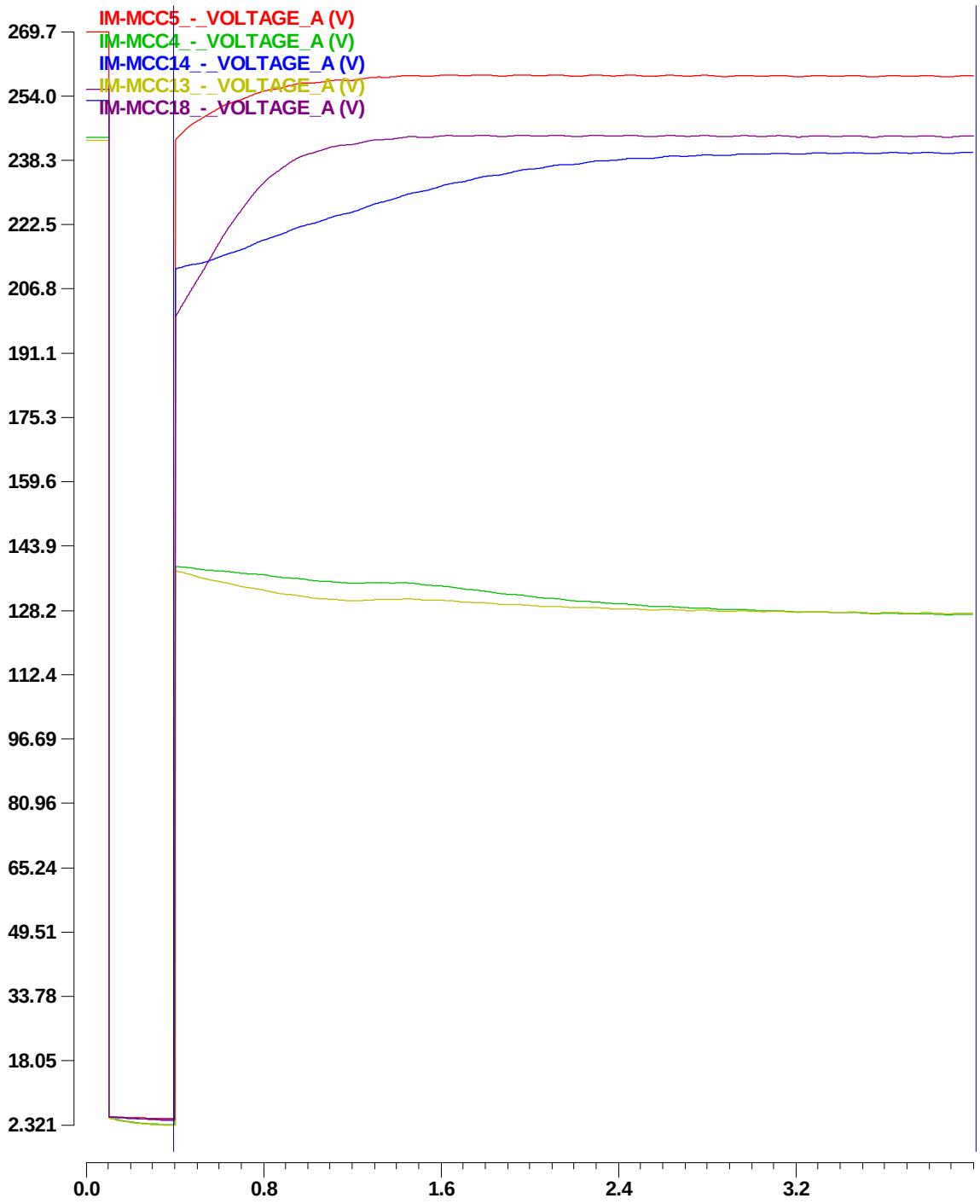

Figure 2.12: Induction Motor Voltages. [16]

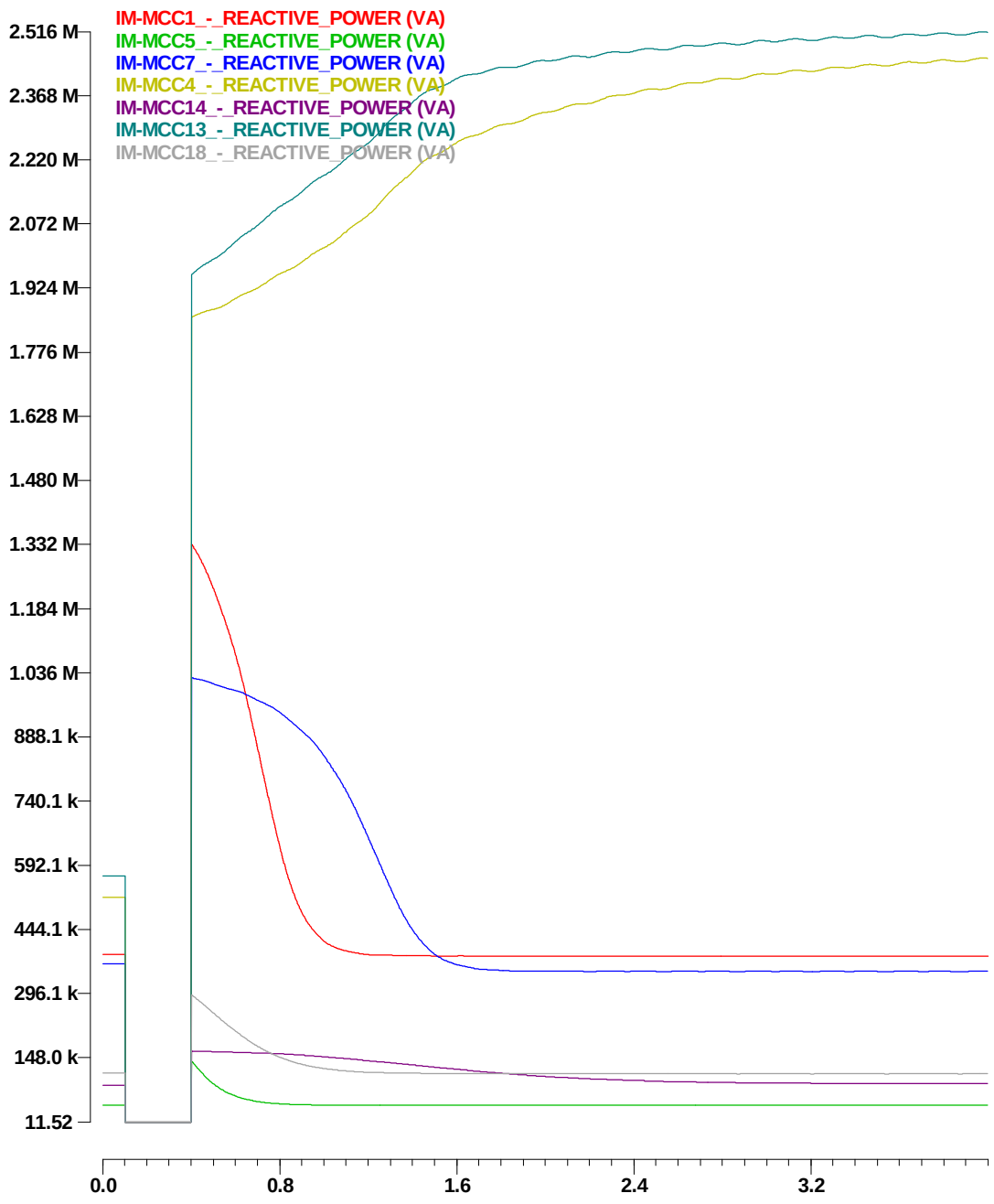

Figure 2.13: Reactive Power absorption by induction motors [16]

2.4 Optimization Algorithms Used in Reactive Power Planning

This section provides an overview of the various optimization algorithms that have been used for reactive power planning based on various objectives and constraints. Previous work has been done in summarizing the algorithms and their efficiency for various objective functions [26].

The problem of reactive power planning to improve system conditions has been solved using many methods in the past few decades. Initially, the location and size of reactive power to be installed was estimated. However, the emergence of various optimization techniques as well as improvement in computational technologies has proved beneficial in solving this problem.

Work was done at Georgia Institute of Technology by [28] in the application of particle swarm optimization to plan allocation of FACTS devices in a power system. This algorithm was tested on the Brazilian power network and showed significant improvements in voltage levels after installation of reactive power. Further, the optimization was done in two stages, the first stage considered the static stability of the system while the second stage considered dynamic stability such as, effect of perturbations, faults etc. This was first validated by brute force method and the results were found to be consistent.

Three classes of optimization techniques have been used in previous research. These are (a) Conventional Methods (b) Intelligent Searches and (c) Fuzzy Theory. Conventional methods include Linear Programming, Nonlinear Programming, Mixed Integer Programming etc. These conventional methods can be relied on to a great extent to yield a global optimum. Attempts have also been made to linearize the nonlinear nature of the problem. However, this method is inaccurate and hence, its use has been

restricted. Nonlinear optimization algorithms have been found to be slow, particularly due to the vastness of the problem.

Intelligent search methods are heuristic techniques that have gained popularity in the recent years. These methods are capable of finding a local optimal point comparatively faster and can sometimes also take into account the probabilistic nature of the problem. Research has also been done to combine two heuristics to solve the problem [27]. Simulated Annealing algorithms can be used when a large number of variables are involved. This inherent advantage has been exploited along with advantages in Genetic Algorithms and Fuzzy Logic in finding optimal location and rating of VAr sources.

Reactive power planning is not without uncertainties in loads, system parameters etc. This has been used as an advantage in the Fuzzy Set Theory [27]. This approach assumes variations in data and hence a certain amount of inaccuracy can be accounted for in the data and the constraints.

A modified approach to dynamic programming has been used to solve the reactive power planning problem [27]. This approach combines dynamic programming with fuzzy set theory to obtain the placement and rating of reactive power in the Croatian power system. A sensitivity analysis for all the buses is done for various cases of reactive power injection and different contingencies. Each of the buses is treated as a node of the dynamic programming problem. For conflicting solutions, fuzzy logic is used to arrive at an optimum.

The various objectives that have been considered while applying the previous approaches have been aimed at (a) Minimizing the cost and (b) Maximizing system performance. Most of the system performance parameters have been aimed at steady state stability as well as reduction in reactive power losses.

To summarize, the issues of voltage stability and voltage recovery under transient conditions have been described. The different approaches used to solve this phenomenon were studied. The next few sections will illustrate research in dynamic programming used as a multistage decision making tool. These stages may span from a few months to a few years, based on the frequency of decision-making. The objectives have been to avoid post fault stalling of dynamic loads at minimum cost of reactive power expansion.

CHAPTER 3

VAR ALLOCATION AS A DYNAMIC PROGRAMMING PROBLEM

3.1 Introduction

It is known that VAr resources can help the system recover from a disturbance and avoid voltage stability problems of the described types. On the other hand dynamic VAr sources are relatively expensive as compared to other VAr sources, such as capacitors. Therefore from an economic point of view dynamic VAr sources should be utilized by placing these resources in strategic locations of the system so that they can control voltage problems over a wider area of the system. The problem of identifying the strategic locations with the greatest impact on the system and the amount of static/dynamic VAr sources required at these locations is the subject of this thesis. We approach the problem as an optimization problem.

3.2 Dynamic Programming

Dynamic programming is a method used to solve multistage decision processes. These decision processes involve a sequence of decisions, usually over a period of time, spanning a planning horizon. This optimization method takes advantage of the fact that although an optimization problem is a complex problem that may contain many dependent variables, it can be decomposed into several subproblems. These subproblems are usually single-stage problems and are computationally less intensive.

During this decomposition into subproblems, the objective function related to each subproblem does not change. Decomposition of the problem into subproblems only increases the computations linearly. However, with an increase in variables, the computations increase exponentially. The method is based on the concept of sequential calculations.

This problem can be approached as either as a forward or a backward dynamic programming problem. In the forward dynamic programming approach, in an optimal path from the first stage to the last stage, the path that begins from the stage after the first stage and ends at the last stage is also optimal. Similarly, in the backward dynamic programming approach, the path that begins in the first stage and ends in the stage before the last stage is an optimal path. These optimal subpaths can further be broken down until we reach a single stage problem that is relatively easy to solve.

The dynamic programming approach consists of two parts, (a) stages, and (b) states. The stages and states contain a description of the system at each hypothetical point that is adequate to solve the system for an optimal solution. A stage in a dynamic programming problem defines the many conditions that the system may exist in, at a point in the planning horizon. The different feasible conditions constituting a stage are called a state. The stage variable indicates how many decisions have been made and is obtained from the recurrence relation. The other variables that describe the state in a stage are called state variables. These state variables are defined by an objective function. [20].

The objective function is used to allocate a numerical value to each state. After decomposition into subproblems, the optimal policy function is used to solve for the best first decision at each subproblem. Further, for each optimal value function, several recurrence relations are obtained.

3.2.1 Problem Definition

The dynamic programming method is based on the principle of optimality which states that independent of the initial state and decision, all the other decisions to any stage are optimal with respect to the initial stage. This principle can be illustrated with the help of Figure 3.1. This figure shows the multistage decision process. It consists of ‘m’ stages and ‘n’ states in each stage.

A stage is defined by the time at which a decision has to be taken, and the states refer to the various decisions that can be taken. An optimal sequence of decisions over this period of ‘m’ stages is to be found using dynamic programming. The principle of optimality implies that any path from the initial stage contains subpaths that are also optimal.

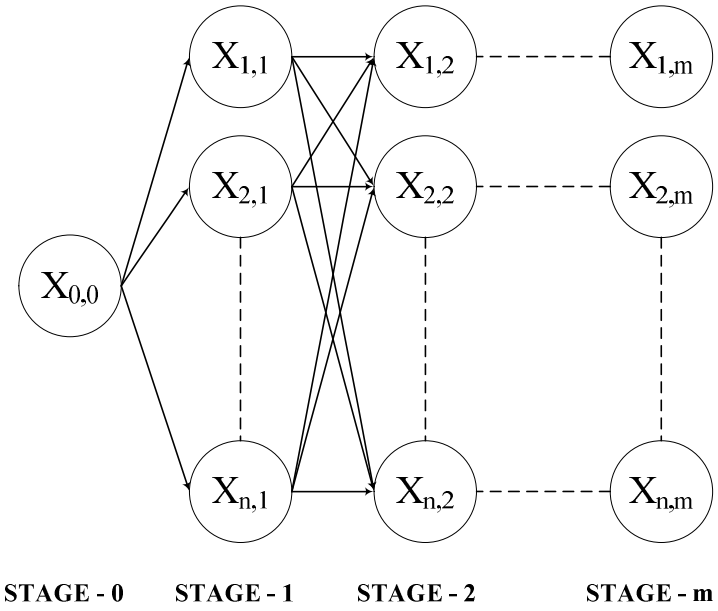

Figure 3.1: Dynamic Programming Formulation

3.2.2 Solution Methodology

Each of the circles in Figure 3.1 represents a state of the system. These can be expanded as shown in Figure 3.2 to contain more information defining the state.

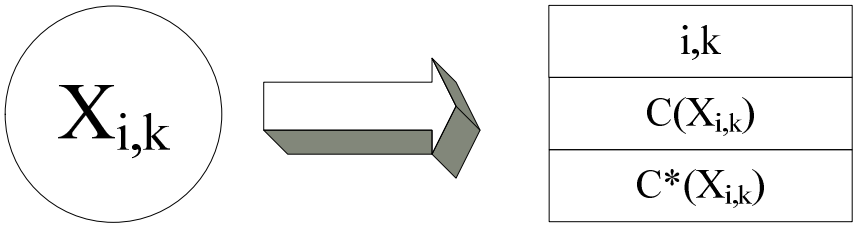

Figure 3.2: State Representation in the Formulation

In this figure, i,k represents the state ‘i’ in stage ‘k’. $C(X_{i,k})$ represents the cost of state ‘i’ at stage ‘k’ over the period of the stage, and $C^*(X_{i,k})$ represents the optimal cost from the start of the planning period to the state $X_{i,k}$.

The dynamic programming approach is a systematic approach for computing the optimal path (transitions) over the entire planning horizon by performing computations only between stages. This is accomplished as follows. Assume that the optimal cost of expanding the system from the start of the planning horizon to state i, stage k has been computed and it is:

$$C^*(X_{i,k})$$

The same optimal cost for each state in the next stage k+1 is computed with the following algorithm:

$$C^*(X_{j,k+1}) = \text{Min}_{\text{(over all states i in stage k)}} [C^*(X_{i,k}) + T(X_{i,k} \rightarrow X_{j,k+1}).C(X_{j,k+1})]$$

Note that the algorithm can be initiated by setting the optimal cost for the initial system equal to zero, i.e. $C^*(X_{0,0})=0.0$, and then start with stage 1.

$T(X_{i,k} \rightarrow X_{j,k+1})$ represents the transition cost from state $X_{i,k}$ to state $X_{j,k+1}$. This cost can be set to 1 for feasible transitions or an infinitely high number for infeasible transitions. Figure 3.3 shows the flowchart for solving a dynamic programming problem.

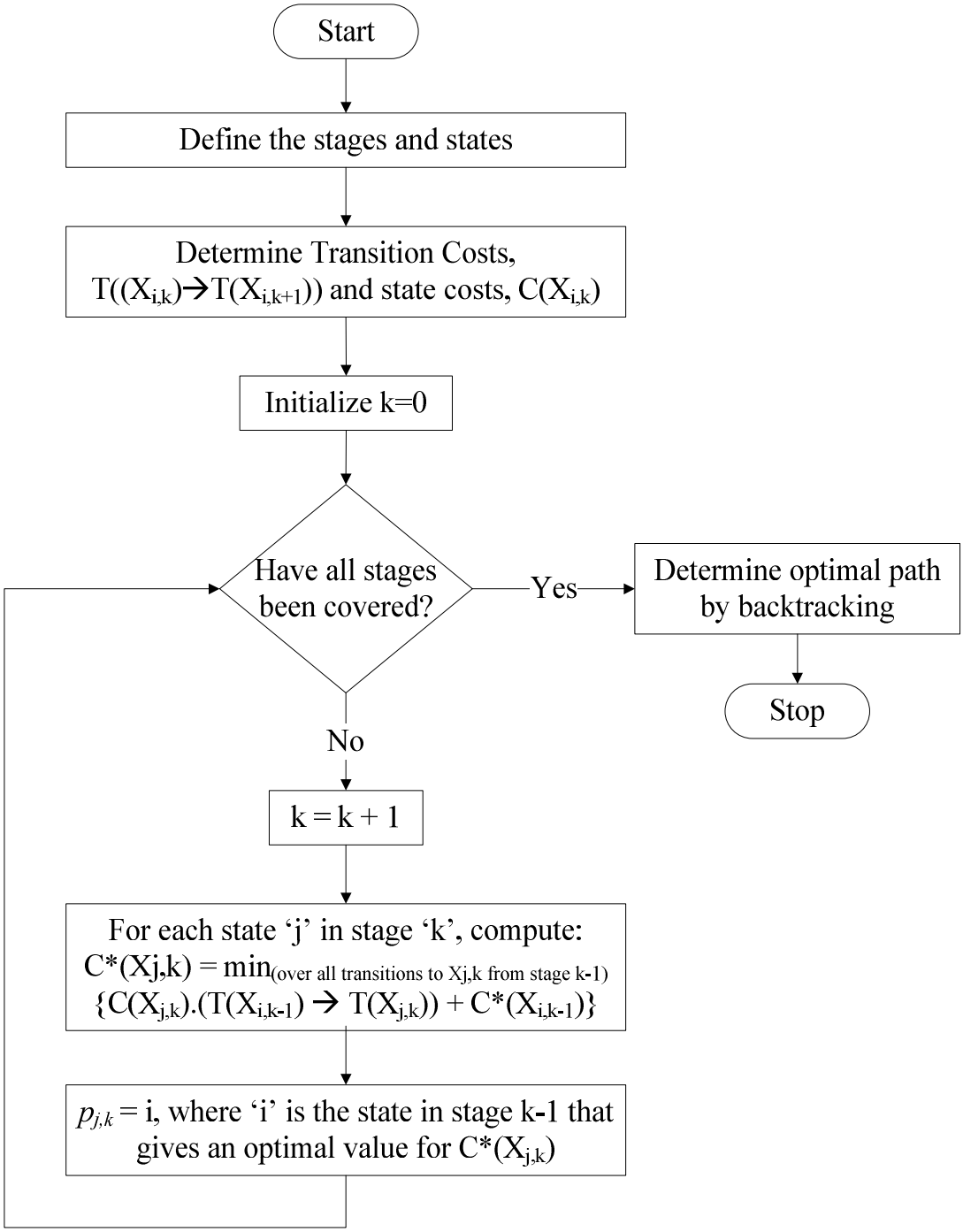

Figure 3.3: Flowchart for Solving the Dynamic Programming Problem

Figure 3.4 shows the calculations involved during transitions from Stage 0 to Stage 1.

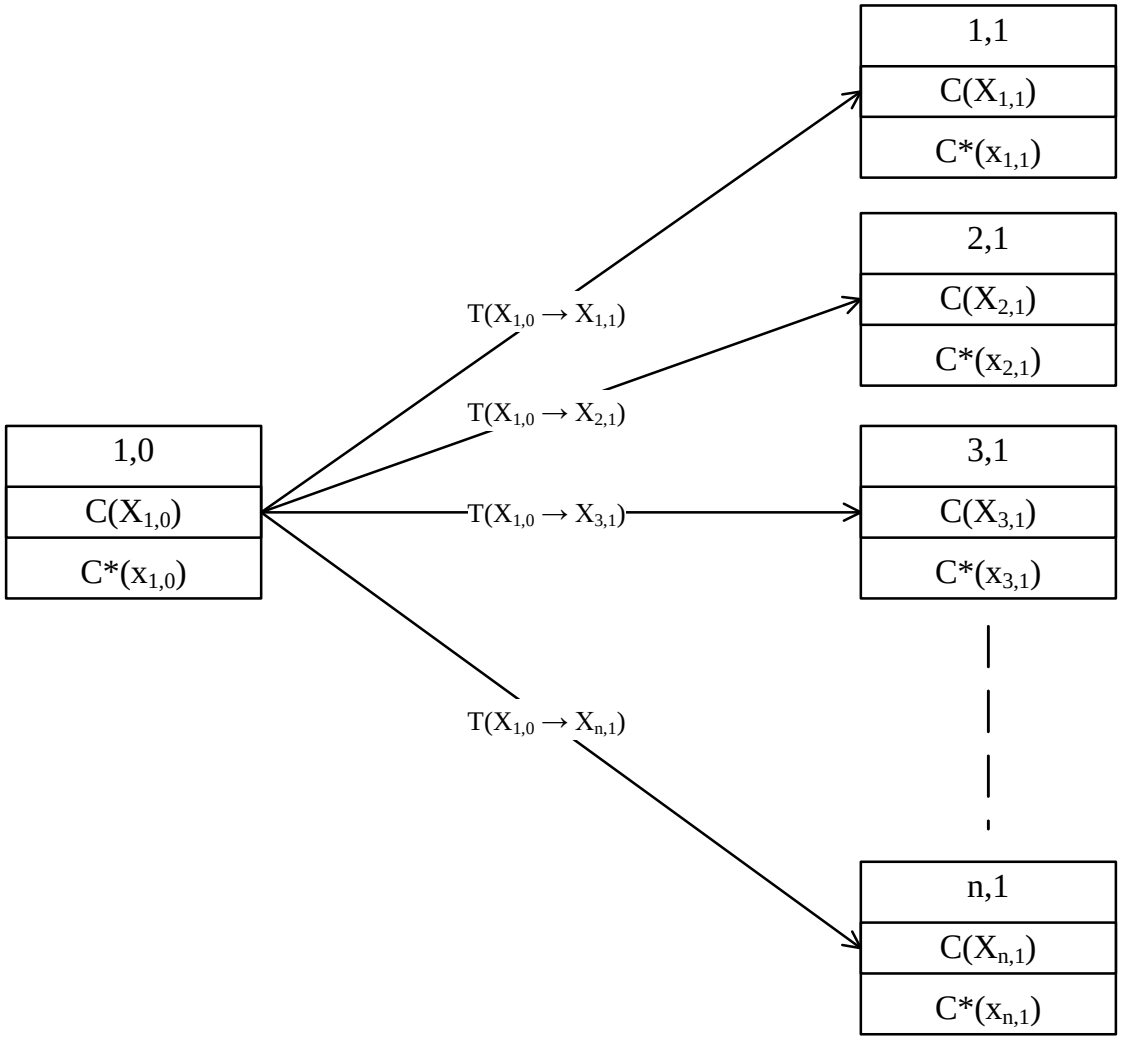

Figure 3.4: Transitions from Stage 0 to Stage 1

For each of these transitions to Stage 1, there is one possible trajectory to each of the states. Hence, for example, applying the equation for optimal path to State 3 in Stage 1,

$$C^*(X_{3,1}) = \text{Min}_{\text{(over all states i in stage 1)}} [C^*(X_{i,0}) + T(X_{i,0} \rightarrow X_{3,1}).C(X_{3,1})] \quad (3.1)$$

Since $X_{3,1}$ has only one path from Stage 0, Equation (3.1) reduces to,

$$C^*(X_{3,1}) = [C^*(X_{1,0}) + T(X_{1,0} \rightarrow X_{3,1}).C(X_{3,1})] \quad (3.2)$$

In a similar manner, Figure 3.5 shows the computations for transitions between Stage k and Stage k+1.

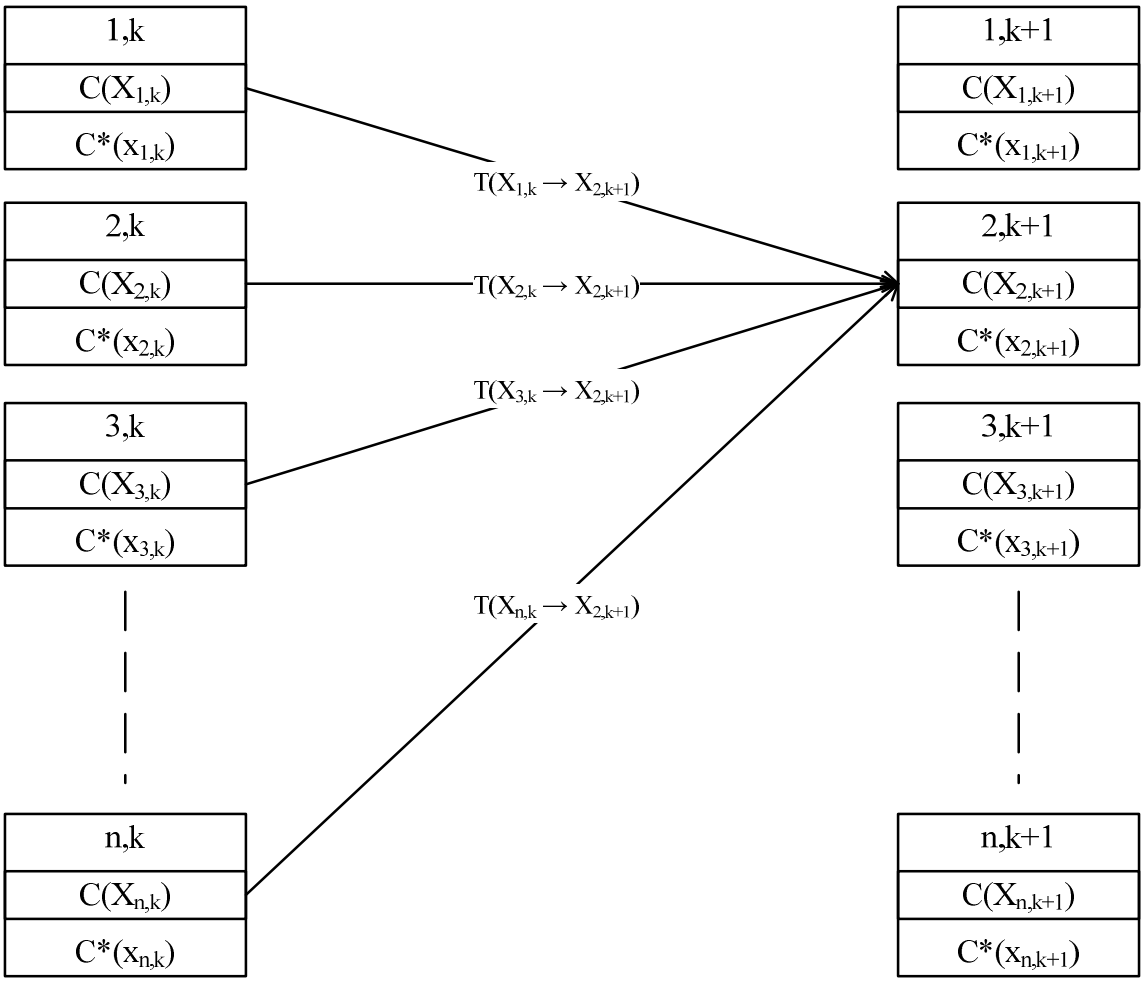

Figure 3.5: Transitions from Stage k to Stage k+1

For transitions from Stage k to a State j in Stage k+1, there are 'n' different possible trajectories. Each of these is characterized by a transition cost as well as an optimal cost. Hence, Equation (3.3) is used for calculating the optimal path to a State j in Stage k+1 is,

$$C^*(X_{j,k+1}) = \text{Min}_{\text{(over all states i in stage k)}} [C^*(X_{i,k}) + T(X_{i,k} \rightarrow X_{j,k+1}).C(X_{j,k+1})] \quad (3.3)$$

[20], [22].

3.3 Summary

This chapter described the dynamic programming methodology and its use as a decision making tool. To summarize, each of the states represents a decision that can be taken and each stage represents a decision making period. This algorithm is tested on a 13.8kV distribution system consisting of both static and dynamic loads and is described in the next chapter.

CHAPTER 4

DESCRIPTIVE EXAMPLE

A base system is considered that may have a number of static and dynamic VAR resources already. The operation of the system over a planning horizon, typically five to fifteen years is considered. Over this planning period it may be necessary to add dynamic VAr sources and/or static VAr sources. The dynamic sources can be of various types, such as synchronous generators, STATCOMs, SVC devices, inverter based interfaces of Wind, PV systems, etc. The decision process involves the addition of specific static and dynamic VAR sources at specific locations of the system at specific levels. Then in terms of the installed sources the state of the system can be defined at a given time as the base case plus the addition of specific amount of static and dynamic VAR sources to specific locations. Thus, a number of states at a number of specific times are defined that will be referred to as stages. In general it is assumed that a decision to add VAR sources can be taken at specific time intervals, for example at intervals of six months. In this case a stage is equivalent to a period of six months. For a planning period of five years, there will be a total of ten stages.

As defined before, the state is denoted as $X_{i,k}$. Using this terminology, the dynamic programming optimization method works on the matrix of all possible states at each stage as it is illustrated in Figure 3.1. Specifically, the matrix shows all the states in a stage in a vertical arrangement. Decisions (additions of specific amounts of VAr sources at specific locations) taken at a state i at stage k will result in a specific state j at stage k+1.

The transition cost has several components. In general, the cost consists of (a) the investment cost, (b) the operating cost and (c) any penalties for non-performance, i.e.

$$T(X_{i,k} \rightarrow X_{j,k+1}) = J_{economic} + J_{penalty} \quad (4.1)$$

The different costs and penalties considered for an optimal planning decision are explained below.

4.1 Transition cost parameters

4.1.1 Economic Costs

It is proposed to use an investment cost which is amortized over a period of one stage. For example assume that a certain transition involves a VAr source that has a total acquisition cost equal to Cx. Further assume that the asset has an expected economic life of m stages. Then the investment cost in one stage is equal to [24]:

$$J_{investment} = \frac{Cx}{\sum_{l=0}^{m} \frac{1}{(1+r)^l}} \quad (4.2)$$

Where, C = Cost per kVAr ($6 for capacitor bank, and $15 for synchronous condenser)

x = kVArs installed

m = 14 years (considering amortization over the lifetime of the equipment)

r = 7%

The second economic cost is the installation cost. This cost has been assumed to be a one-time cost and is represented by $J_{installation}$.

It is important to note also that if the transition requires removal of installed VAR sources, then the transition is infeasible. This is controlled within the dynamic programming optimization approach by assigning a very large cost for these transitions.

The operating cost can be computed by simulating the operating conditions of the system over stage k+1 and assuming the system is at state j. This simulation is in general complicated. The more accurate the simulation procedure is the better the results. Initially, a simple operating cost model is assumed and then replaced with a more sophisticated model. This issue is again addressed later.

The operating cost model used is:

$$J_{operating} = 0.01(MVAr^2) + 110(MVAr) + 12000 \text{ (dollars)} \quad (4.3)$$

Hence,

$$J_{economic}=\alpha_1 J_{investment}+\alpha_2 J_{installation}+\alpha_3 J_{operation} \quad (4.4)$$

The parameters α_1, α_2, α_3 represent the weights. These weights are dimensionless constants and are provided so that all the parameters have equal priority in the objective function. Some parameters are scaled down and some parameters are scaled up using these weights so that we obtain an unbiased solution to the dynamic programming problem.

4.1.2 Performance Penalty Costs

The penalty cost is based on specific performance criteria. The following criteria are proposed, which are illustrated in Figure 4.1.

1. $J_{voltage}$, the cost associated with the voltage deviation of the induction motor buses from the nominal value, at steady state.
2. J_{time}, the cost associated with the time after fault clearance at which the induction motor buses reach 90% of their steady state value.
3. $J_{oscillation}$, the cost associated with the magnitude of oscillations after fault clearance.

These parameters are obtained by simulating the system in WinIGS – Q software.

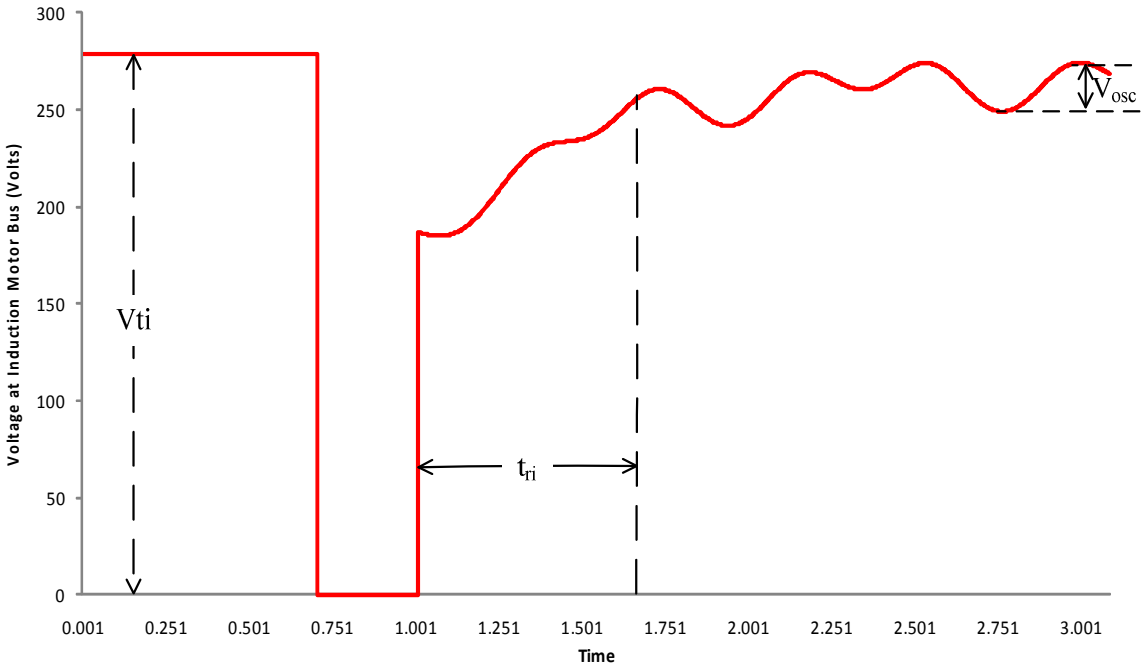

Figure 4.1: Performance Criteria

The penalty function is based on the above technical performance criteria by the following formula that assigns a $ cost to the technical performance of the system:

$$J_{penalty}=f(J_{voltage}, J_{time}, J_{oscillation})$$

The penalty costs are explained as follows.

1. $J_{voltage}$, the cost associated with voltage deviation of the induction motor buses from the nominal value, at steady state.

This cost has been expressed as:

$$J_{voltage} = \sum_{i=0}^{k} \left(\frac{V_{ti} - V_{ni}}{0.05 V_{ni}} \right)^2 \quad (4.5)$$

Where, V_{ti} = actual prefault terminal voltage of the induction motor bus 'i'(Volts)

V_{ni} = prefault rated voltage of the induction motor bus 'i'(Volts)

k = total number of induction motor buses in the system

2. J_{time} is the cost associated with starting the motor if the voltage does not recover to above 95% of its initial value within 500ms after fault clearance. This cost has been represented as a function of (i) Voltage recovery time of the induction motors and (ii) The rating of the induction motors. Further, it has been assumed that if the voltage at these buses stays below 95% of the steady state voltage for a period of 500ms after the fault, the protection system trips these motors. Hence, the cost J_{time} is essentially the cost associated with restarting these motors based on the recovery time and motor ratings.

$$J_{time} = \begin{cases} 0, & if\ t_{ri} < 0.5s \\ \sum_{i=1}^{k} S_i \left(\frac{t_{ri} - 0.5}{0.5} \right)^2, & if\ t_{ri} \geq 0.5s \end{cases} \quad (4.6)$$

Where, t_{ri} = Recovery time of induction motor bus 'i'(seconds) (Figure 4.1)

k = number of induction motor buses

S_i = Rating of induction motor 'i'(kVA)

3. $J_{oscillation}$ is the cost due to oscillations in voltage after fault clearance. Oscillations less than 2% of nominal voltages are ignored, and a cost is applied to oscillation magnitudes above 2% of nominal voltage. This is defined as

$$J_{oscillation} = \begin{cases} 0, & if\ V_{osci} < 0.02V_{ni} \\ \sum_{i=1}^{k} \left(\frac{V_{osci} - 0.02V_{ni}}{0.02V_{ni}}\right)^2, & if\ V_{osci} \geq 0.02V_{ni} \end{cases} \quad (4.7)$$

Where, V_{osci}= oscillation magnitude of induction motor bus 'i'(Volts)

k = number of induction motor buses

V_{ni} = nominal voltage of induction motor 'i'(Volts)

$J_{penalty}$ can now be defined as

$$J_{penalty}=\beta_1 J_{voltage}+\beta_2 J_{time}+\beta_3 J_{oscillation} \quad (4.8)$$

The factors β_1, β_2, β_3 are similar to the weights used in the formulation of $J_{economic}$ in section 3.3.1, used to provide equal priority to all the parameters.

The objective function can now be defined as:

$$\text{Min } J = \alpha_1 J_{investment}+\alpha_2 J_{installation}+\alpha_3 J_{operation}+ \beta_1 J_{voltage}+\beta_2 J_{time}+\beta_3 J_{oscillation} \quad (4.9)$$

The exact constants that translate the performance indices into cost are selected on the basis that force the optimization process to exclude any decisions that violate a threshold of acceptable performance.

4.2 Test System and Calculations

This section provides an overview of the dynamic programming approach used for allocation of reactive sources, both static and dynamic, for an example 13.8kV distribution system.

Figure 4.2 shows the test system used in the computations. This system was built in the software WinIGS – Q and simulations were done for a disturbance in the system. This system consists of two generating stations, rated at 15 kV and 18 kV. The bulk of the system consists of a 13.8kV distribution network. The loads connected are 13.9 kV static loads and 480 V induction motors. A complete description of the ratings of all the equipment in the system is given in Appendix A.

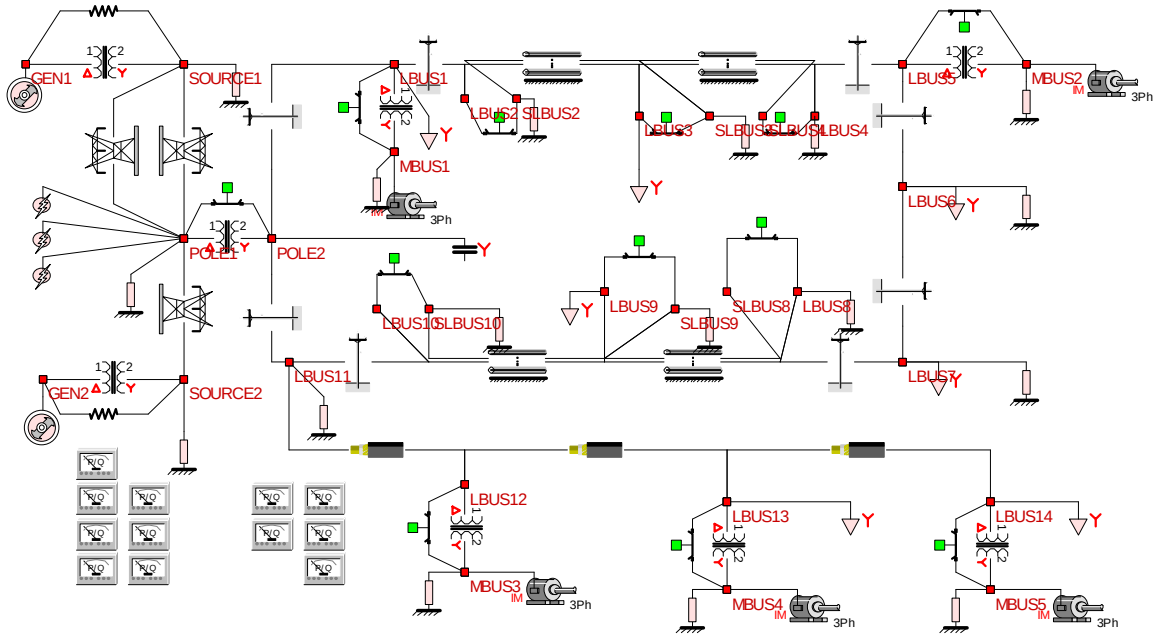

Figure 4.2: Example 13.8 kV distribution system

The various candidate locations for the installation of reactive power were considered to be LBUS1, MBUS2 and MBUS4. At the location LBUS1, the reactive power source is a static source of rating 2MVAr and at the motor buses, MBUS2 and MBUS4, the reactive power sources are dynamic, with a rating of 0.8 MVAr. Table 4.1 shows the various decisions that can be taken over a planning stage.

TABLE 4.3: State Definitions

STATE	**LOCATION**	**CAPACITY (MVAr)**	**TYPE**
1	Base System		
2	LBUS 1	2	Capacitor Bank
3	MBUS 2	0.8	Static VAr Compensator
4	MBUS 4	0.8	Static VAr Compensator
5	LBUS 1	2	Capacitor Bank
	MBUS 2	0.8	Static VAr Compensator
6	MBUS 2	0.8	Static VAr Compensator
	MBUS 4	0.8	Static VAr Compensator
7	LBUS 1	2	Capacitor Bank
	MBUS 4	0.8	Static VAr Compensator

These states have been illustrated as a five stage dynamic programming problem in Figure 4.3.

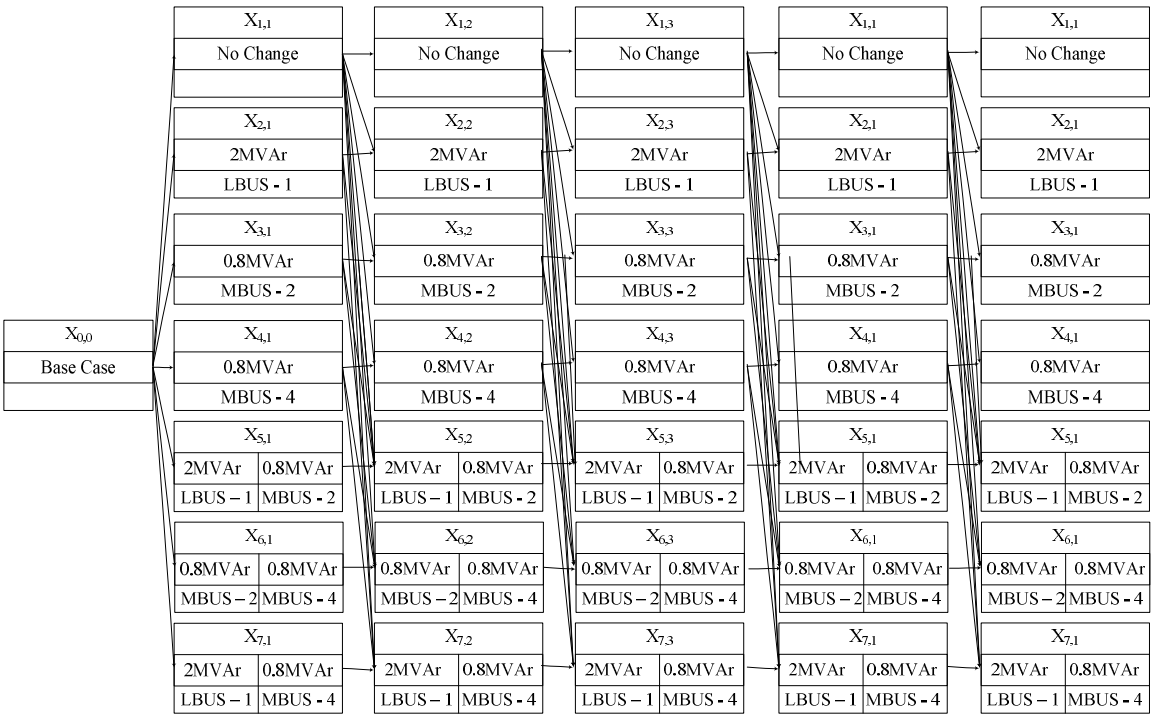

Figure 4.3: Dynamic Programming Formulation

Based on the objective function defined, the following parameters are used as values for the calculations:

$$\text{Min } J = \alpha_1 J_{investment} + \alpha_2 J_{installation} + \alpha_3 J_{operation} + \beta_1 J_{voltage} + \beta_2 J_{time} + \beta_3 J_{oscillation}$$

Where, α_1, α_2, α_3, β_1, β_2, β_3 are constants that have been included to obtain a solution that is not biased towards a particular parameter.

$\alpha_1 = 1/2{,}000$

$\alpha_2 = 1/200$

$\alpha_3 = 1/70{,}000$

$\beta_1 = 1/3$

$\beta_2 = 1/100$

$\beta_3 = 1/200$

$$J_{investment} = \frac{Cx}{\sum_{i=0}^{m} \frac{1}{(1+r)^i}} \text{ (dollars)}$$

Where, C = Cost per kVAr ($6 for capacitor bank, and $15 for synchronous condenser)

x = kVArs installed

m = 14 years (considering amortization over the lifetime of the equipment)

r = 7%

$$J_{operating} = 0.01(MVAr^2) + 110(MVAr) + 12000 \text{ (dollars)}$$

$$J_{installation} = \$4.4 \text{ per kVAr}$$

$$J_{voltage} = \sum_{i=0}^{k} \left(\frac{V_{ti} - V_{ni}}{0.05 V_{ni}} \right)^2$$

Where, $V_{ni} = 480/\sqrt{3}V$ for all buses

$$J_{time} = \begin{cases} 0, & if\ t_{ri} < 0.5s \\ \sum_{i=1}^{k} S_i \left(\frac{t_{ri} - 0.5}{0.5} \right)^2, & if\ t_{ri} \geq 0.5s \end{cases}$$

Where, S_i = rating of each induction motor as follows:

$S_1 = 0.5$ MVA

$S_2 = 1$ MVA

S_3 = 0.5 MVA

S_4 = 1 MVA

S_5 = 0.8 MVA

This MVA rating has been assumed to change after 3 stages to model a realistic system

$$I_{oscillation} = \begin{cases} 0, & if\ V_{osci} < 0.02V_{ni} \\ \sum_{i=1}^{k} \left(\frac{V_{osci} - 0.02V_{ni}}{0.02V_{ni}} \right)^2, & if\ V_{osci} \geq 0.02V_{ni} \end{cases}$$

Figure 4.4 shows the values of steady state voltage, recovery time and oscillation magnitudes for State – 1 of the system. These values are obtained after simulating the three phase fault at the high side of the 115kV/13.8kV transformer as shown in Figure 4.2.

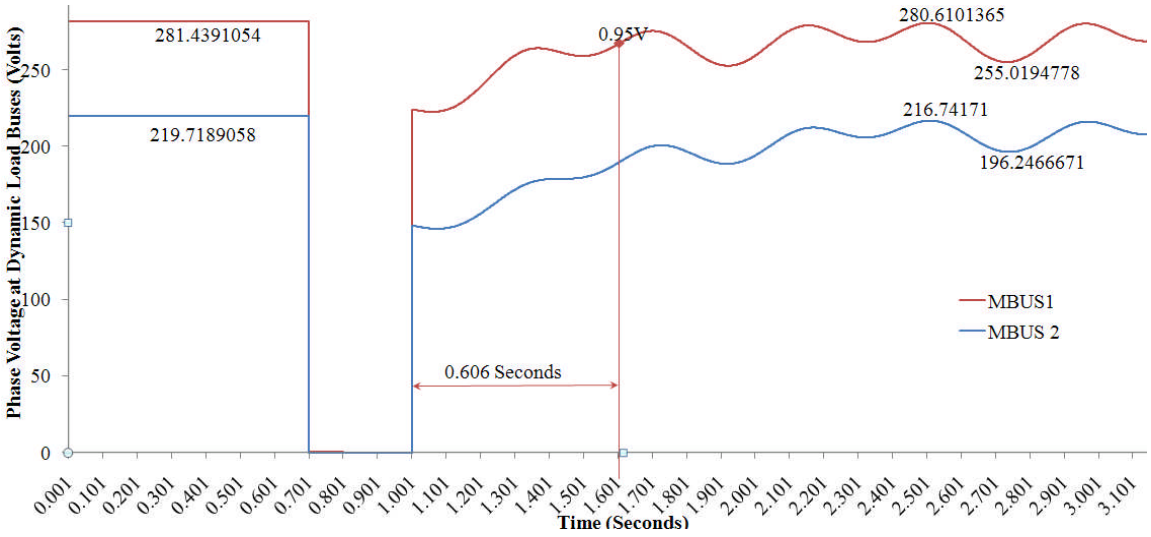

Figure 4.4: Parameters for State - 1

For clarity, only MBUS -1 and MBUS – 2 voltages are shown in the diagram. The procedure remains the same for all the dynamic load buses and all the states. Using these values, the performance parameters can be calculated as follows:

$$J_{voltage} = \left(\frac{281.4391-(480/\sqrt{3})}{0.05\times(480/\sqrt{3})}\right)^2 + \left(\frac{219.7189-(480/\sqrt{3})}{0.05\times(480/\sqrt{3})}\right)^2 + \left(\frac{261.788-(480/\sqrt{3})}{0.05\times(480/\sqrt{3})}\right)^2 + \left(\frac{263.62-(480/\sqrt{3})}{0.05\times(480/\sqrt{3})}\right)^2 + \left(\frac{268.184-(480/\sqrt{3})}{0.05\times(480/\sqrt{3})}\right)^2 = 23.9069$$

$$J_{time} = 500\left(\frac{0.606-0.5}{0.5}\right)^2 + 1000\left(\frac{1.919-0.5}{0.5}\right)^2 + 500\left(\frac{0.711-0.5}{0.5}\right)^2 + 1000\left(\frac{1.099-0.5}{0.5}\right)^2 + 800\left(\frac{1.096-0.5}{0.5}\right)^2 = 10754.3812$$

$$J_{oscillations} = \left(\frac{(280.6101-265.0195)-(0.02)\times(480/\sqrt{3})}{0.02\times(480/\sqrt{3})}\right)^2 + \left(\frac{(216.7417-196.2466)-(0.02)\times(480/\sqrt{3})}{0.02\times(480/\sqrt{3})}\right)^2 + \left(\frac{16.9-(0.02)\times(480/\sqrt{3})}{0.02\times(480/\sqrt{3})}\right)^2 + \left(\frac{16.9-(0.02)\times(480/\sqrt{3})}{0.02\times(480/\sqrt{3})}\right)^2 + \left(\frac{17.7-(0.02)\times(480/\sqrt{3})}{0.02\times(480/\sqrt{3})}\right)^2 = 39.19988$$

Figure 4.5 shows the various values for calculation of the performance parameters as obtained from the simulation of State – 5. For clarity in the diagram, only MBUS – 1 voltage is shows in the figure. The parameters for all the other buses can be obtained using the same procedure.

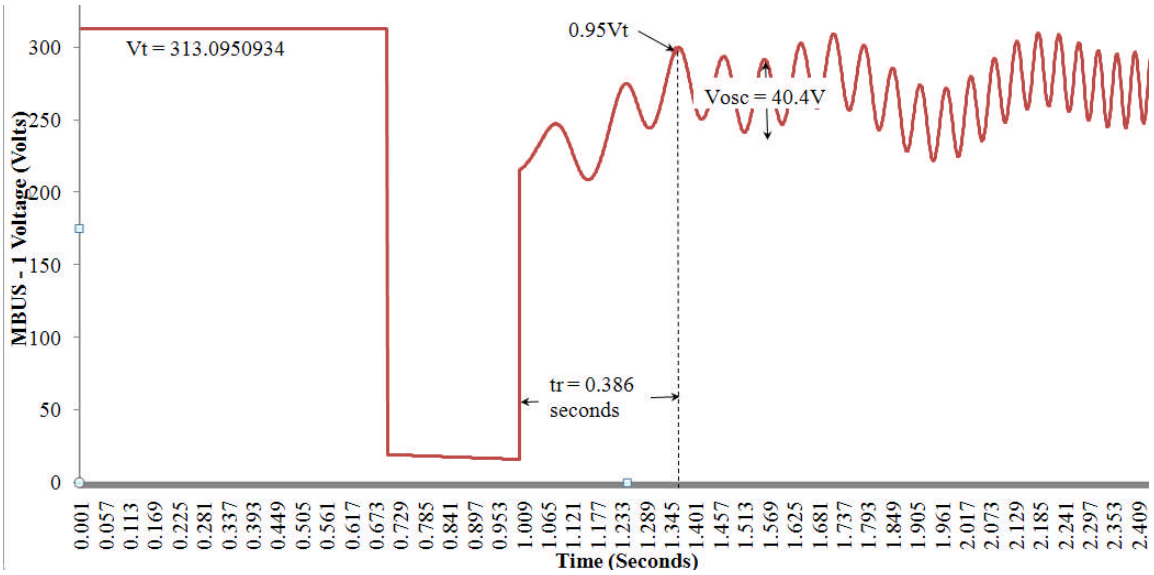

Figure 4.5: Parameters for State – 3

$J_{voltage}$ =

$$\left(\frac{313.095-(480/\sqrt{3})}{0.05\times(480/\sqrt{3})}\right)^2+\left(\frac{269.1928-(480/\sqrt{3})}{0.05\times(480/\sqrt{3})}\right)^2+\left(\frac{2283.1746-(480/\sqrt{3})}{0.05\times(480/\sqrt{3})}\right)^2+\left(\frac{277.7841-(480/\sqrt{3})}{0.05\times(480/\sqrt{3})}\right)^2+\left(\frac{278.2522-(480/\sqrt{3})}{0.05\times(480/\sqrt{3})}\right)^2=7.2643$$

J_{time} =

$$500(0)+1000\left(\frac{0.733-0.5}{0.5}\right)^2+500\left(\frac{0.657-0.5}{0.5}\right)^2+1000\left(\frac{0.682-0.5}{0.5}\right)^2+800\left(\frac{0.682-0.5}{0.5}\right)^2=504.9468$$

$J_{oscillations}$=

$$\left(\frac{40.4-(0.02)\times(480/\sqrt{3})}{0.02\times(480/\sqrt{3})}\right)^2+\left(\frac{187.39-(0.02)\times(480/\sqrt{3})}{0.02\times(480/\sqrt{3})}\right)^2+\left(\frac{32.6-(0.02)\times(480/\sqrt{3})}{0.02\times(480/\sqrt{3})}\right)^2+\left(\frac{30.4-(0.02)\times(480/\sqrt{3})}{0.02\times(480/\sqrt{3})}\right)^2+\left(\frac{30.9-(0.02)\times(480/\sqrt{3})}{0.02\times(480/\sqrt{3})}\right)^2=1180.8766$$

These calculations are carried out for all the buses at all states. Table 4.2 shows the final objective function value, J, for each of the states for transition from Stage 0 to Stage 1.

TABLE 4.2: Objective function computations for transition from Stage- 0 to Stage - 1

FROM	TO	$J_{voltage}$	J_{time}	$J_{oscillation}$	$J_{installation}$	$J_{operation}$	$J_{investment}$	J
0,1	1,1	23.90694152	10754.381	39.19987859	0	0	0	115.7087919
0,1	1,2	13.12190752	1623.3352	121.0434574	800	272000	1231.3375	29.71392151
0,1	1,3	4.642454403	121370.11	1167.327973	480	106400	1231.3375	1225.620865
0,1	1,4	15.47284317	244323.58	1133.559462	480	106400	1231.3375	2458.596892
0,1	1,5	7.264347085	504.9468	1180.876569	1280	398400	2462.6751	26.69806598
0,1	1,6	3.342007229	399366.98	2125.353715	960	213600	2462.6751	4014.493317
0,1	1,7	12.5833973	244241.22	581.4236079	1280	398400	2462.6751	2462.83655

Figure 4.6 shows the various transitions from the base system to the states in Stage 1. It is assumed that the cost of the base system is 0. Each of the states is described in 3 parts. The first part gives the stage number and state number. The second part gives the cost of the state over the entire stage, $C(X_{i,k})$. The third part represents the optimal path of the planning period at the state and stage, $C^*(X_{i,k})$. Let p_i be the state in the previous stage ‘k-1’ that leads to the optimal path in the current state ‘i’ and stage ‘k’.

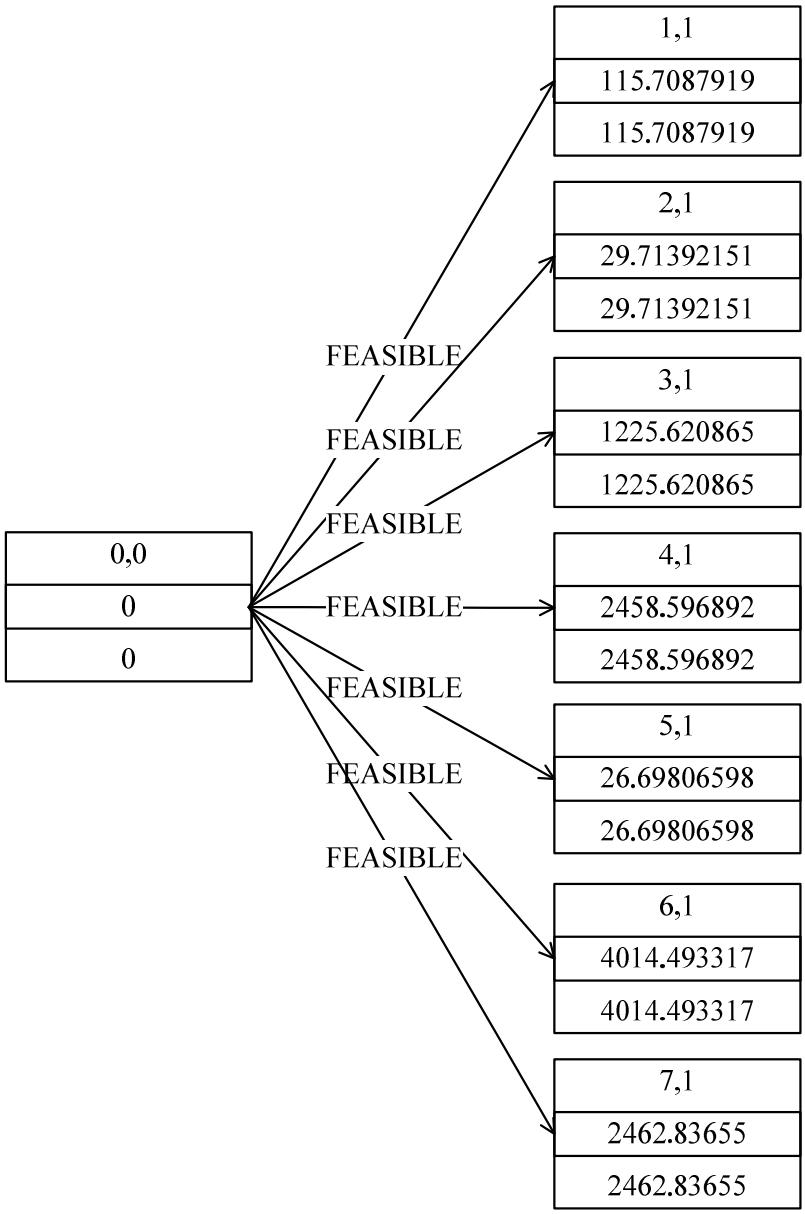

Figure 4.6: Transitions from base case to Stage 1.

Hence, for Stage 1,

$C(X_{1,1}) = 115.7087919$ $C^*(X_{1,1}) = 115.7087919$ $p_1 = 0,0$

$C(X_{2,1}) = 29.71392151$ $C^*(X_{2,1}) = 29.71392151$ $p_2 = 0,0$

$C(X_{3,1}) = 1225.620865$ $C^*(X_{3,1}) = 1225.620865$ $p_3 = 0,0$

$C(X_{4,1}) = 2458.596892$ $C^*(X_{4,1}) = 2458.596892$ $p_4 = 0,0$

$C(X_{5,1}) = 26.69806598$ $C^*(X_{5,1}) = 26.69806598$ $p_5 = 0,0$

$C(X_{6,1}) = 4014.493317$ $C^*(X_{6,1}) = 4014.493317$ $p_6 = 0,0$

$C(X_{7,1}) = 2462.83655$ $C^*(X_{7,1}) = 2462.83655$ $p_7 = 0,0$

Similar computations can be carried out for Stages 2 to 5. These calculations are shown in Appendix B. After the values of $C(X_{i,k})$ and $C^*(X_{i,k})$ are found for all the states and stages, the optimal planning decision sequence can be obtained by backtracking. This is shown in Figure 4.7.

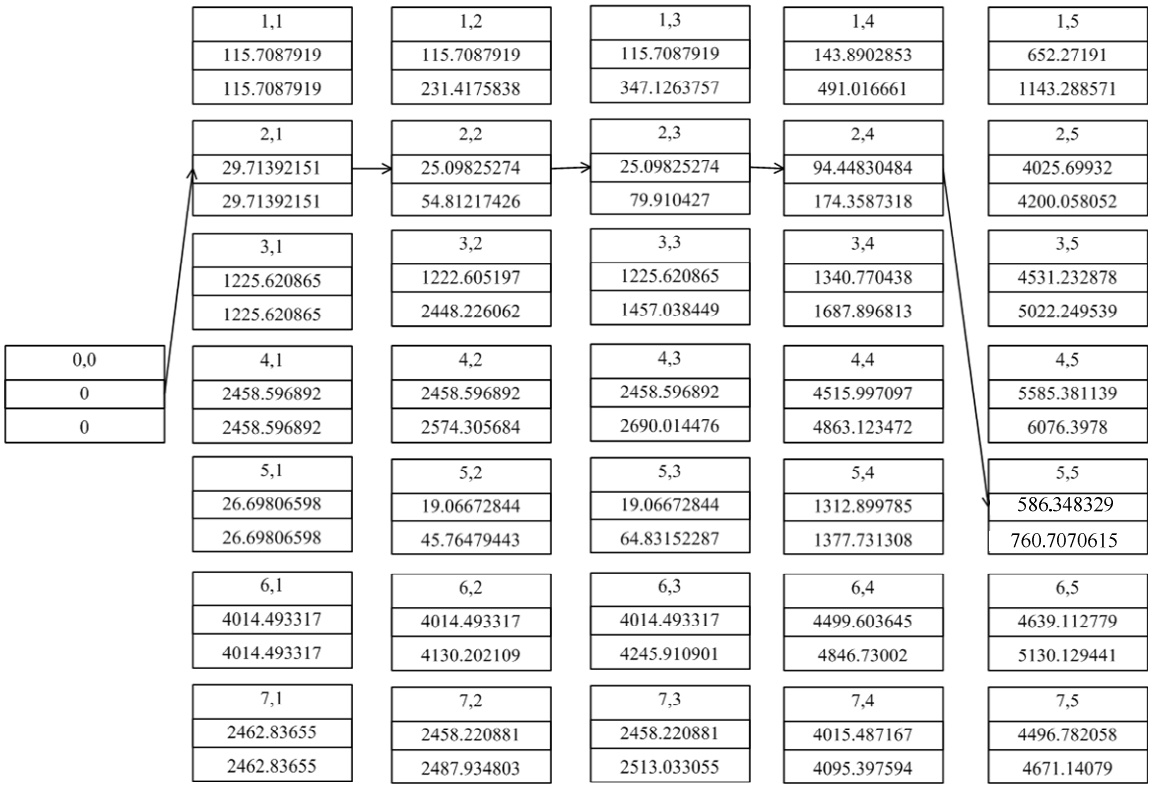

Figure 4.7: Optimal Planning Sequence

4.3 Summary

This chapter covered an example that showed how the dynamic programming algorithm can be used to perform reactive power planning for a test distribution network. The network is simulated on a custom software, WinIGS – Q. The parameters of the system are given in Appendix A. The results obtained show a mix of static and dynamic reactive power sources that have to be installed for optimal operation. Details of simulation data and in-depth calculations are covered in Appendix B. The next chapter provides conclusions and future work that can be carried out in this field.

CHAPTER 5

CONCLUSIONS AND FUTURE WORK

The work performed in this thesis focused on post fault voltage stability in power systems. A method to apply dynamic programming algorithm for reactive power planning was devised. This took into account both static and dynamic voltage stability. The steady state voltages were monitored to ensure that they stayed within nominal limits. The focus was on recovery time and oscillations during the post fault period.

The recovery time after a major contingency plays an important role in ensuring reliability from the loads. The protective mechanism for many dynamic loads do not allow stalling and hence cease supply to the loads during periods of prolonged undervoltage. Supplying reactive power, particularly during the post fault period ensured shorter recovery time for all the motors in the system, ensuring continued service.

Preliminary results were obtained from the IEEE 24-Substation system, which are outlined in Appendix C. The multiobjective optimization problem can be further refined to include more parameters and constraints so as to obtain a practical solution for larger distribution networks.

APPENDIX A:

DESCRIPTION OF TEST SYSTEM

FIGURE A.1 shows the 13.8kV test distribution system.

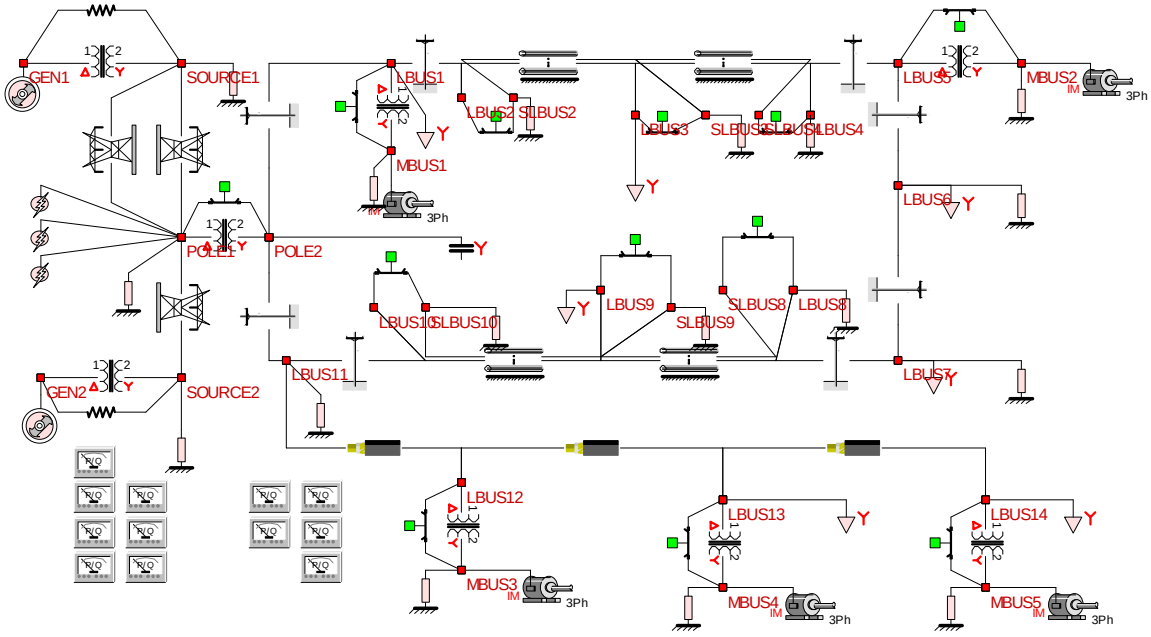

FIGURE A.1: Test 13.8kV System

The ratings of each of the units are given from FIGURE A.2 to FIGURE A.11.

It was found that a three phase fault at the high voltage side of the step down 115/13.8kV transformer yielded the most deviations from steady state conditions. Hence, this type of fault was considered for computations. The fault clearing time is considered to be 300ms.

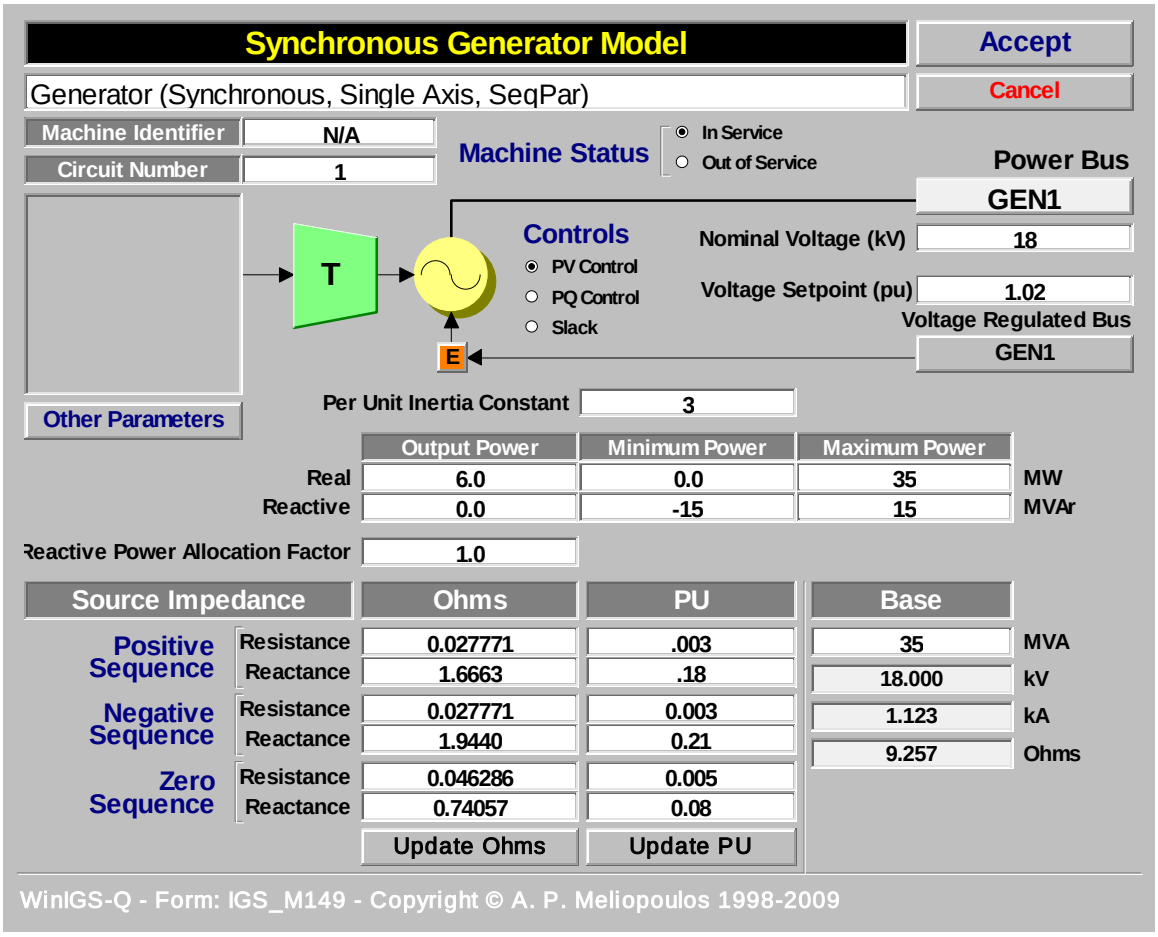

FIGURE A.2: Parameters of 18kV Generator

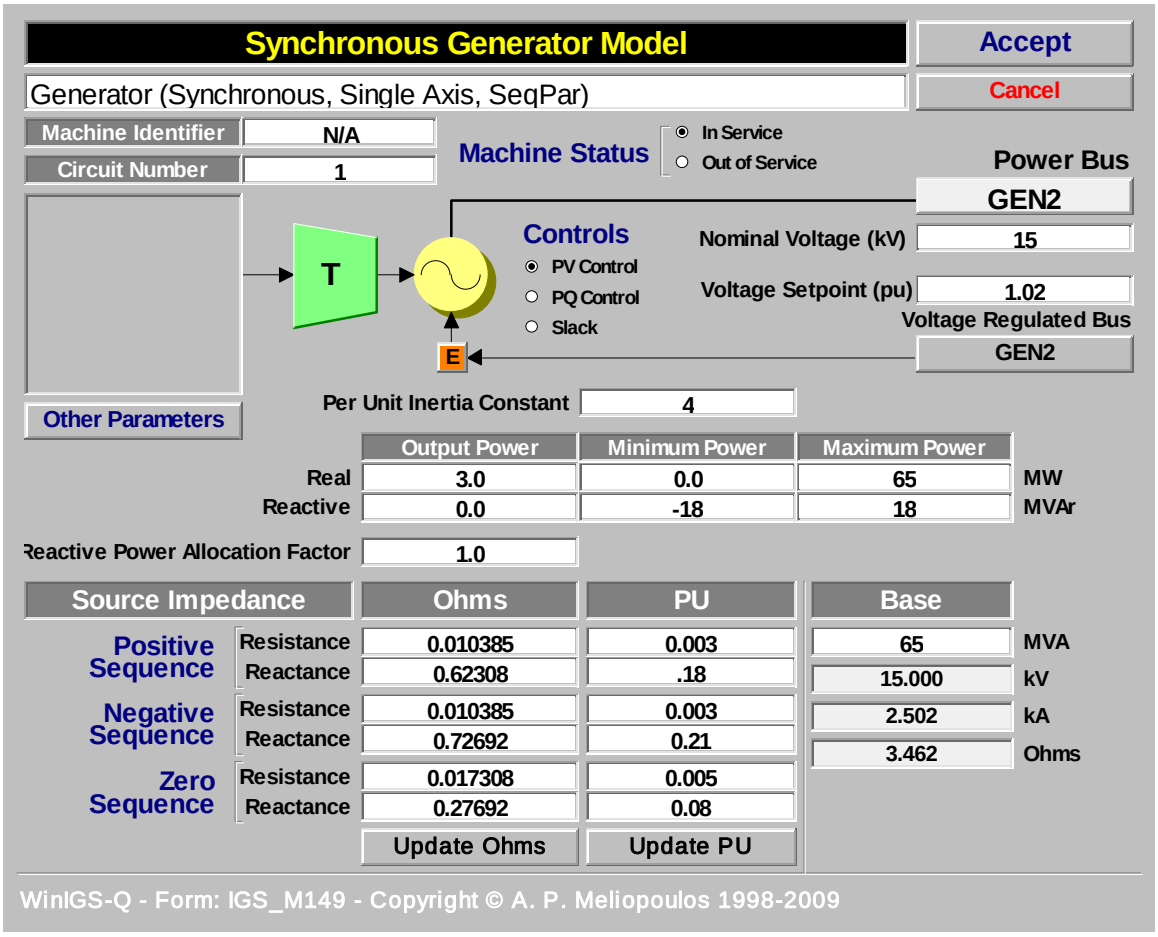

FIGURE A.3: Parameters of 15kV Generator

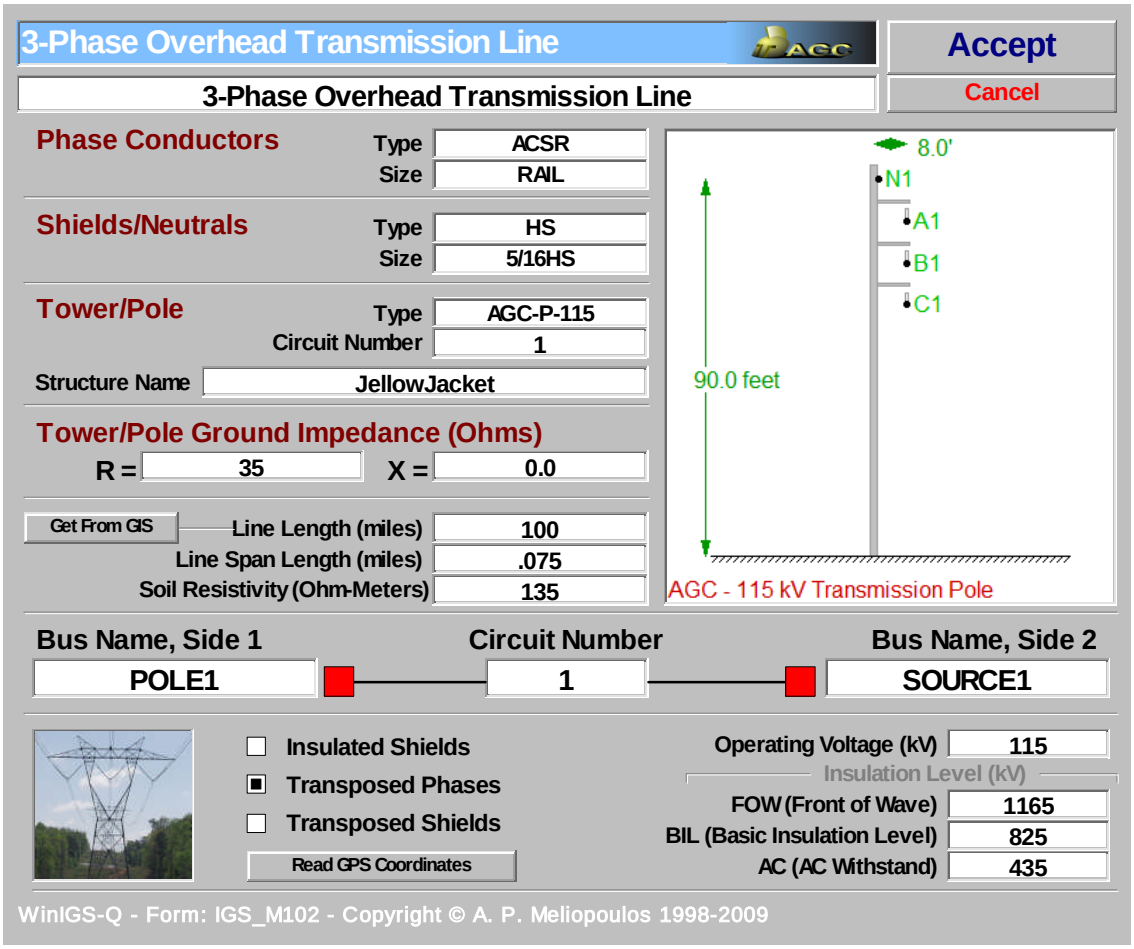

FIGURE A.4: Parameters of 115kV Overhead Transmission line

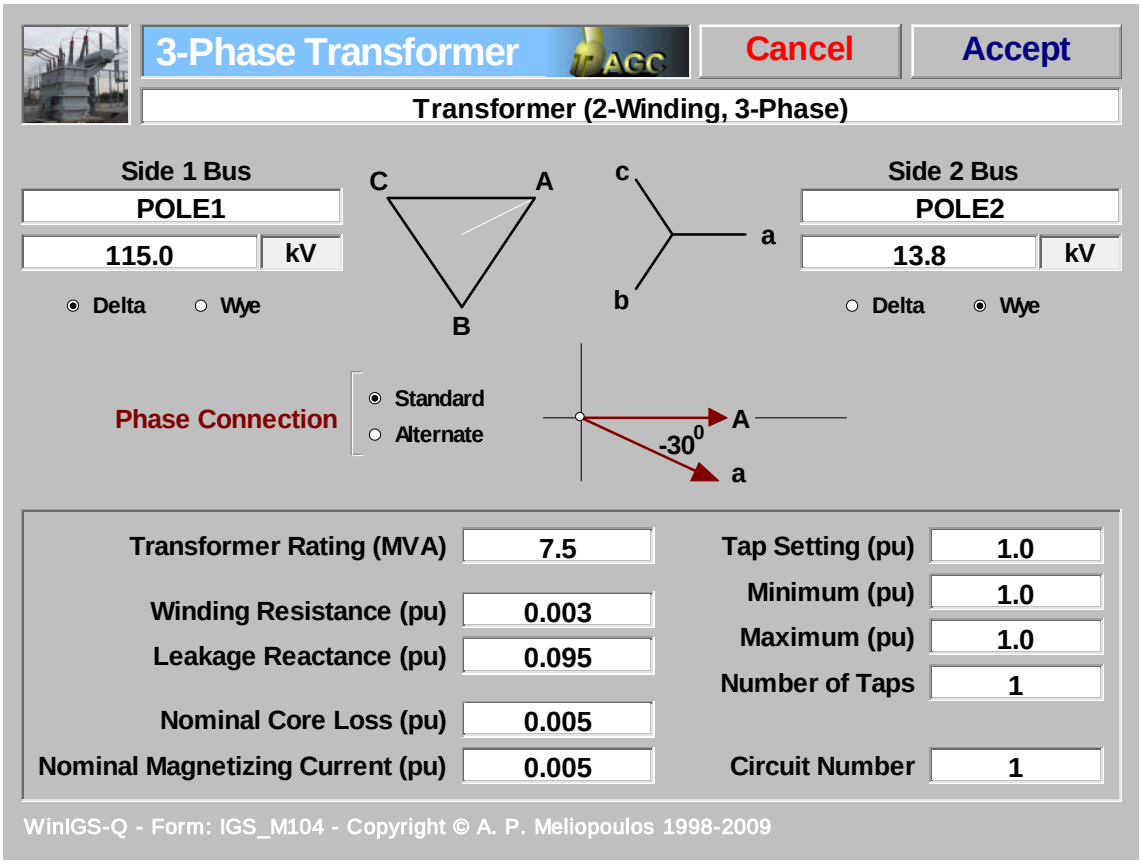

FIGURE A.5: Parameters of Step Down Transformer

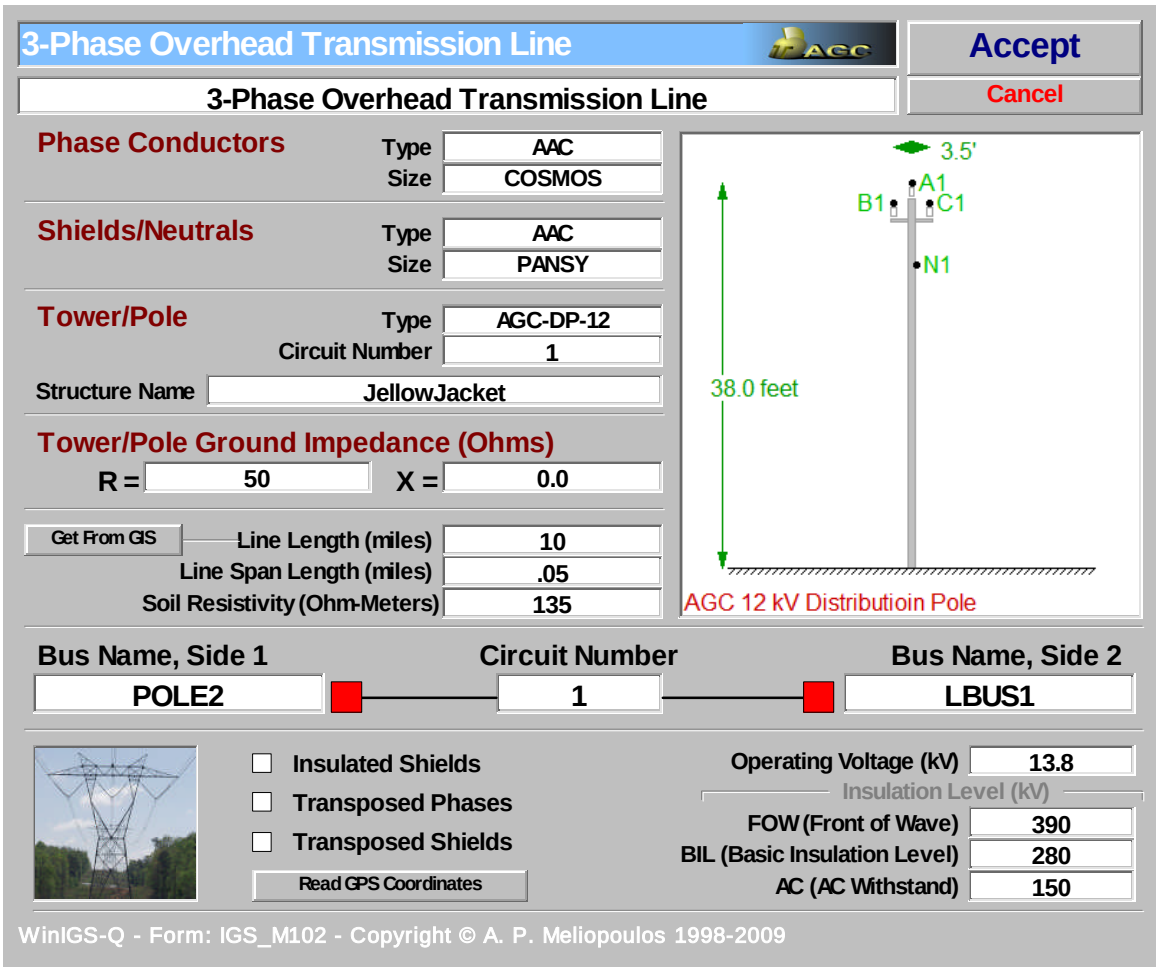

FIGURE A.6: Parameters of 13.8kV Distribution Line

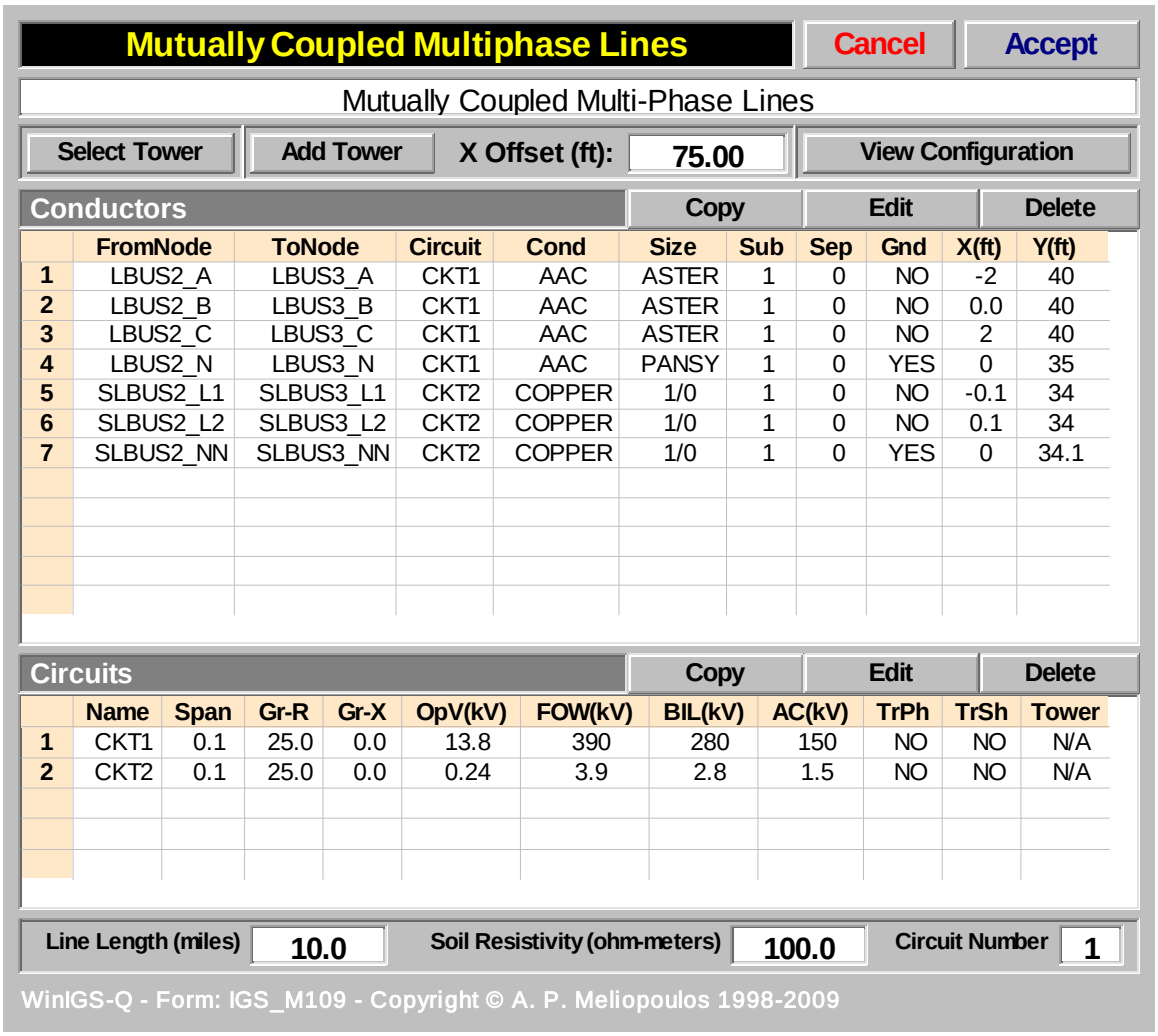

Mutually Coupled Multiphase Lines | Cancel | Accept

Mutually Coupled Multi-Phase Lines

Select Tower | Add Tower | X Offset (ft): 75.00 | View Configuration

Conductors | Copy | Edit | Delete

	FromNode	ToNode	Circuit	Cond	Size	Sub	Sep	Gnd	X(ft)	Y(ft)
1	LBUS2_A	LBUS3_A	CKT1	AAC	ASTER	1	0	NO	-2	40
2	LBUS2_B	LBUS3_B	CKT1	AAC	ASTER	1	0	NO	0.0	40
3	LBUS2_C	LBUS3_C	CKT1	AAC	ASTER	1	0	NO	2	40
4	LBUS2_N	LBUS3_N	CKT1	AAC	PANSY	1	0	YES	0	35
5	SLBUS2_L1	SLBUS3_L1	CKT2	COPPER	1/0	1	0	NO	-0.1	34
6	SLBUS2_L2	SLBUS3_L2	CKT2	COPPER	1/0	1	0	NO	0.1	34
7	SLBUS2_NN	SLBUS3_NN	CKT2	COPPER	1/0	1	0	YES	0	34.1

Circuits | Copy | Edit | Delete

	Name	Span	Gr-R	Gr-X	OpV(kV)	FOW(kV)	BIL(kV)	AC(kV)	TrPh	TrSh	Tower
1	CKT1	0.1	25.0	0.0	13.8	390	280	150	NO	NO	N/A
2	CKT2	0.1	25.0	0.0	0.24	3.9	2.8	1.5	NO	NO	N/A

Line Length (miles): 10.0 | Soil Resistivity (ohm-meters): 100.0 | Circuit Number: 1

WinIGS-Q - Form: IGS_M109 - Copyright © A. P. Meliopoulos 1998-2009

FIGURE A.7: Parameters of 13.8kV Multiphase Line

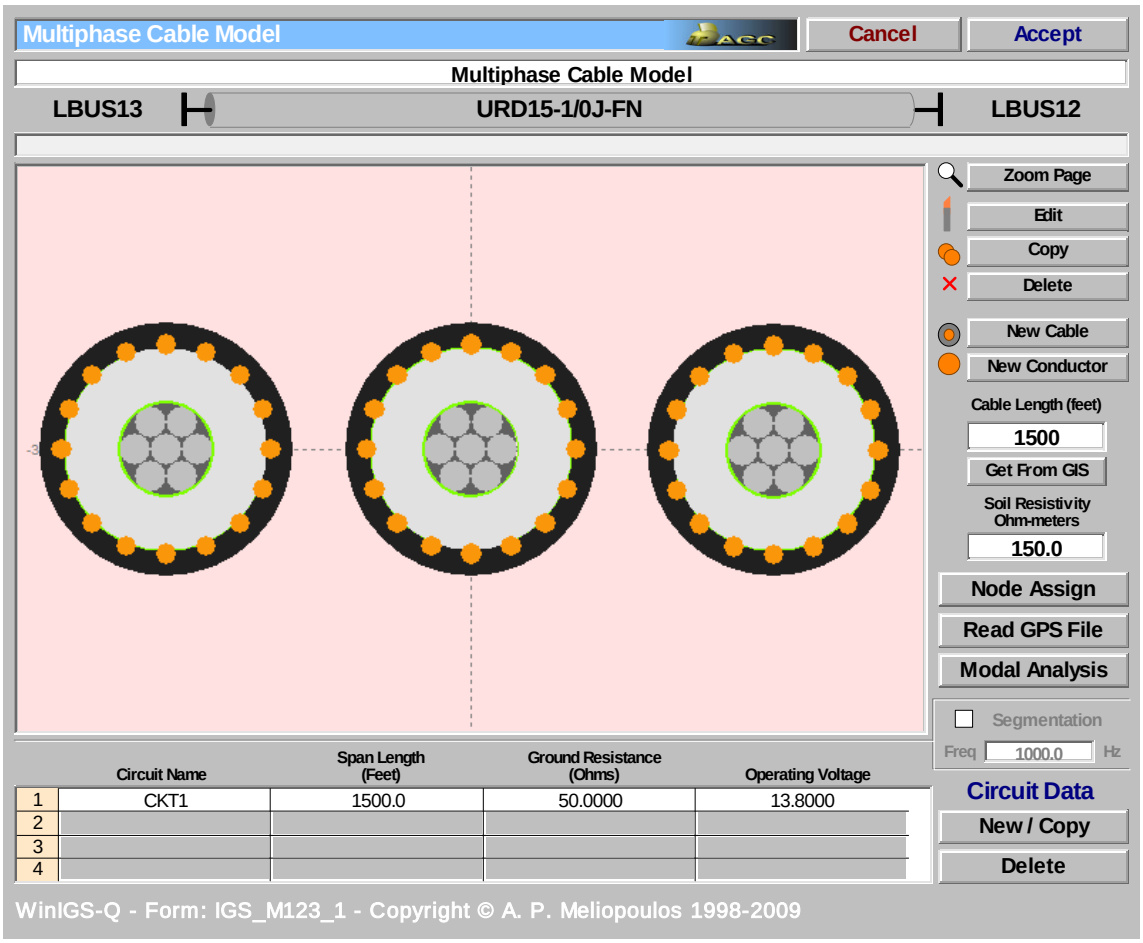

FIGURE A.8: Parameters of Multiphase Underground Cable

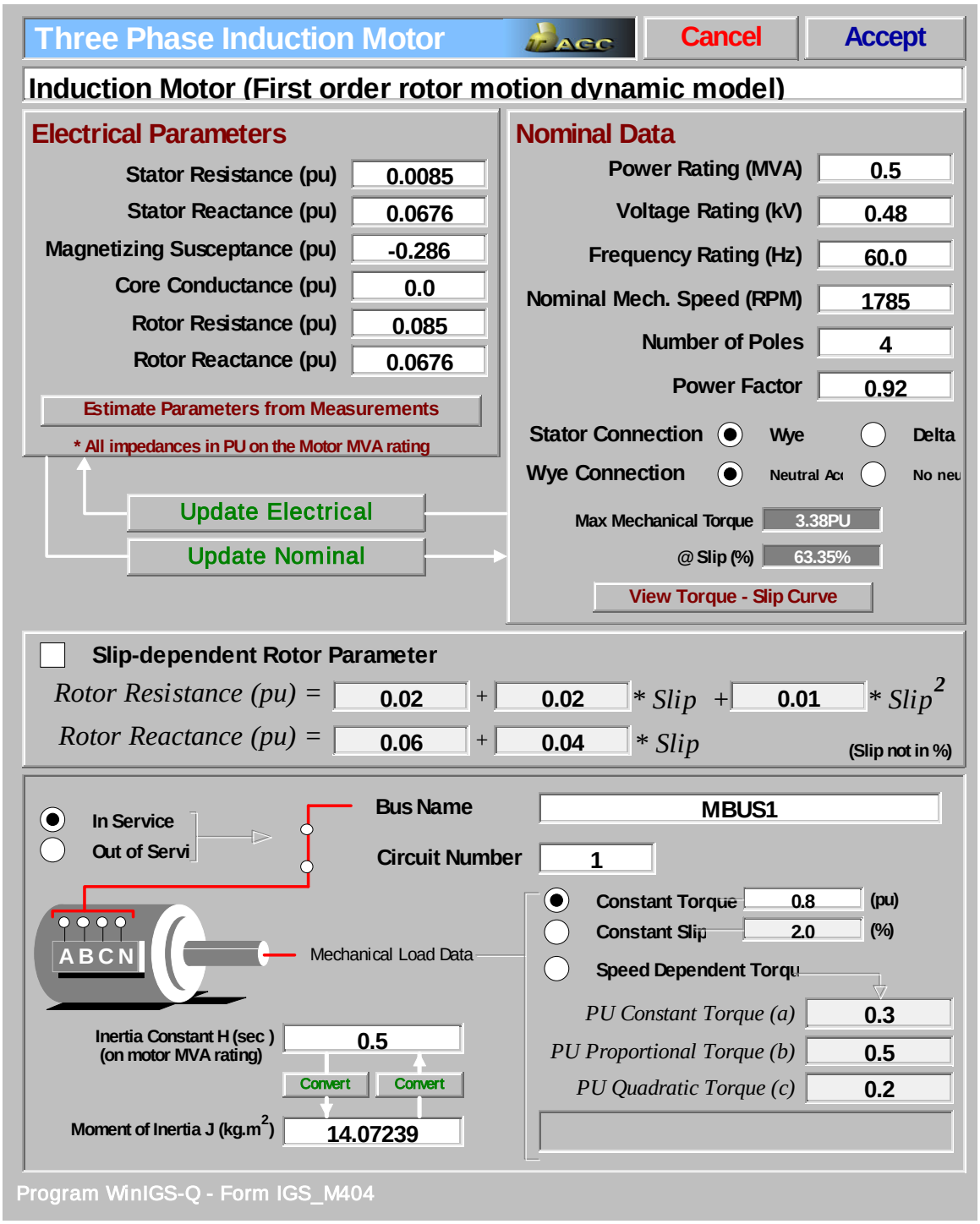

FIGURE A.9: Parameters of Induction Motor Load

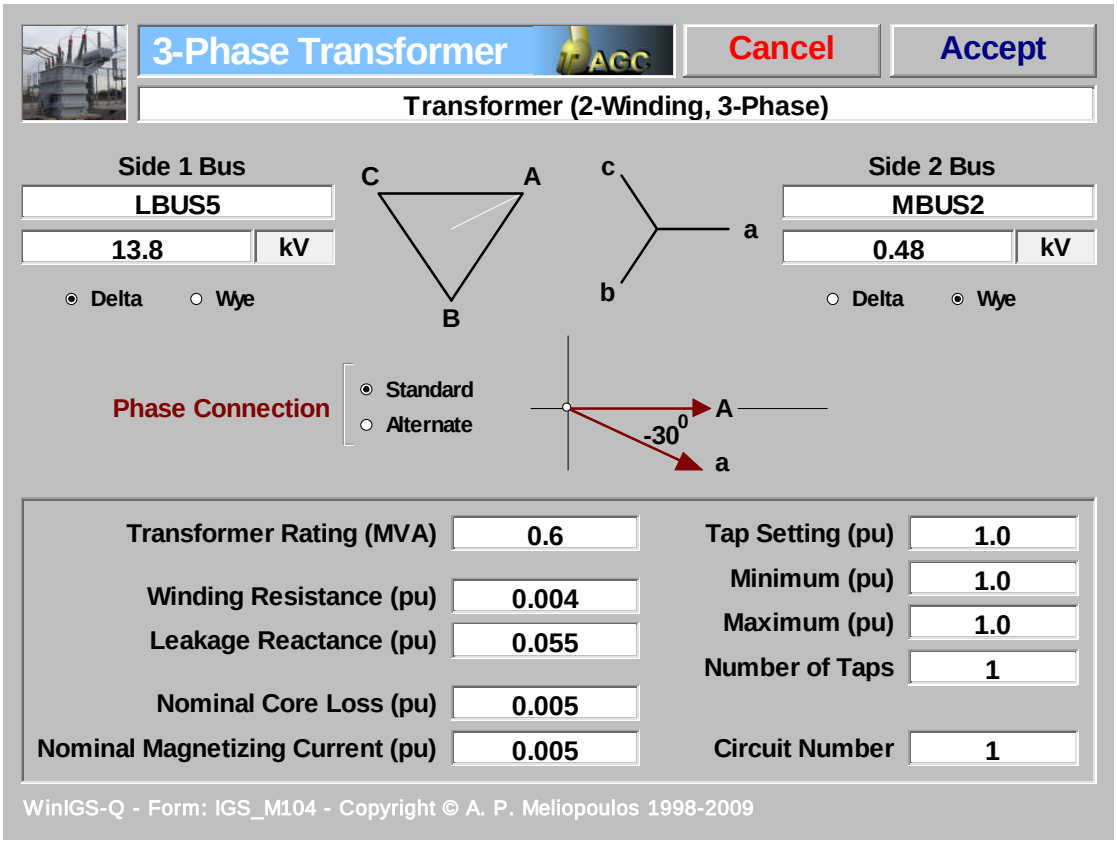

FIGURE A.10: Parameters of Step Down Transformer for Induction Motor Load

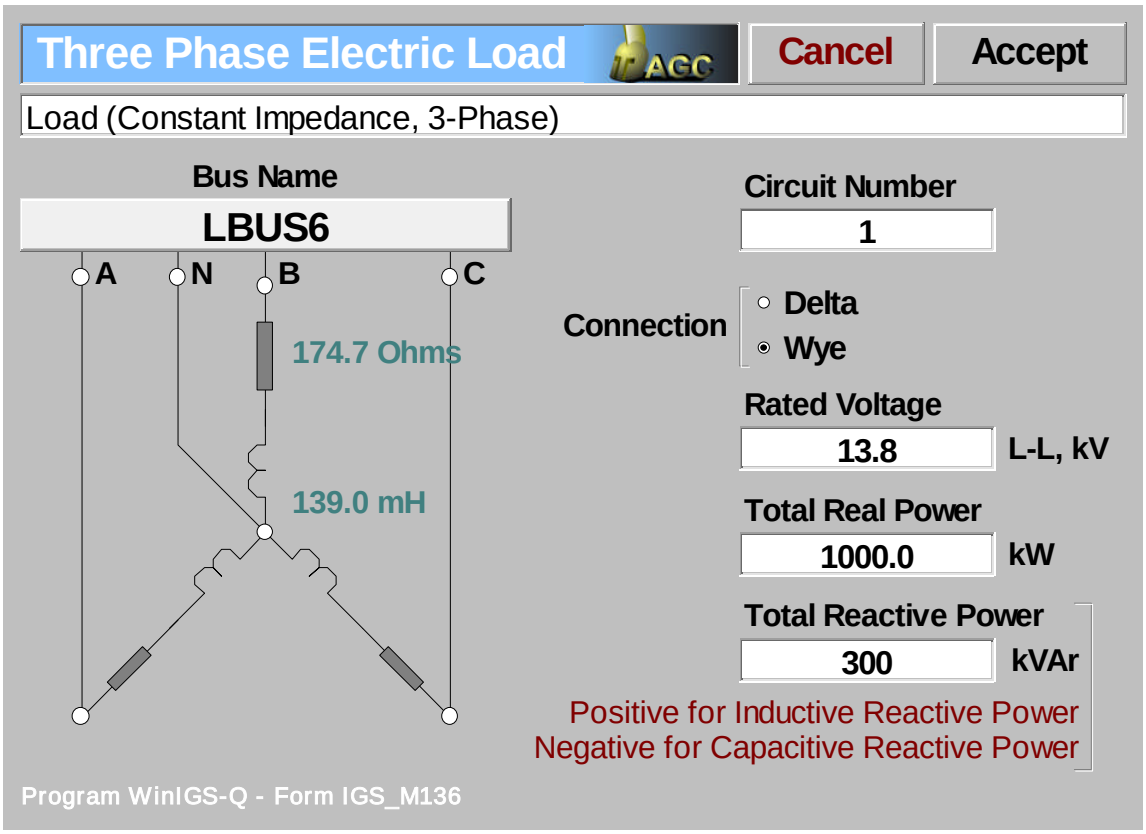

FIGURE A.11: Parameters of 13.8kV Static Load

APPENDIX B:

COMPUTATION OF RESULTS FOR THE TEST SYSTEM

B.1 Introduction

The test system is considered as shown in FIGURE B.1. The ratings of the equipment and transmission lines are given in Appendix A.

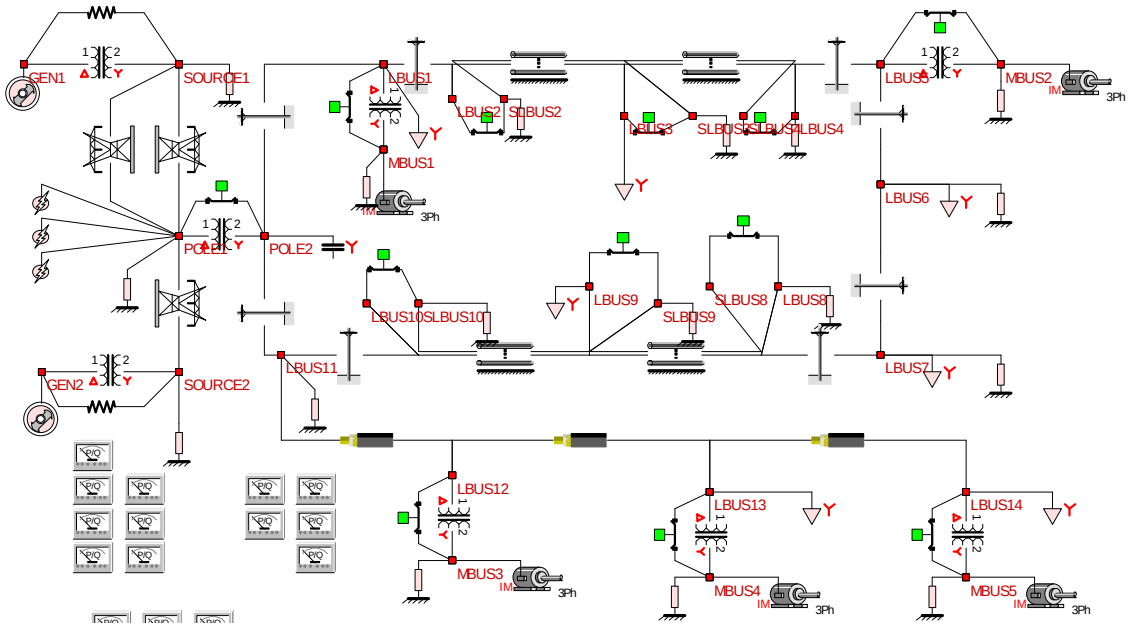

FIGURE B.1: Test System used for computations

A three phase fault was considered at the high voltage side of the substation transformer. This type of fault at this location was determined to cause the most severe effect on the induction motors. The reactive power compensation was done in three stages. The candidate locations for reactive power allocation were considered to be (i) LBUS – 1 (ii) MBUS – 2 and (iii) MBUS – 4. For each of the options, the amount of reactive power allocated at each location was considered to be 2MVAr (for a static source) and 0.8MVAr (for a dynamic source). Table B.1 shows the different options

considered for reactive power allocation. The transitions between these states are considered over a period of 3 planning stages. Each stage is separated by a period of six months. It has also been assumed that once a reactive power source has been installed it cannot be removed.

TABLE B.4: State Definitions

STATE	LOCATION	CAPACITY (MVAr)	TYPE
1	Base System		
2	LBUS - 1	2	Capacitor Bank
3	MBUS - 2	0.8	Static VAr Compensator
4	MBUS - 4	0.8	Static VAr Compensator
5	LBUS - 1	2	Capacitor Bank
	MBUS - 2	0.8	Static VAr Compensator
6	MBUS - 2	0.8	Static VAr Compensator
	MBUS - 4	0.8	Static VAr Compensator
7	LBUS - 1	2	Capacitor Bank
	MBUS - 4	0.8	Static VAr Compensator

The objective function which was defined in Chapter 3 is,

$$\text{Min } J = \alpha_1 J_{investment} + \alpha_2 J_{installation} + \alpha_3 J_{operation} + \beta_1 J_{voltage} + \beta_2 J_{time} + \beta_3 J_{oscillation}$$

Where, α_1, α_2, α_3, β_1, β_2, β_3 are constants that have been included to obtain a solution that is not biased towards a particular parameter.

$\alpha_1 = 1/2{,}000$

$\alpha_2 = 1/200$

α_3 = 1/70,000

β_1 = 1/3

β_2 = 1/100

β_3 = 1/200

$$J_{investment} = \frac{Cx}{\sum_{i=0}^{m} \frac{1}{(1+r)^i}} \text{ (dollars)}$$

Where, C = Cost per kVAr ($6 for Capacitor Bank, and $15 for Synchronous Condenser)

x = kVArs installed

m = 14 years

r = 7%

$J_{operating}$ = 0.01(MVAr^2) + 110(MVAr) + 12000 (dollars)

$J_{installation}$ = $4.4 per kVAr

$$J_{voltage} = \sum_{i=0}^{k} \left(\frac{V_{ti} - V_{ni}}{0.05 V_{ni}} \right)^2$$

Where, V_{ni} = 480V for all buses

$$J_{time} = \begin{cases} 0, & if\ t_{ri} < 0.5s \\ \sum_{i=1}^{k} S_i \left(\frac{t_{ri} - 0.5}{0.5} \right)^2, & if\ t_{ri} \geq 0.5s \end{cases}$$

Where S_i = rating of each induction motor as follows:

S_1 = 0.5MVA

S_2 = 1MVA

S_3 = 0.5MVA

S_4 = 1MVA

S_5 = 0.8MVA

$$I_{oscillation} = \begin{cases} 0, & if\ V_{osci} < 0.02V_{ni} \\ \sum_{i=1}^{k} \left(\frac{V_{osci} - 0.02V_{ni}}{0.02V_{ni}} \right)^2, & if\ V_{osci} \geq 0.02V_{ni} \end{cases}$$

The values of V_{osci}, t_{ri} and V_{ti} are obtained from the simulations as shown in Figure C.2.

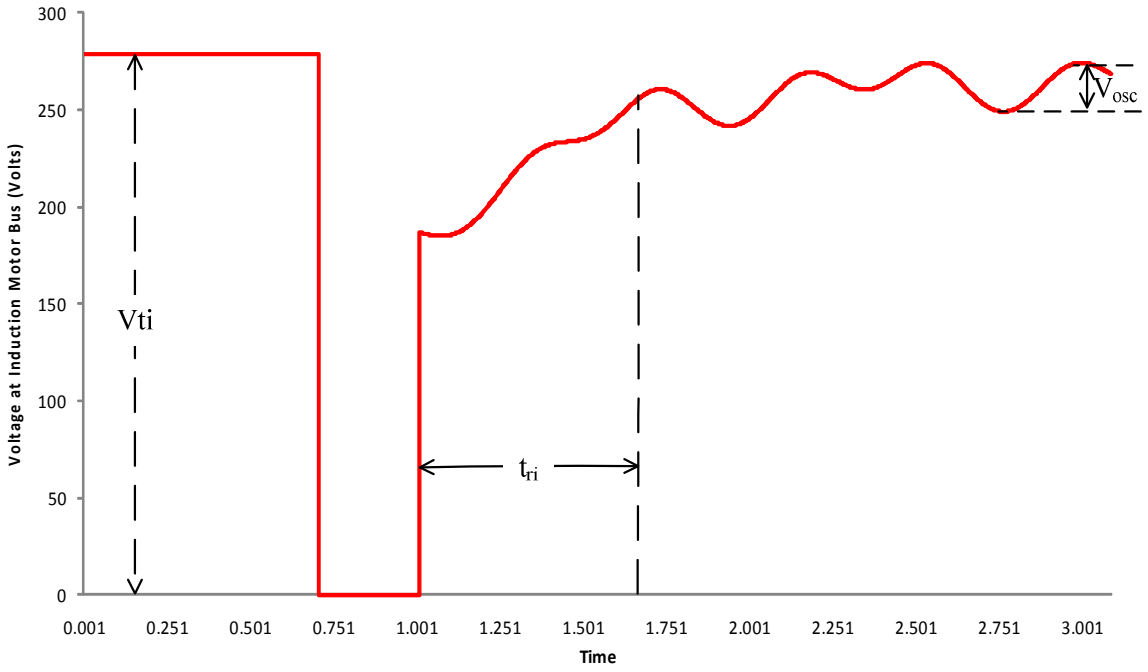

FIGURE B.2: Simulation parameters

B.2 Simulation Data

Table B.2 shows the simulation data for all the induction motor buses for States 1 to 7 as defined in Table B.1. An example describing the simulation parameters and the calculation of the three performance penalties is given in Section 3.

TABLE B.2: Simulation data for States 1 to 7

Motor Bus Number	Nominal Voltage, V_n (Volts)	Actual Value, V_t (Volts)	Deviation from Nominal Value (Volts)	95% of Steady State Value (Volts)	Time taken to reach 95% of Steady State Value, t_r (Seconds)	Oscillation Magnitude, V_{osc} (Volts)
STATE – 1						
MBUS1	277.128	281.439	-4.310870789	267.36705	0.640	26.501
MBUS 2	277.128	219.719	57.40912921	208.73305	1.919	24.495
MBUS 3	277.128	261.738	15.39007924	248.651147	0.711	16.900
MBUS 4	277.128	253.520	23.60844573	240.843699	1.099	16.900
MBUS 5	277.128	255.184	21.94374171	242.425168	1.096	17.700
STATE – 2						
MBUS-1	277.128	306.12332	173.87668	290.81715	0.606	35.9
MBUS-2	277.128	236.98836	243.01164	225.13894	1.102	29.6
MBUS-3	277.128	276.51139	203.48861	262.68582	0.622	33
MBUS-4	277.128	271.09781	208.90219	257.54292	0.629	32.6
MBUS-5	277.128	271.58384	208.41616	258.00464	0.631	32.6
STATE – 3						
MBUS-1	277.128	288.49418	191.50582	274.06947	0.631	39.3
MBUS-2	277.128	254.08335	225.91665	241.37918	6	184.21
MBUS-3	277.128	272.15988	207.84012	258.55188	0.665	41.4
MBUS-4	277.128	266.72214	213.27786	253.38603	0.699	31.4
MBUS-5	277.128	267.22185	212.77815	253.86076	0.696	34.6

STATE – 4						
MBUS-1	277.128	284.50636	195.49364	270.28104	0.671	30.9
MBUS-2	277.128	224.3566	255.6434	213.13877	6	35.2
MBUS-3	277.128	271.87388	208.12612	258.28019	1.142	70.4
MBUS-4	277.128	275.97993	204.02007	262.18093	6	163.3
MBUS-5	277.128	266.99959	213.00041	253.64961	1.171	70.4
STATE – 5						
MBUS-1	277.128	313.0937568	-35.96562756	297.439069	0.386	40.4
MBUS-2	277.128	269.1925204	7.93560886	255.732894	0.733	187.39
MBUS-3	277.128	283.174647	-6.046517785	269.015915	0.657	32.6
MBUS-4	277.128	277.7841619	-0.656032678	263.894954	0.682	30.4
MBUS-5	277.128	278.2522423	-1.124113055	264.33963	0.682	30.9
STATE – 6						
MBUS-1	277.128	290.14045	189.85955	275.63343	0.683	59.5
MBUS-2	277.128	256.33438	223.66562	243.51766	6	201.77
MBUS-3	277.128	275.92305	204.07695	262.12689	6	83.5
MBUS-4	277.128	275.96818	204.03182	262.16977	6	114.3
MBUS-5	277.128	271.03164	208.96836	257.48005	6	82.8
STATE -7						
MBUS-1	277.128	307.08019	172.91981	291.72618	0.653	15.2
MBUS-2	277.128	238.35698	241.64302	226.43913	6	21.6
MBUS-3	277.128	278.51399	201.48601	264.58829	1.149	46.8
MBUS-4	277.128	275.94332	204.05668	262.14615	6	124.38
MBUS-5	277.128	273.61245	206.38755	259.93183	1.15	46.6

Table B.3 shows the computations for objective function calculations for transition from stage – 0 to stage – 1.

B.3 Calculations

TABLE B.3: Objective function computations for transition from Stage- 0 to Stage - 1

FROM	TO	$J_{voltage}$	J_{time}	$J_{oscillation}$	$J_{installation}$	$J_{operation}$	$J_{investment}$	J
0,1	1,1	23.90694152	10754.381	39.19987859	0	0	0	115.7087919
0,1	1,2	13.12190752	1623.3352	121.0434574	800	272000	1231.3375	29.71392151
0,1	1,3	4.642454403	121370.11	1167.327973	480	106400	1231.3375	1225.620865
0,1	1,4	15.47284317	244323.58	1133.559462	480	106400	1231.3375	2458.596892
0,1	1,5	7.264347085	504.9468	1180.876569	1280	398400	2462.6751	26.69806598
0,1	1,6	3.342007229	399366.98	2125.353715	960	213600	2462.6751	4014.493317
0,1	1,7	12.5833973	244241.22	581.4236079	1280	398400	2462.6751	2462.83655

Figure B.3 shows the various transitions from the base system to the states in stage – 1. It is assumed that the cost of the base system is 0. Each of the states is described in 3 parts. The first part gives the stage number and state number. The second part gives the cost of the state over the entire stage, $C(X_{i,k})$. The third part represents the optimal path of the planning period at the state and stage, $C^*(X_{i,k})$. Let p_i be the state in the previous stage ‘k-1’ that leads to the optimal path in the current state ‘i’ and stage ‘k’.

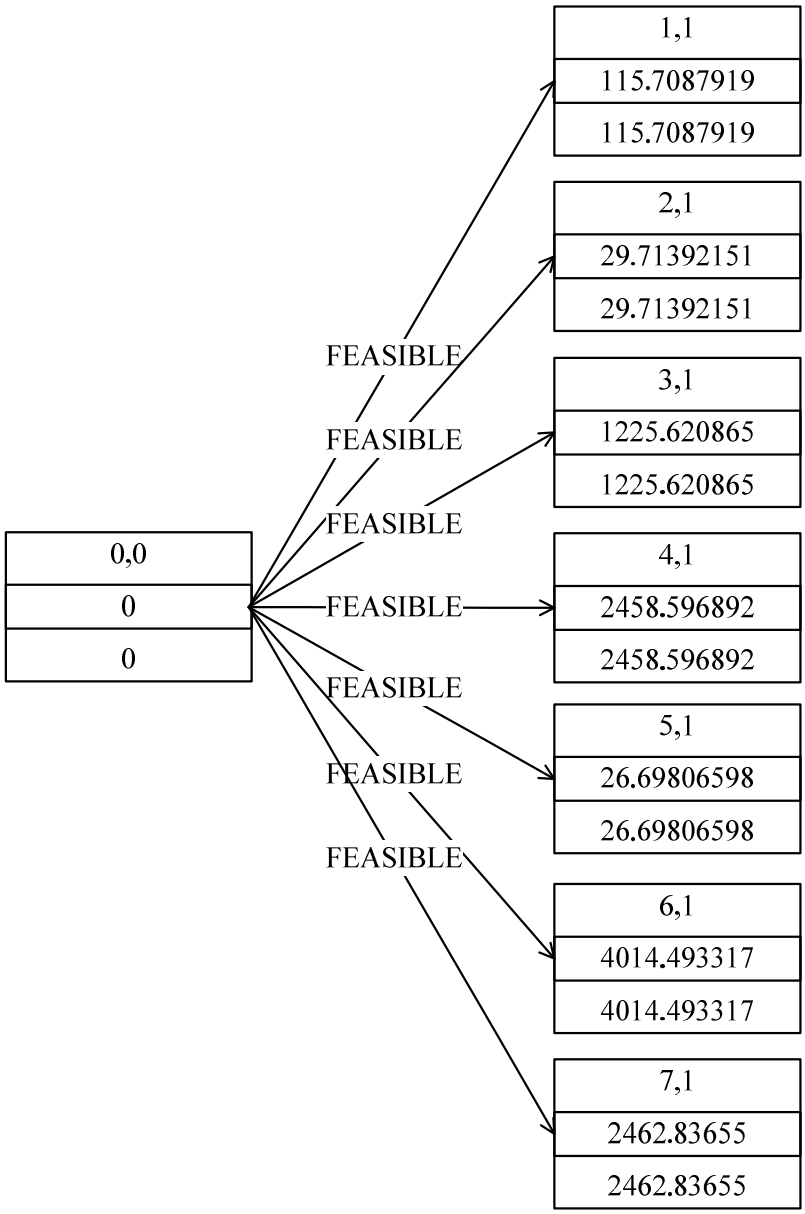

FIGURE B.3: Transitions from base case to Stage – 1.

Hence, for Stage – 1,

$C(X_{1,1}) = 115.7087919$ $C^*(X_{1,1}) = 115.7087919$ $p_1 = 0,0$

$C(X_{2,1}) = 29.71392151$ $C^*(X_{2,1}) = 29.71392151$ $p_2 = 0,0$

$C(X_{3,1}) = 1225.620865$ $C^*(X_{3,1}) = 1225.620865$ $p_3 = 0,0$

$C(X_{4,1}) = 2458.596892$ $C^*(X_{4,1}) = 2458.596892$ $p_4 = 0,0$

$C(X_{5,1}) = 26.69806598$ $C^*(X_{5,1}) = 26.69806598$ $p_5 = 0,0$

$C(X_{6,1}) = 4014.493317$ $C^*(X_{6,1}) = 4014.493317$ $p_6 = 0,0$

$C(X_{7,1}) = 2462.83655$ $C^*(X_{7,1}) = 2462.83655$ $p_7 = 0,0$

Hence, for the transition between Stage – 0 and Stage – 1, there is only one possible transition for all the stages. The ease of dynamic programming method to find optimal path is evident in the forthcoming calculations where we have multiple states between stages and multiple transitions.

Table B.4 shows the objective function computations for each of the states in Stage – 2

TABLE B.4: Objective function calculations for Stage - 2

FROM	TO	$J_{voltage}$	J_{time}	$J_{oscillation}$	$J_{installation}$	$J_{operation}$	$J_{investment}$	J
1,1	1,2	23.906941	10754.3812	39.199878	0	0	0	115.70879
1,1	2,2	13.121907	1623.3352	121.04345	800	272000	1231.33	29.713921
2,1	2,2	13.121907	1623.3352	121.04345	0	272000	0	25.09825
1,1	3,2	4.6424544	121370.107	1167.3279	480	106400	1231.33	1225.6208
3,1	3,2	4.6424544	121370.107	1167.3279	0	106400	0	1222.6051
1,1	4,2	15.472843	244323.581	1133.5594	480	106400	1231.33	2458.5968
4,1	4,2	15.472843	244323.581	1133.5594	0	106400	0	2455.5812
1,1	5,2	7.2643470	504.9468	1180.87656	1280	398400	2462.67	26.698065
2,1	5,2	7.2643470	504.9468	1180.87656	480	398400	1231.33	22.082397
3,1	5,2	7.2643470	504.9468	1180.87656	800	398400	1231.33	23.682397
5,1	5,2	7.2643470	504.9468	1180.87656	0	398400	0	19.066728
1,1	6,2	3.3420072	399366.978	2125.35371	960	213600	2462.67	4014.4933
3,1	6,2	3.3420072	399366.978	2125.35371	480	213600	1231.33	4011.4776

4,1	6,2	3.3420072	399366.978	2125.35371	480	213600	1231.33	4011.4776
6,1	6,2	3.3420072	399366.978	2125.35371	0	213600	0	4008.4618
1,1	7,2	12.583397	244241.22	581.423607	1280	398400	2462.67	2462.836
2,1	7,2	12.583397	244241.22	581.423607	480	398400	1231.33	2458.2208
4,1	7,2	12.583397	244241.22	581.423607	800	398400	1231.33	2459.8208
7,1	7,2	12.583397	244241.22	581.423607	0	398400	0	2455.2052

For state-2, stage -2,

$C^*(X_{2,2})$ = min{29.71392151 + 115.7087919, 25.09825274 + 29.71392151 ,∞, ∞, ∞, ∞, ∞} = 54.81217426

Figure B.4 shows the transitions from the states in stage 1 to state 2 in stage 2. Similar computations are carried out for each of the states in stage 2. The transitions from States 3,4,5,6,7 in Stage – 1 to State – 2, Stage – 2 would involve removing a reactive power source. Since this has been considered infeasible, the transition costs of these sources are ∞, thereby eliminating these options.

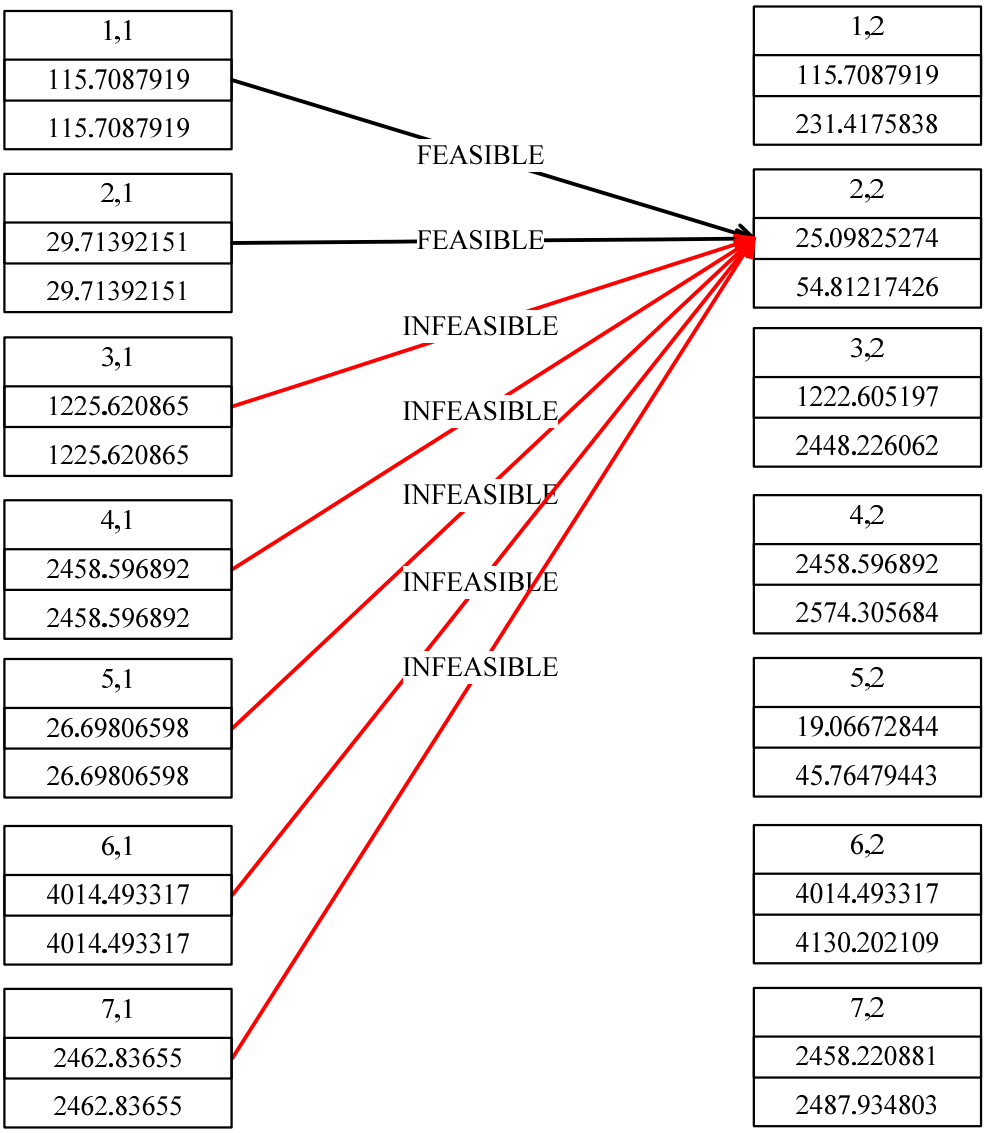

FIGURE B.4: Computations from Stage - 1 to Stage - 2

$C(X_{1,2}) = 115.7087919$ $C^*(X_{1,2}) = 231.4175838$ $p_1 = 1,1$

$C(X_{2,2}) = 25.09825274$ $C^*(X_{2,2}) = 54.81217426$ $p_2 = 2,1$

$C(X_{3,2}) = 1222.605197$ $C^*(X_{3,2}) = 2448.226062$ $p_2 = 3,1$

$C(X_{4,2}) = 2458.596892$ $C^*(X_{4,2}) = 2574.305684$ $p_4 = 1,1$

$C(X_{5,2})$ = 19.06672844 $C^*(X_{5,2})$ = 45.76479443 p_5 = 5,1

$C(X_{6,2})$ = 4014.493317 $C^*(X_{6,2})$ = 4130.202109 p_6 = 1,1

$C(X_{7,1})$ = 2458.220881 $C^*(X_{7,1})$ = 2487.934803 p_7 = 2,1

The above values are illustrated in Figure B.5. This figure shows the most optimal transitions between Stage – 1 and Stage – 2.

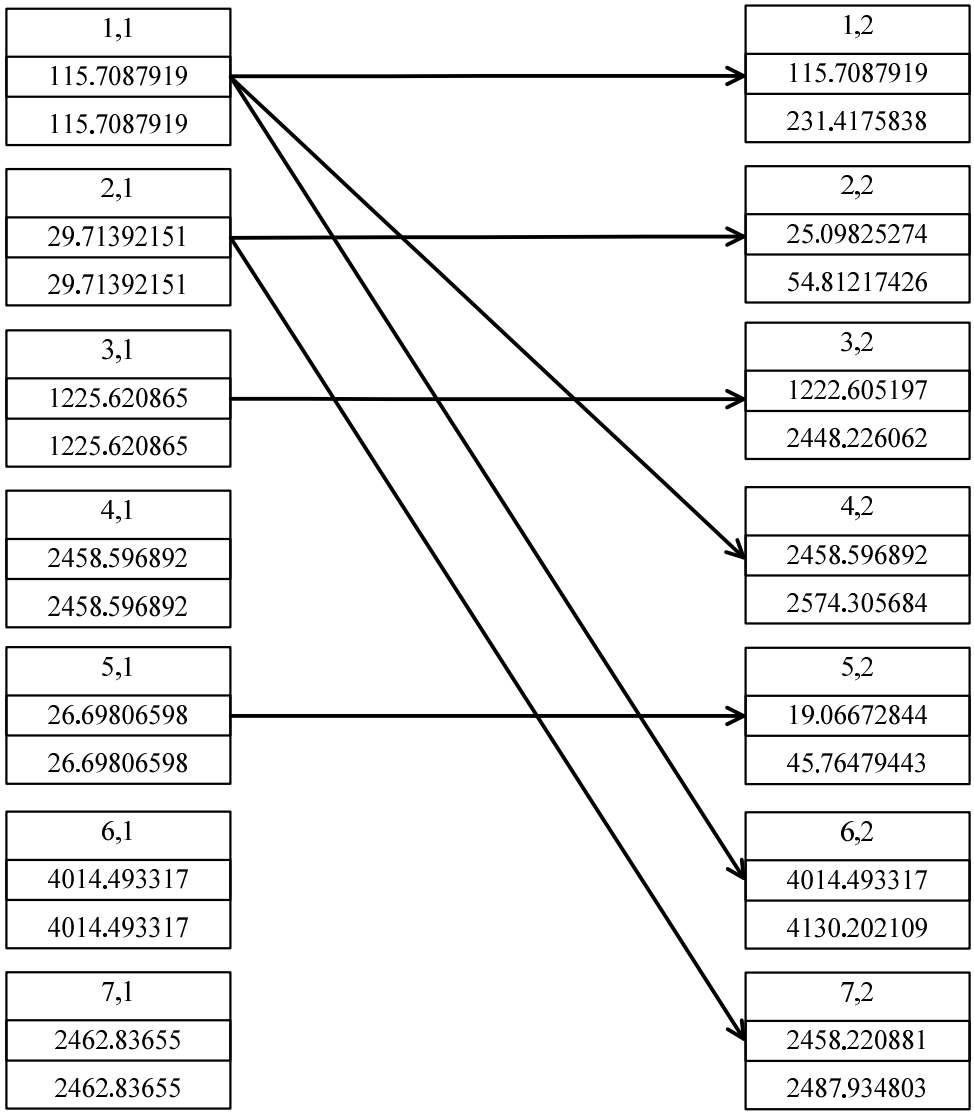

FIGURE B.5: Optimal Transitions from Stage – 1 to Stage - 2

TABLE B.5: Objective Function Calculations for Stage – 3

FROM	TO	$J_{voltage}$	J_{time}	$J_{oscillation}$	$J_{installation}$	$J_{operation}$	$J_{investment}$	J
1,2	1,3	23.90694152	10754.3812	39.199878	0	0	0	115.70879
1,2	2,3	13.12190752	1623.3352	121.04345	800	272000	1231.3375	29.713921
2,2	2,3	13.12190752	1623.3352	121.04345	0	272000	0	25.098252
1,2	3,3	4.642454403	121370.1072	1167.3279	480	106400	1231.3375	1225.6208
3,2	3,3	4.642454403	121370.1072	1167.3279	0	106400	0	1222.6051
1,2	4,3	15.47284317	244323.5812	1133.5594	480	106400	1231.3375	2458.5962
4,2	4,3	15.47284317	244323.5812	1133.5594	0	106400	0	2455.5812
1,2	5,3	7.264347085	504.9468	1180.8765	1280	398400	2462.6750	26.698065
2,2	5,3	7.264347085	504.9468	1180.8765	480	398400	1231.3375	22.082397
3,2	5,3	7.264347085	504.9468	1180.8765	800	398400	1231.3375	23.682397
5,2	5,3	7.264347085	504.9468	1180.8765	0	398400	0	19.066728
1,2	6,3	3.342007229	399366.978	2125.3537	960	213600	2462.6750	4014.4933
3,2	6,3	3.342007229	399366.978	2125.3537	480	213600	1231.3375	4011.4776
4,2	6,3	3.342007229	399366.978	2125.3537	480	213600	1231.3375	4011.4776
6,2	6,3	3.342007229	399366.978	2125.3537	0	213600	0	4008.4619
1,2	7,3	12.5833973	244241.22	581.42360	1280	398400	2462.6750	2462.8365
2,2	7,3	12.5833973	244241.22	581.42360	480	398400	1231.3375	2458.2208
4,2	7,3	12.5833973	244241.22	581.42360	800	398400	1231.3375	2459.8208
7,2	7,3	12.5833973	244241.22	581.42360	0	398400	0	2455.2052

For example, in State – 5 in Stage – 3, the optimal value from the base case to the current stage is calculated as:

$C^*(X_{5,3})$ = min{ 26.69806598 + 231.4175838, 22.08239721 + 54.81217426, 3.68239721 + 2448.226062, ∞, 19.06672844 + 45.76479443, ∞, ∞} = 64.83152287

Figure B.6 shows the transitions from Stage – 2 to State – 5, Stage – 3.

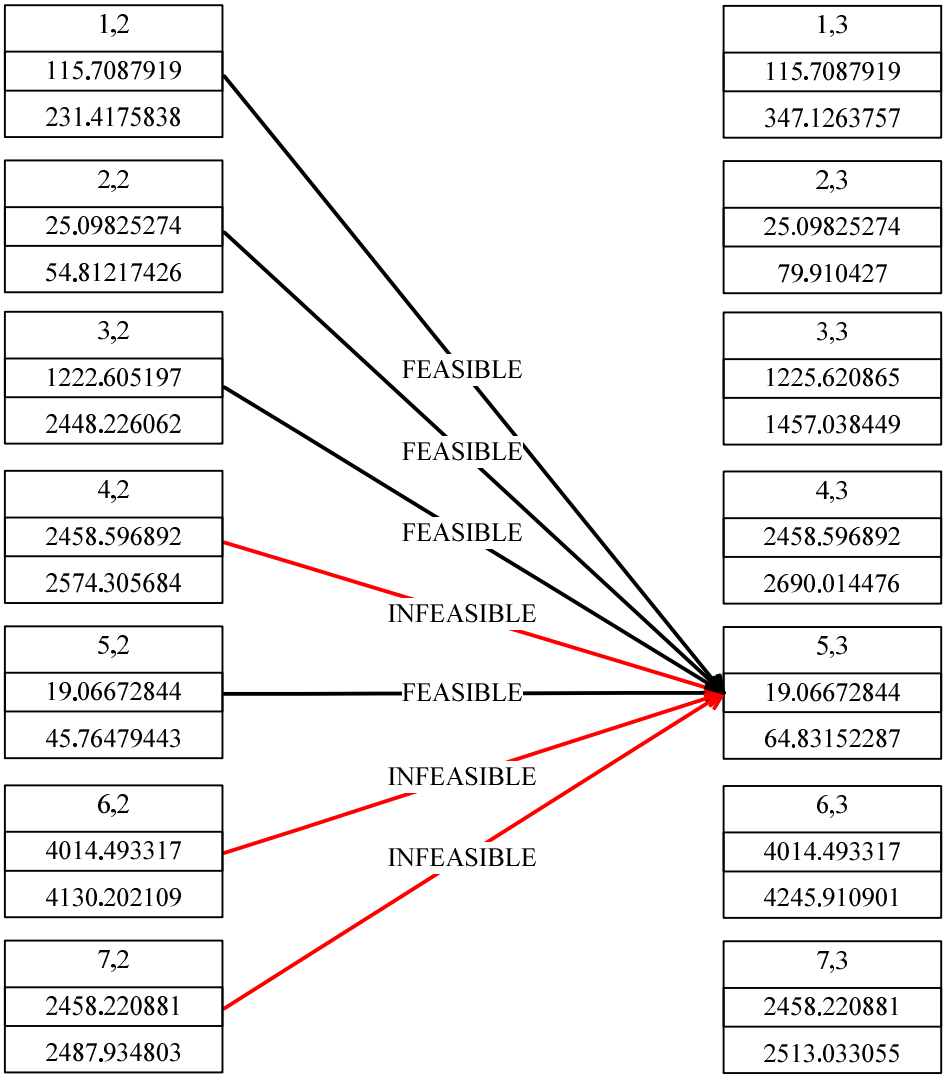

FIGURE B.6: Transitions from Stage – 2 to State – 5, Stage – 3

This gives the most optimal value of $C^*(X_{5,3})$ as 64.83152287 from the base case to Stage – 5. These computations are carried out for all the states in this stage and the following values of $C^*(X_{i,3})$ and p_i for all the states i in Stage – 3 are obtained as follows:

$C(X_{1,3}) = 115.7087919$ $C^*(X_{1,3}) = 347.1263757$ $p_1 = 1,1$

$C(X_{2,3}) = 25.09825274$ $C^*(X_{2,3}) = 79.910427$ $p_2 = 2,1$

$C(X_{3,3}) = 1225.620865$ $C^*(X_{3,3}) = 1457.038449$ $p_2 = 3,1$

$C(X_{4,3}) = 2458.596892$ $C^*(X_{4,3}) = 2690.014476$ $p_4 = 1,1$

$C(X_{5,3}) = 19.06672844$ $C^*(X_{5,3}) = 64.83152287$ $p_5 = 5,1$

$C(X_{6,3}) = 4014.493317$ $C^*(X_{6,3}) = 4245.910901$ $p_6 = 1,1$

$C(X_{7,3}) = 2458.220881$ $C^*(X_{7,3}) = 2513.033055$ $p_7 = 2,1$

These values are illustrated in Figure B.7. This figure shows the most optimal transitions for all the states from Stage – 2 to Stage – 3.

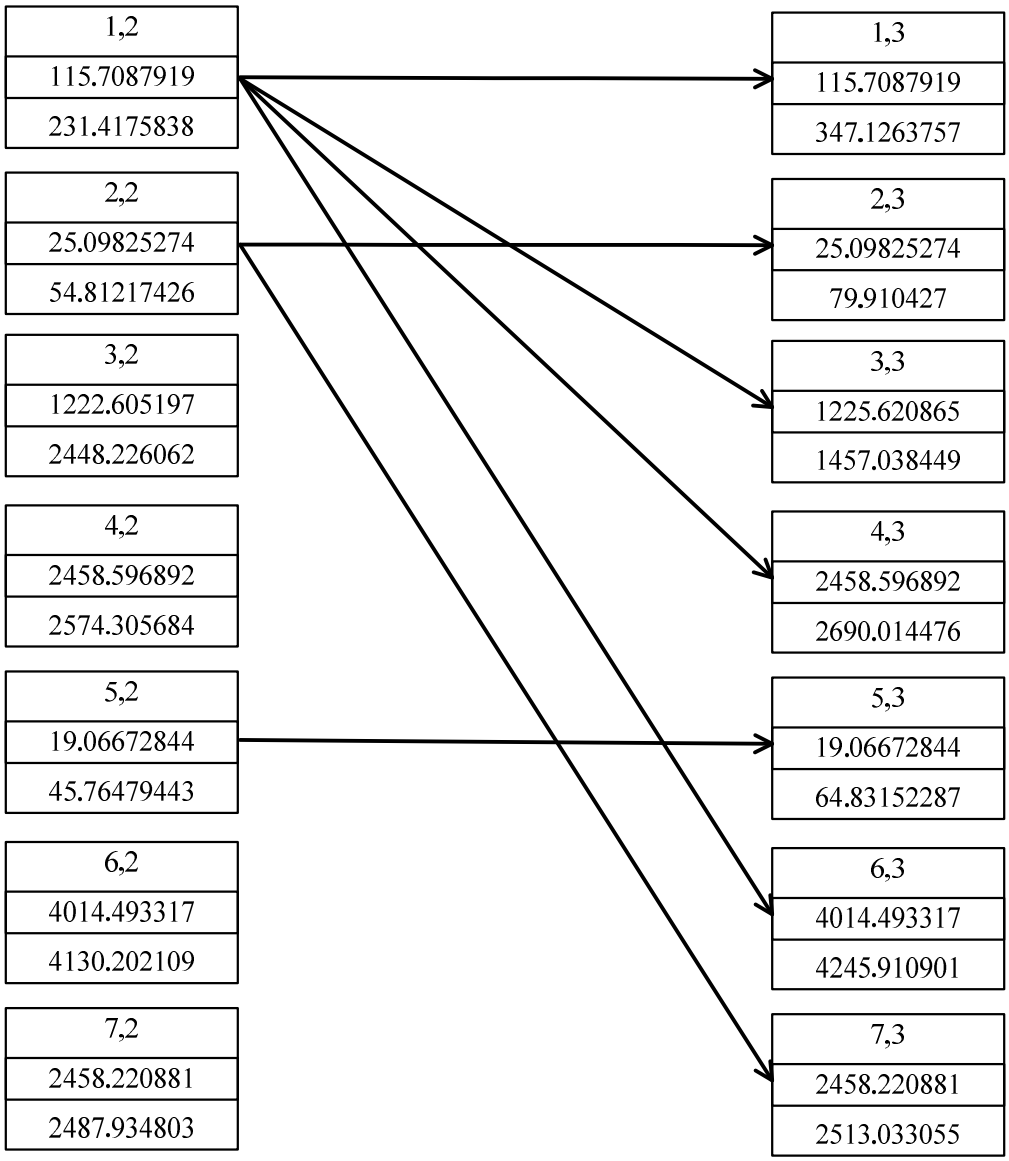

FIGURE B.7: Most optimal transitions from State – 2 to State – 3

After Stage – 3, we assume that there is an increase in dynamic load at MBUS – 4 by 0.4 MVA. Table B.6 gives the objective function computations for Stage – 4.

TABLE B.6: Objective function computations for Stage - 4

FROM	TO	$J_{voltage}$	J_{time}	$J_{oscillation}$	$J_{installation}$	$J_{operation}$	$J_{investment}$	J
1,3	1,4	37.4855	13105.3036	68.4186	0	0	0.0000	143.8903
1,3	2,4	21.6382	8256.3348	157.3038	800	272000	1231.3375	99.0640
2,3	2,4	21.6382	8256.3348	157.3038	0	272000	0.0000	94.4483
1,3	3,4	12.4274	132675.9484	1066.5633	480	106400	1231.3375	1340.7704
3,3	3,4	12.4274	132675.9484	1066.5633	0	106400	0.0000	1337.7548
1,3	4,4	22.8379	449930.2720	909.2135	480	106400	1231.3375	4515.9971
4,3	4,4	22.8379	449930.2720	909.2135	0	106400	0.0000	4512.9814
1,3	5,4	8.0584	129867.9152	1168.6164	1280	398400	2462.6751	1320.5311
2,3	5,4	8.0584	129867.9152	1168.6164	480	398400	1231.3375	1315.9155
3,3	5,4	8.0584	129867.9152	1168.6164	800	398400	1231.3375	1317.5155
5,3	5,4	8.0584	129867.9152	1168.6164	0	398400	0.0000	1312.8998
1,3	6,4	5.8508	447795.9220	2122.2815	960	213600	2462.6751	4499.6036
3,3	6,4	5.8508	447795.9220	2122.2815	480	213600	1231.3375	4496.5880
4,3	6,4	5.8508	447795.9220	2122.2815	480	213600	1231.3375	4496.5880
6,3	6,4	5.8508	447795.9220	2122.2815	0	213600	0.0000	4493.5723
1,3	7,4	16.5589	399658.2500	935.5847	1280	398400	2462.6751	4020.1028
2,3	7,4	16.5589	399658.2500	935.5847	480	398400	1231.3375	4015.4872
4,3	7,4	16.5589	399658.2500	935.5847	800	398400	1231.3375	4017.0872
7,3	7,4	16.5589	399658.2500	935.5847	0	398400	0.0000	4012.4715

Similar computations are carried out, resulting in FIGURE B.8, which gives the optimal path to each of the states in Stage – 4.

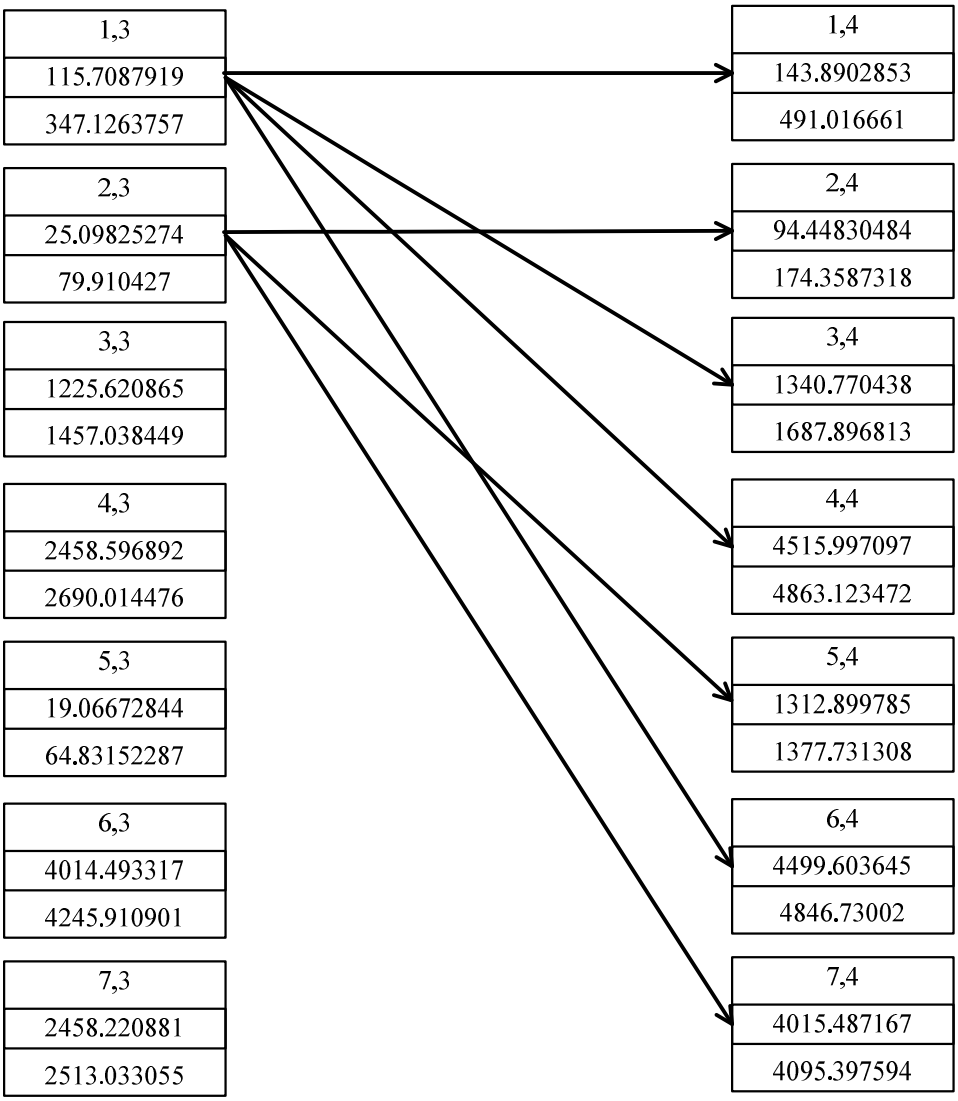

FIGURE B.8: Optimal paths between Stage -3 and Stage – 4

At Stage – 5, we assume an increase in load at MBUS – 1 by 0.4MVA. Table B.7 gives the objective function values for Stage – 5 and FIGURE B.9 gives the shortest paths between states in Stage – 4 and Stage – 5.

TABLE B.7: Objective function for Stage – 5

FROM	TO	$J_{voltage}$	J_{time}	$J_{oscillation}$	$J_{installation}$	$J_{operation}$	$J_{investment}$	J
1,4	1,5	51.6629	63448.8760	112.4344	0	0	0.0000	652.2719
1,4	2,5	449.3363	387200.0000	6.9665	800	272000	1231.3375	4030.3150
2,4	2,5	449.3363	387200.0000	6.9665	0	272000	0.0000	4025.6993
1,4	3,5	20.4157	451497.0244	984.3449	480	106400	1231.3375	4531.2329
3,4	3,5	20.4157	451497.0244	984.3449	0	106400	0.0000	4528.2172
1,4	4,5	31.0770	556600.0000	897.2971	480	106400	1231.3375	5585.3811
4,4	4,5	31.0770	556600.0000	897.2971	0	106400	0.0000	5582.3655
1,4	5,5	9.9677	56897.4916	1068.7490	1280	398400	2462.6751	590.9640
2,4	5,5	9.9677	56897.4916	1068.7490	480	398400	1231.3375	586.3483
3,4	5,5	9.9677	56897.4916	1068.7490	800	398400	1231.3375	587.9483
5,4	5,5	9.9677	56897.4916	1068.7490	0	398400	0.0000	583.3327
1,4	6,5	8.4339	461389.0000	2665.7434	960	213600	2462.6751	4639.1128
3,4	6,5	8.4339	461389.0000	2665.7434	480	213600	1231.3375	4636.0971
4,4	6,5	8.4339	461389.0000	2665.7434	480	213600	1231.3375	4636.0971
6,4	6,5	8.4339	461389.0000	2665.7434	0	213600	0.0000	4633.0814
1,4	7,5	17.8587	447705.4744	1013.4637	1280	398400	2462.6751	4501.3977
2,4	7,5	17.8587	447705.4744	1013.4637	480	398400	1231.3375	4496.7821
4,4	7,5	17.8587	447705.4744	1013.4637	800	398400	1231.3375	4498.3821
7,4	7,5	17.8587	447705.4744	1013.4637	0	398400	0.0000	4493.7664

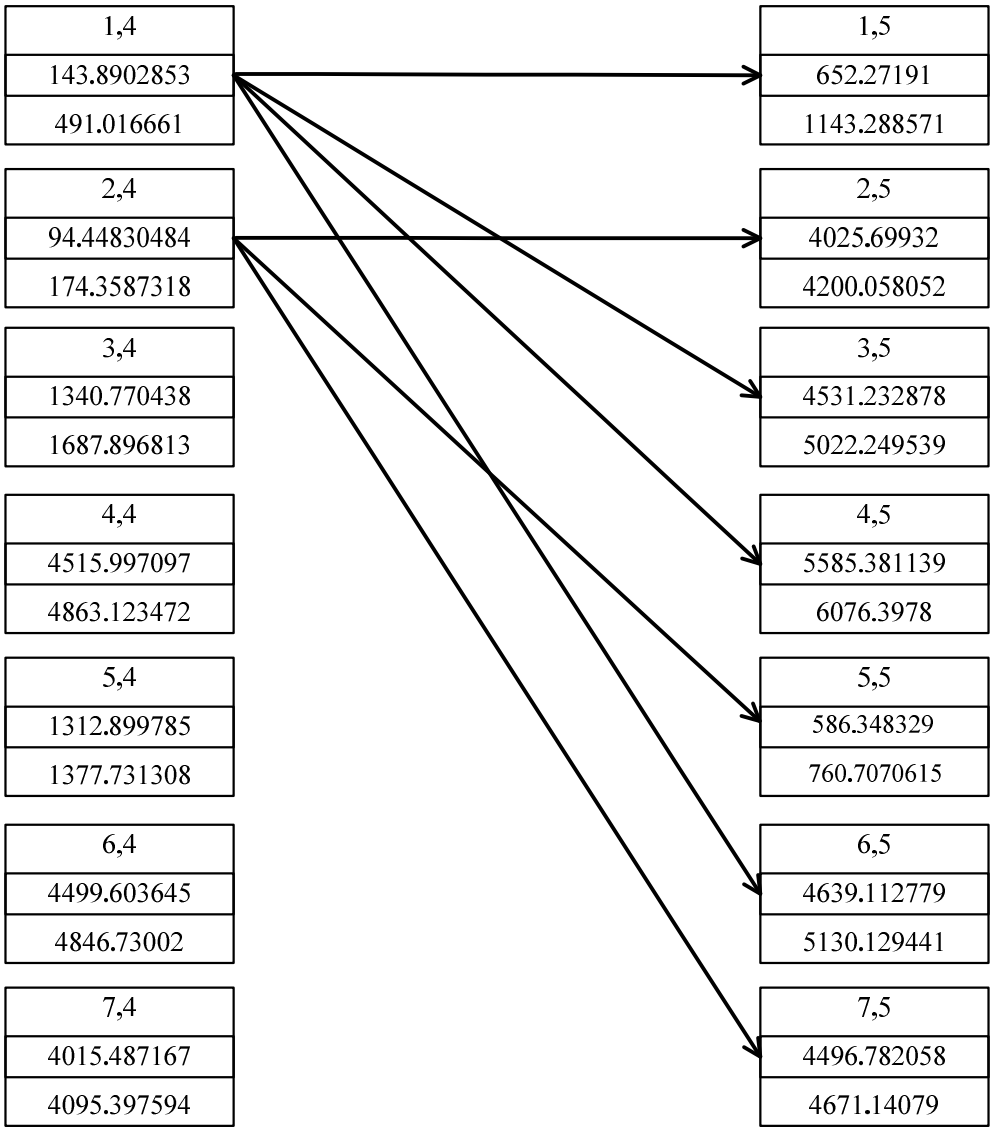

FIGURE B.9: Optimal paths between Stage -4 and Stage – 5

In this stage we see that the minimum $C^*(x_{i,j})$ value is at State – 5 in Stage – 5. This stage is reached optimally from State – 2 in Stage – 4. By backtracking in this manner, the optimal planning path is obtained as shown in FIGURE B.10.

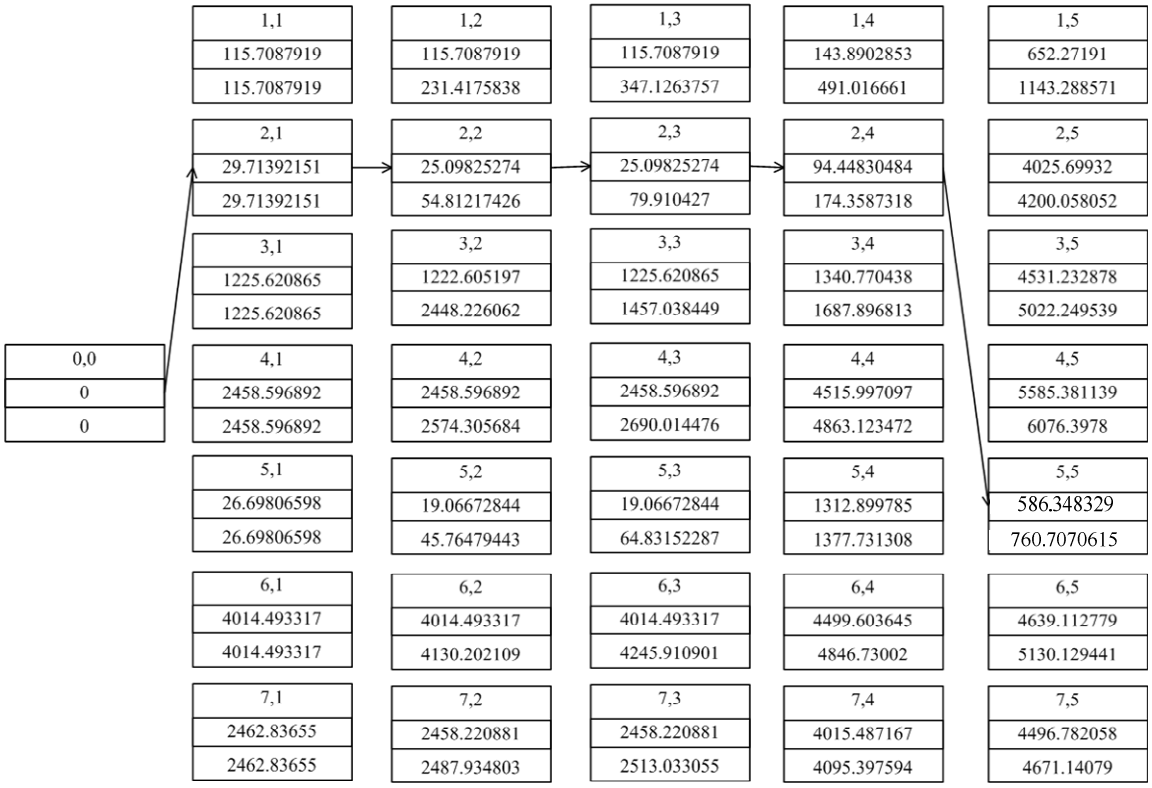

FIGURE B.10: Optimal Planning Trajectory

This appendix described the calculations involved with the application of dynamic programming to a multistage decision process involving allocation of static and dynamic reactive power sources. This method was then tested on the IEEE 24-Substation Reliability Test System (RTS - 96). The distribution substation is appended to one of the substations and similar simulations are calculations are performed. These have been described in Appendix C.

APPENDIX C:

RESULTS FROM IEEE – 24 BUS RTS

The dynamic programming algorithm illustrated in Appendix B was tested on the IEEE -24 Substation Reliability Test System. This is a one-area system and consists of three main interconnections. Two of these are 230kV interconnections and one of them is a 138kV interconnection. The system is shown in FIGURE C.1. FIGURE C.2 shows the connection of the 13.8kV distribution system to SUB170. This substation is a 230kV substation and the distribution system is connected through a 230/13.8kV transformer. The other parameters and states of the dynamic programming algorithm remain the same. In this simulation, only one load change has been enforced. This has been done at the beginning of Stage – 4.

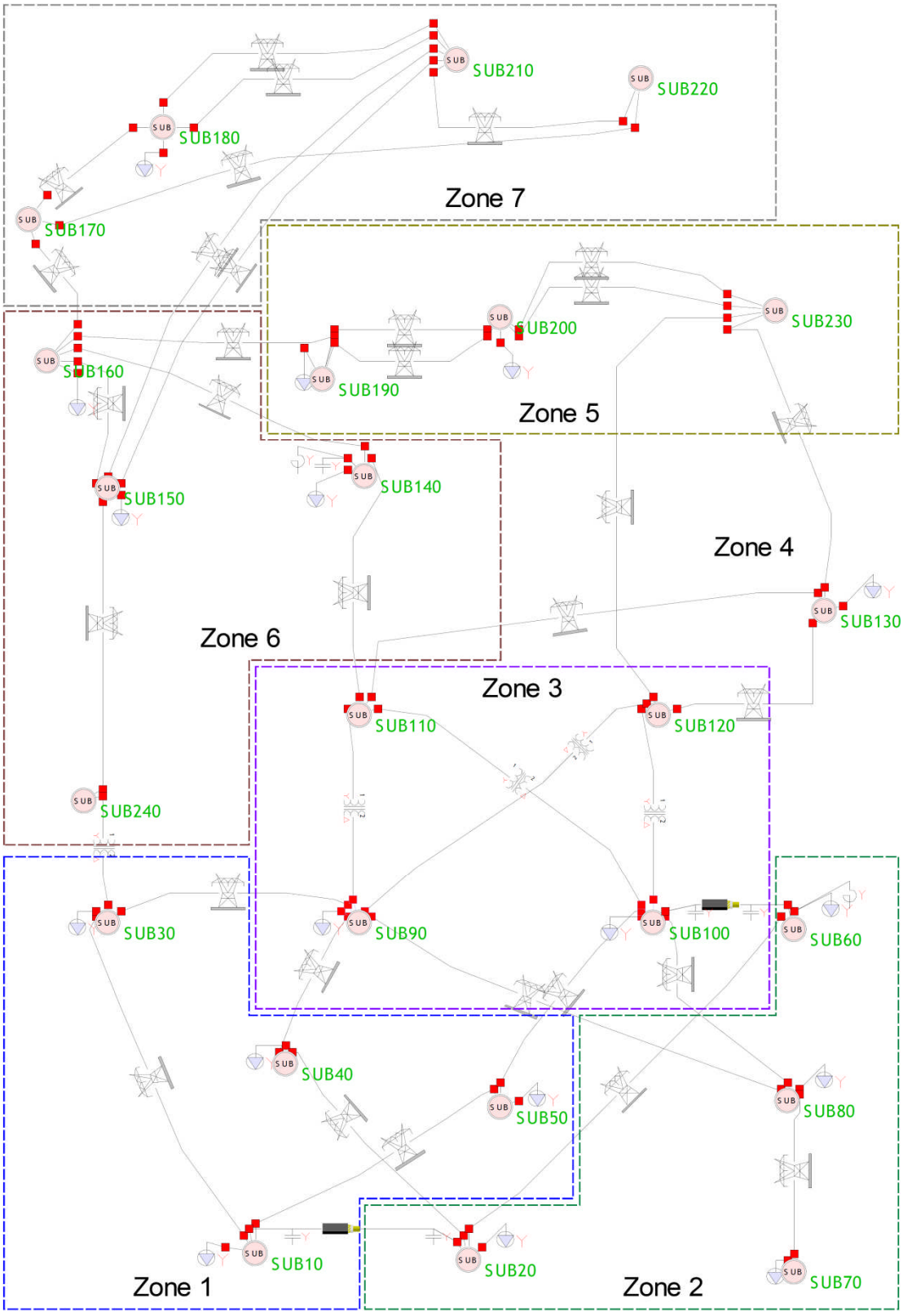

FIGURE C.1: IEEE 24-Substation RTS

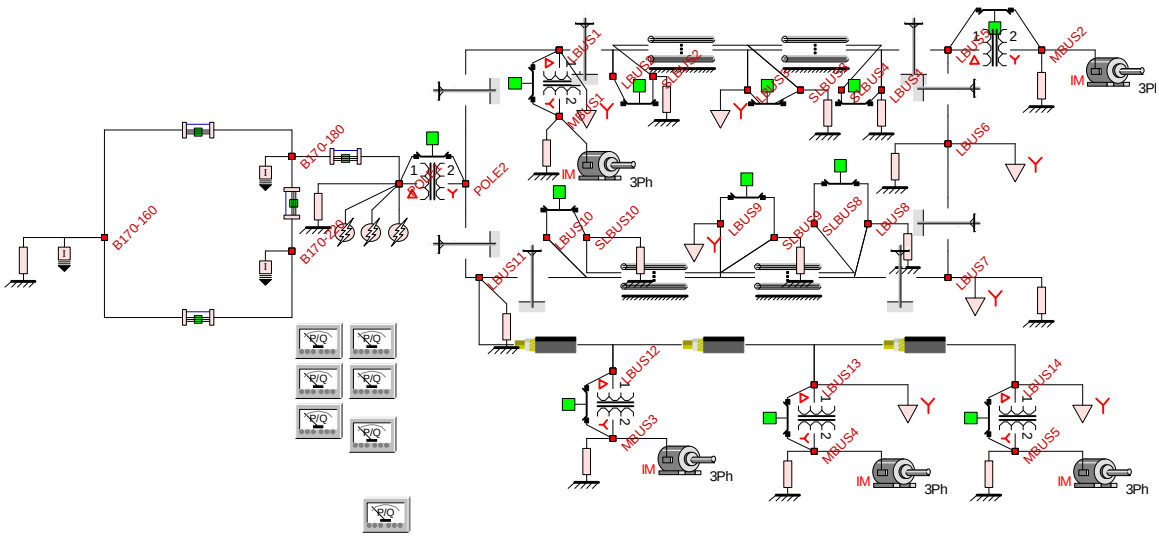

FIGURE C.2: Connection of 13.8kV Distribution System to Substation 170

Simulations similar to the system in Appendix B were carried out for the same decisions in WinIGS – Q. Table C.1 shows the objective functions for these simulations.

TABLE C.1: Objective function computations

FROM	TO	$J_{voltage}$	J_{time}	$J_{oscillation}$	$J_{installation}$	$J_{operation}$	$J_{investment}$	J
STAGE 1								
0,0	1,1	39.8849	1462.2	4.00914	0	0	0	16.1634
0,0	2,1	30.6915	693.6	111.71	800	272000	1231.34	10.1016
0,0	3,1	25.564	4871.26	1617.42	480	106400	1231.34	7.61599
0,0	4,1	23.7867	4139.91	1825.08	480	106400	1231.34	7.18572
0,0	5,1	19.88	4343.76	1862.79	1280	398400	2462.68	10.5538
0,0	6,1	15.2335	4410.68	3409.16	960	213600	2462.68	7.32695
0,0	7,1	18.2053	3100.96	2029.58	1280	398400	2462.68	10.0651
STAGE 2								
1,1	1,2	39.8849	1462.2	4.00914	0	0	0	8.18645
1,1	2,2	30.6915	693.6	111.71	800	272000	1231.34	10.1016
2,1	2,2	30.6915	693.6	111.71	0	272000	0	9.88001
1,1	3,2	25.564	4871.26	1617.42	480	106400	1231.34	7.61599

3,1	3,2	25.564	4871.26	1617.42	0	106400	0	7.45842
1,1	4,2	23.7867	4139.91	1825.08	480	106400	1231.34	7.18572
4,1	4,2	23.7867	4139.91	1825.08	0	106400	0	7.02815
1,1	5,2	19.88	4343.76	1862.79	1280	398400	2462.68	10.5538
2,1	5,2	19.88	4343.76	1862.79	480	398400	1231.34	10.3322
3,1	5,2	19.88	4343.76	1862.79	800	398400	1231.34	10.3962
5,1	5,2	19.88	4343.76	1862.79	0	398400	0	10.1746
1,1	6,2	15.2335	4410.68	3409.16	960	213600	2462.68	7.32695
3,1	6,2	15.2335	4410.68	3409.16	480	213600	1231.34	7.16938
4,1	6,2	15.2335	4410.68	3409.16	480	213600	1231.34	7.16938
6,1	6,2	15.2335	4410.68	3409.16	0	213600	0	7.01182
1,1	7,2	18.2053	3100.96	2029.58	1280	398400	2462.68	10.0651
2,1	7,2	18.2053	3100.96	2029.58	480	398400	1231.34	9.84356
4,1	7,2	18.2053	3100.96	2029.58	800	398400	1231.34	9.90756
7,1	7,2	18.2053	3100.96	2029.58	0	398400	0	9.68599
STAGE 3								
1,2	1,3	39.8849	1462.2	4.00914	0	0	0	8.18645
1,2	2,3	30.6915	693.6	111.71	800	272000	1231.34	10.1016
2,2	2,3	30.6915	693.6	111.71	0	272000	0	9.88001
1,2	3,3	25.564	4871.26	1617.42	480	106400	1231.34	7.61599
3,2	3,3	25.564	4871.26	1617.42	0	106400	0	7.45842
1,2	4,3	23.7867	4139.91	1825.08	480	106400	1231.34	7.18572
4,2	4,3	23.7867	4139.91	1825.08	0	106400	0	7.02815
1,2	5,3	19.88	4343.76	1862.79	1280	398400	2462.68	10.5538
2,2	5,3	19.88	4343.76	1862.79	480	398400	1231.34	10.3322
3,2	5,3	19.88	4343.76	1862.79	800	398400	1231.34	10.3962
5,2	5,3	19.88	4343.76	1862.79	0	398400	0	10.1746
1,2	6,3	15.2335	4410.68	3409.16	960	213600	2462.68	7.32695
3,2	6,3	15.2335	4410.68	3409.16	480	213600	1231.34	7.16938
4,2	6,3	15.2335	4410.68	3409.16	480	213600	1231.34	7.16938
6,2	6,3	15.2335	4410.68	3409.16	0	213600	0	7.01182
1,2	7,3	18.2053	3100.96	2029.58	1280	398400	2462.68	10.0651

2,2	7,3	18.2053	3100.96	2029.58	480	398400	1231.34	9.84356
4,2	7,3	18.2053	3100.96	2029.58	800	398400	1231.34	9.90756
7,2	7,3	18.2053	3100.96	2029.58	0	398400	0	9.68599
STAGE – 4								
1,3	1,4	39.9351	4050.19	0.53598	0	0	0	8.56569
1,3	2,4	25.8624	2705.33	2.76381	800	272000	1231.34	9.40757
2,3	2,4	25.8624	2705.33	2.76381	0	272000	0	9.18601
1,3	3,4	28.207	6024.16	1524.5	480	106400	1231.34	8.29601
3,3	3,4	28.207	6024.16	1524.5	0	106400	0	8.13844
1,3	4,4	27.5936	8638.12	1326.54	480	106400	1231.34	8.51848
4,3	4,4	27.5936	8638.12	1326.54	0	106400	0	8.36092
1,3	5,4	97.5233	63000	1019.43	1280	398400	2462.68	34.3414
2,3	5,4	97.5233	63000	1019.43	480	398400	1231.34	34.1199
3,3	5,4	97.5233	63000	1019.43	800	398400	1231.34	34.1839
5,3	5,4	97.5233	63000	1019.43	0	398400	0	33.9623
1,3	6,4	22.3593	15288.8	3295.67	960	213600	2462.68	10.2899
3,3	6,4	22.3593	15288.8	3295.67	480	213600	1231.34	10.1324
4,3	6,4	22.3593	15288.8	3295.67	480	213600	1231.34	10.1324
6,3	6,4	22.3593	15288.8	3295.67	0	213600	0	9.9748
1,3	7,4	171.223	175000	755.901	1280	398400	2462.68	65.0437
2,3	7,4	171.223	175000	755.901	480	398400	1231.34	64.8221
4,3	7,4	171.223	175000	755.901	800	398400	1231.34	64.8861
7,3	7,4	171.223	175000	755.901	0	398400	0	64.6646
STAGE – 5								
1,4	1,5	39.9351	4050.19	0.53598	0	0	0	8.56569
1,4	2,5	25.8624	2705.33	2.76381	800	272000	1231.34	9.40757
2,4	2,5	25.8624	2705.33	2.76381	0	272000	0	9.18601
1,4	3,5	28.207	6024.16	1524.5	480	106400	1231.34	8.29601
3,4	3,5	28.207	6024.16	1524.5	0	106400	0	8.13844
1,4	4,5	27.5936	8638.12	1326.54	480	106400	1231.34	8.51848
4,4	4,5	27.5936	8638.12	1326.54	0	106400	0	8.36092
1,4	5,5	97.5233	63000	1019.43	1280	398400	2462.68	34.3414
2,4	5,5	97.5233	63000	1019.43	480	398400	1231.34	34.1199
3,4	5,5	97.5233	63000	1019.43	800	398400	1231.34	34.1839
5,4	5,5	97.5233	63000	1019.43	0	398400	0	33.9623
1,4	6,5	22.3593	15288.8	3295.67	960	213600	2462.68	10.2899
3,4	6,5	22.3593	15288.8	3295.67	480	213600	1231.34	10.1324
4,4	6,5	22.3593	15288.8	3295.67	480	213600	1231.34	10.1324
6,4	6,5	22.3593	15288.8	3295.67	0	213600	0	9.9748

1,4	7,5	171.223	175000	755.901	1280	398400	2462.68	65.0437
2,4	7,5	171.223	175000	755.901	480	398400	1231.34	64.8221
4,4	7,5	171.223	175000	755.901	800	398400	1231.34	64.8861
7,4	7,5	171.223	175000	755.901	0	398400	0	64.6646

FIGURE C.3 gives the dynamic programming results computed for the system. It can be seen that at Stage – 5, State – 4 has the minimum optimal value. Thus, by backtracking, it was concluded that optimal planning would involve allocation of a dynamic reactive power source at MBUS – 4 at the start of Stage – 2.

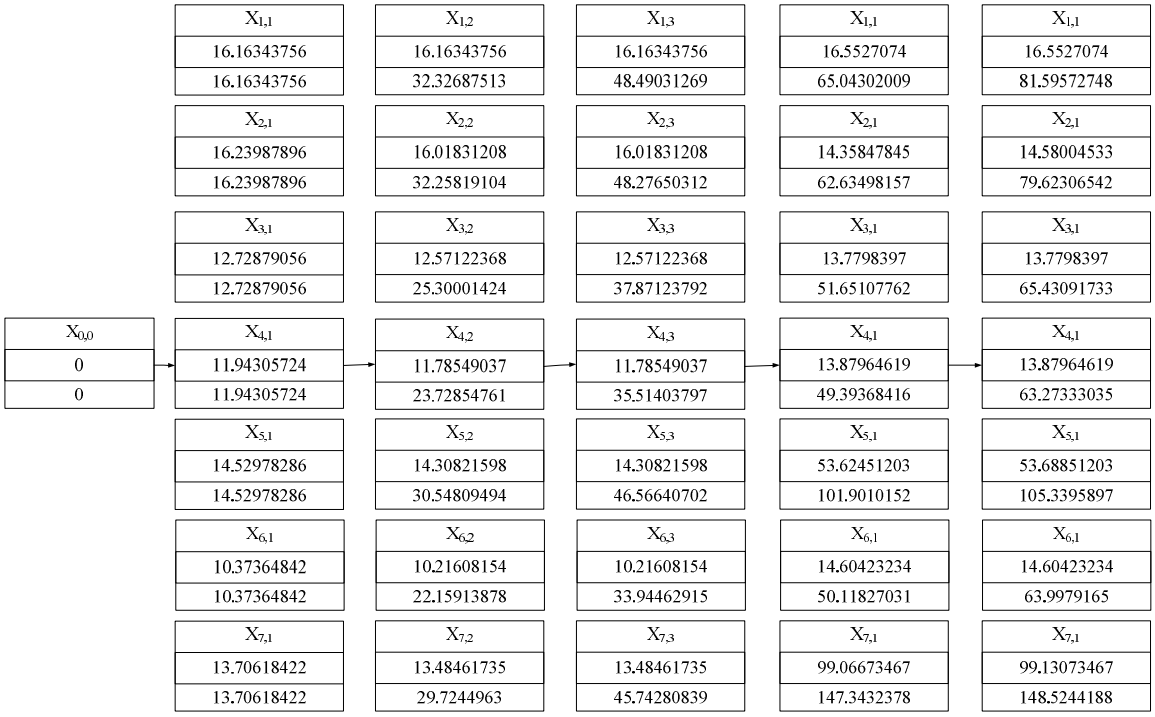

FIGURE C.3: Optimal Planning Trajectory for the IEEE 24 Bus RTS

REFERENCES

[1] N. Martins, L.T.G. Lima, “Determination of Suitable Locations for Power System Stabilizers and Static VAr Compensators for Damping Electromechanical Oscillations in Large Scale Power Systems”, IEEE Power Industry Computer Applications Conference, 1989.

[2] “AMSC SVC” Brochure, American Superconductors, http://www.amsc.com/pdf/PESSVC_BRO_0410_A4_forweb.pdf.

[3] E.H. Camm, T. Adu, “Evaluating Advanced VAr Compensators for Improving Power System Voltage Stability”, IEEE Power Systems Conference and Exposition, 2004.

[4] V.S. Kolluri, S. Mandal, S. Datta, R.D. Powell, D. Mader, “Application of Static VAr Compensator in Entergy System to Address Voltage Stability Issues – Planning and Design Considerations”, IEEE PES Transmission and Distribution Conference and Exhibition, 2005.

[5] M.A. Yalcin, M. Turan, Z. Demir, “Effects of Transmission Line Faults on Dynamic Voltage Stability”, PowerTech Budapest, IEEE International Conference on Electric Power Engineering, 1999.

[6] A.P. Sakis Meliopoulos, G. Cokkinides, G. Stefopoulos, “Voltage Stability and Voltage Recovery: Load Dynamics and Dynamic VAr Sources”, IEEE Power Systems Conference and Exposition, 2006.

[7] G.M. Huang, N.K.C. Nair, “Detection of Dynamic Voltage Collapse”, Power Engineering Society Summer Meeting, Vol. 3, Pages 1284 – 1289, 2002.

[8] X. Lei, D. Retzmann, “Static and Dynamic Approaches for Analyzing Voltage Stability”, European Transactions on Electric Power, Vol. 16, Iss. 3, 2006.

[9] G. Huang, H, Zhang, “Dynamic Voltage Stability Reserves for Deregulated Environment”, IEEE Power Engineering Society Summer Meeting, Vol. 1, Pages 301 – 306, 2001.

[10] Y.H. Moon, H.S. Ryu, J. Lee, B. Kim, “Uniqueness of Voltage Stability Analysis in Power Systems”, IEEE Power Engineering Society Summer Meeting, Vol. 3, Pages 1536 – 1541, 2001.

[11] S.C. Tripathy, “Study of Dynamic Voltage Stability of Power Systems”, International Journal of Electrical Engineering Education, Vol. 37, Iss. 4, 2000.

[12] E.B. Cano, “Static Voltage Stability Analysis for Electric Subtransmission System”, http://ebcano.files.wordpress.com/2008/07/microsoft-word-ebcano_vs_0908.pdf, 2008.

[13] G. Radman, A. Pama, “Static Voltage Stability Analysis of Power Systems Considering Induction Motor Components of Loads”, European Power and Energy Systems, 2007.

[14] Mohan, Undeland, Robbins, “Power Electronic Converters, Applications and Design”, 2005, Publisher: Wiley, 3rd Edition, ISBN: 978-0471226932.

[15] C. Mozina, “Undervoltage Load Shedding – Part 1”, electricenergyonline.com.

[16] A.P. Sakis Meliopoulos, G.J. Cokkinides, G. Stefopoulos, S. Choi, F. Lambert, “Feeder Voltage Phenomena – Phase 1: Characterization”, 2008.

[17] L.Y. Taylor, H, Shih-Min, “Transmission Voltage Recovery following a fault event in the Metro Atlanta Area”, IEEE Power Engineering Society Summer Meeting, Vol. 1, Pages 537 – 542, 2000.

[18] M.H.J. Bollen, “Voltage Recovery after Unbalanced and Balanced Voltage Dips in Three Phase Power Systems”, IEEE Transactions on Power Delivery, Iss. 4, Vol. 18, Pages 1376 – 1381, 2003.

[19] J.W. Bialek. “Recent Blackouts in US/Canada and Continental Europe: Is liberalization to blame?”, PowerTech, IEEE Russia, 27-30 June 2005, Pages 1 – 7.

[20] S.E.Dreyfus, A.M. Law, “The Art and Theory of Dynamic Programming”, Publisher: Academic Press, 1997, ISBN: 978-0122218606.

[21] R. Bellman, “Dynamic Programming”, Publisher: Princeton University Press, 1962, ISBN: 978-0486428093 .

[22] G. Stefopoulos, “Quadratic Power System Modeling and Simulation with Application to Voltage Recovery and Optimal Allocation of VAr Support”, PhD Thesis, Georgia Institute of Technology, August 2009.

[23] C. Tufon, A. Isemonger, B. Kirby, J. Kueck, L. Fangxing, “A Tariff for Reactive Power”, Power Systems Conference and Exposition, 2009, PSCE 2009, IEEE/PES, Pages 1 – 7.

[24] “Engineering Economic Analysis” Coursework Slides, R. Bales, University of California at Merced, 2006, https://eng.ucmerced.edu/people/rbales/Courses/ENGR155files

[25] “Reactive Power Pricing in Competitive Electric Markets Using a Sequential Linear Programming with Considered Investment Cost of Capacitor Banks”, S.G. Seifossadat et al, International Journal of Innovations in Energy Systems and Power, Vol. 4 No. 1, April 2009.

[26] “Review of Reactive Power Planning: Objectives, Constraints and Algorithms”, W. Zhang, F. Li, L.M. Tolbert, IEEE Transactions on Power Systems, Vol. 22, No. 4, November 2007.

[27] “Modified Dynamic Programming Method for Reactive Power Compensating Device Allocation”, G. Majstrovic, D. Bajs, M. Majstrovic, Power Tech, 2005 IEEE Russia, June 2005.

[28] Y. del Valle, “Optimization of Power System Performance using FACTS Devices”, PhD Thesis, Georgia Institute of Technology, August 2009.